LUND UNIVERSITY

Dynamic Shear Rheometer for rheological investigation of bitumen in road applications

The impact of measurement technique

Sheidaei, Maya

2025

Document Version:
Publisher's PDF, also known as Version of record

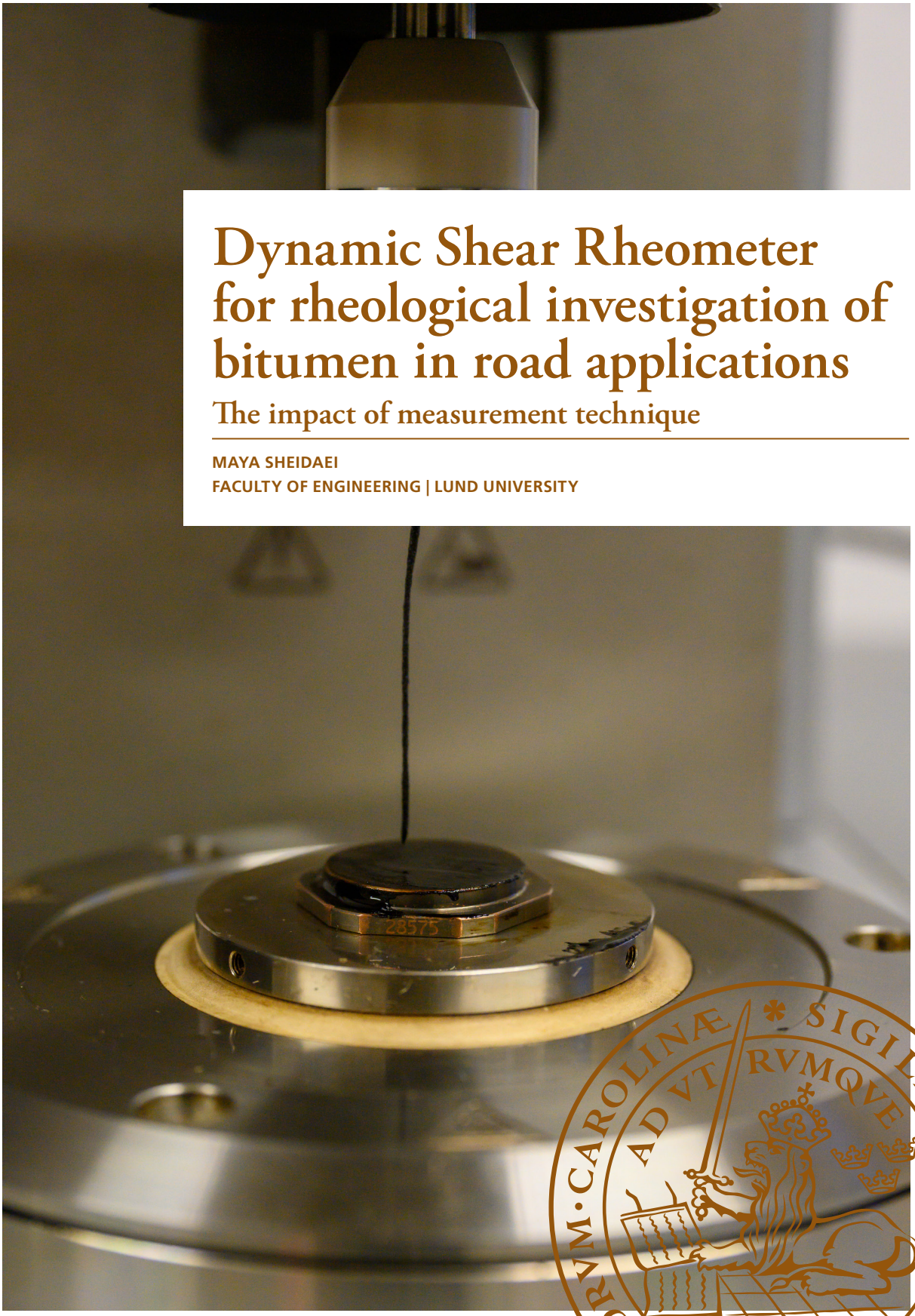

Dynamic Shear Rheometer for rheological investigation of bitumen in road applications

The impact of measurement technique

MAYA SHEIDAEI
FACULTY OF ENGINEERING | LUND UNIVERSITY

Dynamic Shear Rheometer for rheological investigation of bitumen in road applications

Dynamic Shear Rheometer for rheological investigation of bitumen in road applications

The impact of measurement technique

Maya Sheidaei

LUND
UNIVERSITY

DOCTORAL DISSERTATION

by due permission of the Faculty of Engineering, LTH, Lund University, Sweden.To be defended in auditorium V:C, V-house, John Ericsson väg 1, Lund on Thursday, the 6th of March 2025, at 9:00 AM.

Faculty opponent
Associate Professor Augusto Cannone Falchetto,
University of Padua

Organization: LUND UNIVERSITY	**Document name:** DOCTORAL DISSERTATION
Author: Maya Sheidaei	**Date of issue:** 2025-03-06
	Sponsoring organization: SBUF Development Fund of the Swedish Construction Industry

Title and subtitle:
Dynamic Shear Rheometer for rheological investigation of bitumen in road applications_
The impact of measurement technique

Abstract: The rheological properties of bituminous binders tested with a dynamic shear rheometer (DSR) as a function of loading time and temperature can more accurately represent real road situations with rising traffic loads and densities combined with climatic change. This method is more effective than traditional methods such as measuring the softening point and penetration. Complex shear modulus and phase angle which describe the materials' viscoelastic response at a given frequency and temperature can be measured using a DSR following European standard EN 14770.

Even though EN 14770 primarily describes the preparation and conditioning of specimens, various steps in the DSR testing setup result in nonconformity. Therefore, an investigation was conducted to review several areas of test method practices and the underlying impact on results. Data from round-robin tests on bitumen types 20/30 in 2018 and polymer-modified bitumen 45/80-55 in 2019 and 2020, as well as from laboratory experiments on neat bitumen and modified bitumen with wax, SBS, and filler were analysed. The variability in testing conditions and how the testing conditions may affect the measures, as well as the precision of the test technique, are statistically examined. After that, a two-level, three-factor experimental design was used to investigate the effects of the oven setting temperature (HT), bonding temperature (BT) to the rheometer, and trimming state of the specimen on outcomes. Finally, DSR and conventional tests were used to examine the stiffening impact of the fillers when added to bitumen (mastics).

The results based on round-robin test data demonstrate an improved precision on measured |G*| and δ discarding data from inappropriate plate geometry. It was discovered that when using PP25, the BT and HT had a considerable impact on the results, whereas when using PP08, the trimming state significantly affected the measured parameters. The HT showed higher material type dependency compared to Trim and BT. The mastic results from DSR and traditional tests are somewhat in agreement and can be related to the properties of the filler. However, determining a temperature at which |G*| achieves a particular value and its corresponding δ would be useful for the universality of the result expression.

According to the findings, a thorough standard for specimen preparation and test setup that is strictly followed can enhance the uniformity of DSR testing. Since these empirical tests are insufficient to characterise and choose material based on desired criteria in today's demanding conditions and eventually reduce maintenance work, it is advantageous to have specifications that consider more than only the penetration and softening point for bitumen and mastics.

Keywords: Bitumen, Dynamic Shear Rheometer, complex modulus, phase angle, rheology, filler, mastic, sample, specimen preparation

Supplementary bibliographical information		**Language** English
ISSN 1653-1930 Bulletin 335 Lund University, Faculty of Engineering, Department of Technology and Society		**ISBN** 978-91-8104-364-8 (print) **ISBN** 978-91-8104-365-5 (e-print)
Recipient's notes	**Number of pages** 105	Price
	Security classification	

Signature Date 2025-02-13

Dynamic Shear Rheometer for rheological investigation of bitumen in road applications

The impact of measurement technique

Maya Sheidaei

LUND
UNIVERSITY

Front coverphoto by Joacim Lundberg
Back coverphoto by Ebbe Parhamifar

‘

Faculty of Engineering
Department of Technology and Society

ISBN 978-91-8104-364-8 (print), 978-91-8104-365-5 (e-print)
ISSN 1653-1930 (2025-335-1074)

Printed in Sweden by Media-Tryck, Lund University
Lund 2025

To Poyzone & T-A.L

Table of Contents

Acknowledgment

This PhD work was carried out at the Division of Transport and Road at the Department of Technology and Society at Lund University. The author is thankful to those who have contributed with financing, research data, guidance, and moral support.

This study was financed by the Development Fund of the Swedish Construction Industry (Svenska Byggbranschens utvecklingsfond) and co-financed by Lund University and Peab Asfalt AB. All support is gratefully acknowledged. Further, Study I relied on data from round-robin tests that the Bureau de Normalisation du Pétrole announced. Study IV was done in collaboration with Lusófona University and the National Laboratory for Civil Engineering in Lisbon.

I thank my supervisor András Varhelyi for his guidance and wise counsel and my co-supervisor Anders Gudmarsson for his specialist knowledge and expertise, especially during the first two years of my PhD project. A special thanks to Michael Langfjell at Peab Asfalt AB, for his indefatigable helpfulness in providing technical and practical support.

Other contributors I would like to thank are Sven Agardh and Carl-William Palmqvist at Lund Institute of Technology (LTH), Jiqing Zhu at Swedish National Road and Transport Research Institute (VTI) for their helpful feedback, and Jenny-Ann Östlund and Mats Wendel at Peab Asfalt AB for their project management and supervision.

Finally, I want to thank the support I received from Ebbe Parhamifar, Joacim Lundberg, Pajtim Sulejmani, and other members of the Transport and Road division.

The encouragement given to me by my family has been invaluable. ☺

Abstract

The rheological properties of bituminous binders tested with a dynamic shear rheometer (DSR) as a function of loading time and temperature can more accurately represent real road situations with rising traffic loads and densities combined with climatic change. This method is more effective than traditional methods such as measuring the softening point and penetration. Complex shear modulus and phase angle which describe the materials' viscoelastic response at a given frequency and temperature can be measured using a DSR following European standard EN 14770. Even though EN 14770 primarily describes the preparation and conditioning of specimens, various steps in the DSR testing setup result in nonconformity. Therefore, an investigation was conducted to review several areas of test method practices and the underlying impact on results. Data from round-robin tests on bitumen types 20/30 in 2018 and polymer-modified bitumen 45/80-55 in 2019 and 2020, as well as from laboratory experiments on neat bitumen and modified bitumen with wax, SBS, and filler were analysed. The variability in testing conditions and how the testing conditions may affect the measures, as well as the precision of the test technique, are statistically examined. After that, a two-level, three-factor experimental design was used to investigate the effects of the oven setting temperature (HT), bonding temperature (BT) to the rheometer, and trimming state of the specimen on outcomes. Finally, DSR and conventional tests were used to examine the stiffening impact of the fillers when added to bitumen (mastics).

The results based on round-robin test data demonstrate an improved precision on measured |G*| and δ discarding data from inappropriate plate geometry. It was discovered that when using PP25, the BT and HT had a considerable impact on the results, whereas when using PP08, the trimming state significantly affected the measured parameters. The HT showed higher material type dependency compared to Trim and BT. The mastic results from DSR and traditional tests are somewhat in agreement and can be related to the properties of the filler. However, determining a temperature at which |G*| achieves a particular value and its corresponding δ would be useful for the universality of the result expression.

According to the findings, a thorough standard for specimen preparation and test setup that is strictly followed can enhance the uniformity of DSR testing. Since these empirical tests are insufficient to characterise and choose material based on desired criteria in today's demanding conditions and eventually reduce maintenance work, it is advantageous to have specifications that consider more than only the penetration and softening point for bitumen and mastics.

Popular science summary

If the material behaviour in the lab can be predicted early on, a better design of asphalt pavement becomes achievable, resulting in increased asphalt durability. Rheological measurements can provide information on how a road material will behave (flow and deform) to variations in temperature and loads. This is especially beneficial since heavier vehicles will use our roads in the future, and climate change can cause higher daily average temperatures, putting further stress on the materials in our road bodies. New binders (modified bitumen) are required to fulfil the new expectations. However, traditional empirical methods are inadequate for properly evaluating them, as they are insufficient to account for the requirements that must be met. There is also a need for a common view of test methods and a uniform way of working within the industry. The study aims to investigate the influence of variation in a number of phases of testing on bituminous binders using a Dynamic Shear Rheometer to characterise the rheological properties via Study I, II, and III. In Study IV the properties of bitumen mixed with fillers (mastics) are evaluated based on physical and mechanical assessment.

The precision results based on data in Study I clearly show the consequences of departing from the operating stiffness ranges advised by the standard. Also, the statistical analyses show that the temperature of DSR plates when mounting bitumen (BT) and the sample manufacturing temperature (HT) significantly affect the results compared to other phases. In Studies II and III, the effect of these factors and the trimming state of samples on results were investigated for neat and modified bitumen. Regardless of bitumen type, the trimming state has significant effects on the measured parameters when the parallel plate of 8-mm diameter (PP08) is used as measuring geometry. Thereby, to promote result consistency trimming might need to be mandatory in the future version of EN 14770. When using PP25, the BT and HT have a greater impact on the results. Since HT has a higher material type dependency among the studied factors, supplementary research on exact temperature settings can be conducted in the form of interlaboratory tests in the future. The stipulated BT in EN 14770 needs to be closely adhered to or updated to a smaller interval. The softening point and penetration test results are comparable with those obtained from DSR testing of mastics according to Study IV. However, DSR is required to monitor the behaviour of mastics over an extensive temperature and frequency range. The Filler-to-Bitumen content strongly affects the mastic behaviour. The relative strength of the mineral fillers to each other changes when they are replaced partially with an active filler which is attributed to the variation in interaction degree between the active filler and different fillers. Overall, the void in dry compacted filler (Rigden Voids), particle size distribution, and content of finer particles of the filler can explain the variation in properties of mastics.

Populärvetenskaplig sammanfattning

Om man redan i ett tidigt skede i labbet kan förutsäga ett materials lämplighet möjliggörs en bättre design av asfaltbeläggning, vilket medför bättre hållbarhet hos den. Reologiska mätningar kan t.ex. ge information om hur ett vägmaterial kommer svara mot t.ex. laster, vilket är mycket användbart då tyngre fordon kommer trafikera våra vägar i framtid. Vidare kan klimatförändringar medföra en högre temperatur förändringshastighet vilket ger ytterligare påfrestningar på materialen i våra vägkroppar. Nya bindemedel (modifierad bitumen) kan krävas för att uppfylla de nya förväntningarna, men de kan inte utvärderas ordentligt med traditionella, empiriska metoder eftersom de är otillräckliga för att ta hänsyn till de krav som måste uppfyllas. Det behövs också en gemensam syn på testmetoder och ett enhetligt arbetssätt inom branschen. Studien syftar till att undersöka påverkan av variation i ett antal faser av bituminösa bindemedel mättning med hjälp av en Dynamic Shear Rheometer för att karakterisera de reologiska egenskaperna. Dessutom utvärderas egenskaperna hos bitumen blandat med filler (asfaltbruk) baserat på fysisk och mekanisk bedömning.

Noggrannhetsresultaten visar tydligt konsekvenserna av att avvika från de arbetsstyvhetsintervall som rekommenderas av europeiska standarden EN 14770. De statistiska analyserna visar också att temperaturen på DSR-plattor vid montering av bitumen provkropp (BT) och provtillverkningstemperaturen (HT) signifikant påverkar resultaten jämfört med andra faser. Effekten av dessa faktorer och trimningstillståndet av provkropp på resultaten undersöktas för ren och modifierad bitumen. Oavsett bitumentyp har trimningstillståndet betydande effekter på de uppmätta parametrarna när parallellplattan med 8-mm diameter (PP08) används som mätgeometri. För att främja resultatet kan trimning därför behöva vara obligatoriskt i den framtida versionen av EN. När man använder PP25 har BT och HT en större inverkan på resultaten. Eftersom HT har ett högre materialtypsberoende bland de studerade faktorerna kan kompletterande forskning om exakt temperaturinställning göras i form av interlaboratorietest i framtiden. Den föreskrivna bindningstemperaturen (BT) i EN måste följas noga eller uppdateras till ett mindre intervall. Mjukningspunkten och penetreringstestresultaten är överens med de som erhålls från DSR-mättning av asfaltbruk. DSR krävs dock för att övervaka asfaltbruks beteende över ett omfattande temperatur- och frekvensområde. Förhållande mellan filler och bitumen påverkar kraftigt beteendet av asfaltbruk. Mineralfillers relativa styrka i förhållande till varandra förändras när de delvis ersätts med ett aktivt filler, vilket tillskrivs variationen i interaktionsgrad mellan det aktiva fyllmedel och minerala fyllmedlen. Sammantaget kan tomrummet i torrt kompakterat filler (Rigden Voids), partikelstorleksfördelning och innehåll av finare partiklar i filler förklara variationen i egenskaper hos asfaltbruk.

List of included papers

Paper I

Maya Sheidaei & Anders Gudmarsson (2023). Sample preparation techniques on dynamic shear rheometer testing: round robin tests on bitumen. Road Materials and Pavement Design.

https://doi.org/10.1080/14680629.2023.2213775

Paper II

Maya Sheidaei, Anders Gudmarsson, & Michael Langfjell (2023). Effect of Various Dynamic Shear Rheometer Testing Methods on the Measured Rheological Properties of Bitumen. Materials, vol. 16, no. 7, p. 2745, 2023.

https://doi.org/10.3390/ma16072745

Paper III

Maya Sheidaei, Jiqing Zhu, & Sven Agardh (2024). Assessing the Effect of Specimen Preparation Methods on DSR Test Results of Bitumen Using Factorial Design Analysis. Materials, vol. 17, no. 20, p. 5117, 2024.

https://doi.org/10.3390/ma17205117

Paper IV

Maya Sheidaei, Jenny-Ann Östlund, Vítor Antunes & Ana-Cristina Freire (2025). Effect of the geometrical and physical nature of filler on mastics rheological properties/ (Manuscript)

https://doi.org/ / (Manuscript)

Author's contribution to the papers

Paper I

Conceptualization, methodology, software (RStudio), data curation, formal analysis, investigation, visualization, writing original draft, writing manuscript after review & editing.

Paper II

Conceptualization, methodology, software (RheoCompass, Matlab, RStudio), data curation, formal analysis, investigation, visualization, writing original draft, writing manuscript after review & editing.

Paper III

Conceptualization, methodology, software (RheoCompass, RStudio), data curation, formal analysis, investigation, visualization, writing original draft, writing manuscript after review & editing.

Paper IV

Conceptualization, methodology, software (RheoCompass, Matlab), data curation, formal analysis, investigation, visualization, writing original draft, writing manuscript after review & editing.

Glossary of Terms/Definitions

Bitumen: A dark sticky liquid or a solid mass that acts like a liquid over long time scales with a complex chemical composition derived from crude oil.

Complex shear modulus |G*|: The amplitude ratio of the shear stress to the shear strain in harmonic sinusoidal oscillation, in Pa (EN14770:2023).

Dynamic Shear Rheometer: An equipment with different measuring geometry (cone-plate, parallel plate, concentric cylinder, etc.) that through rotational or oscillation tests can characterise the viscous and elastic behaviour of materials, including Bitumen. It measures the viscosity, transient response (relaxation modulus, creep compliance, and creep recovery), and viscoelastic properties concerning time, temperature, frequency, and stress-strain relationship.

Filler: Fine particles that are derived from crushed natural rocks, industrial products, or waste material, which pass through a 0.063 mm screen (EN1097-7:2022).

Loss modulus G″: viscous component of G*.

Mastic: A mixture of bitumen and graded fine filler. The right proportion of filler to bitumen contributes to a more desired asphalt mixture production.

Phase angle δ: phase difference between shear stress and strain in harmonic oscillation, in ° (EN14770:2023). Describes the relationship between G*, G′, and G″.

Repeatability r: test-retest reliability is often used to measure the variation in successive measurements of the same variable taken under the same conditions.

Reproducibility R: It is the degree of agreement between test results achieved by various operators, using different equipment, in separate laboratories, when testing the same material under specified conditions.

Rheology: The science of flow and deformation of time-temperature dependent materials in response to applied stress or strain. Bitumen is a viscoelastic material that exhibits viscous and elastic responses depending on the temperature and the duration of a certain applied force. Elastic deformation is reversible and returns to its original shape once the stress is removed. Plastic deformation, on the other hand, is permanent and occurs once the material surpasses its yield point. Fluids, however, do not have a yield point and flow continuously under applied stress.

Storage modulus G′: elastic component of G*.

Abbreviations

AASHTO	American Association of State Highway and Transportation Officials
A-sweep	Amplitude sweep
ASTM	American Society for Testing and Materials
BT	Bonding temperature
Comb	combination(s)
DSR	Dynamic Shear Rheometer
EN	European Standard
HT	Heating Temperature
LVE	linear viscoelastic
Mfg.	manufacturing
PMB	Polymer modified bitumen
PP	Parallel Plate
PG	Performance Grade
RTFO	Rolling Thin Film Oven
RV	Rigden voids
SHRP	Strategic Highway Research Program
T-f-sweep	Temperature-frequency-sweeps
VG	Viscosity Grade

1 Introduction

The increase in traffic loading combined with climate change has accelerated pavement degradation, leading to increased annual investments in construction, maintenance, and repairs of roads. This situation necessitates more careful consideration of design and material selection. Existing European Standards such as EN 12591 and EN 14023 provide a framework for specifying various properties and relevant test methods for bitumen, suitable for use in the construction and maintenance of roads, and other paved areas, along with requirements for conformity evaluation. In Sweden, the quality of bitumen is currently defined using empirical requirements for each of its constituents, including properties like needle penetration, ring and ball softening point, and the Fraass breaking point test. Although these tests are straightforward, they do not accurately reflect the actual stress-strain behaviour of materials at different temperatures and frequencies. The Strategic Highway Research Program (SHRP) that was carried out in the U.S.A. between 1988 and 1993 (Anderson et al., 1994; Petersen et al., 1994) has led to the Superpave mix design method. This in turn increased interest in performance-based methods for characterizing bituminous binders, among other things. The new approaches distinguish the rheological properties of bituminous binders as a function of loading time and temperature to simulate actual behaviour in practice rather than empirical properties such as softening point temperature and penetration value, among others. The complex shear modulus (G*) is one of the most used rheological properties for performing bitumen analysis and modelling, which can be defined as $G^* = |G^*| e^{i\delta}$ The dynamic shear modulus |G*| describes the material's stiffness, and phase angle δ, describes the extent of viscous and elastic behaviour of the material at a given frequency and temperature, and i is the imaginary unit ($i^2 = -1$). A dynamic shear rheometer (DSR) can be used to obtain the |G*| and δ of bitumen following several testing standards (AASHTO-T315, 2022; ASTM-D7175, 2023; EN14770, 2023).

However, there is concern about ensuring conformity between laboratories on sample preparation and or testing methods which may lead to discrepancies in results. The procedure for preparing and conditioning the specimens is primarily specified in EN 14770, utilized in Sweden and other European countries. It appears there is so much leeway in the standard that operators have too much latitude to influence the test results when running the tests, implying the need to clarify factors related to the set-up of the laboratory testing that possibly can affect the outcomes.

Blending pure bitumen with additives which is essential to achieve desired bitumen qualities and improve performance in a variety of traffic and temperature conditions makes the DSR testing of modified bitumen more sensitive to variations in the test set-up than the testing of neat bitumen (Zhu et al., 2017; Soenen et al., 2008; Airey, 2003). Various studies have shown how variables such as the limit of linear viscoelasticity (Airey et al., 2002b), the equipment sensitivity to measure torque (Divya and Krishnan, 2019), and the sample manufacturing method (Airey et al., 2017) affect the consistency of results. The dependence of bitumen rheological properties on the impact of various plate geometries and gap sizes was also investigated in a different study with inconsistent results due to variation of susceptibility to changes for different studied materials (Liu et al., 2020; Carswell et al., 1998; Singh et al., 2016). Other research has emphasized the importance of applying the same thermal treatment to achieve acceptable precision on the complex modulus, phase angle, and SHRP parameter ($G^*/\sin \delta$) (Soenen et al., 2005; Mouillet et al., 2004; Eckmann et al., 2012). Numerous investigations emphasized the overfilling or underfilling of the gap and concerns with reproducibility since the DSR does not accurately capture the sample diameter in the low-temperature test (Laukkanen, 2017; Alisov, 2017). There for improvements on testing method should be made.

1.1 Literature review

The following section primarily reviews the influence of various stages of sample conditioning and preparation on the rheological properties of bitumen using a Dynamic Shear Rheometer with parallel plates. The first two sections are focused on bitumen in terms of definition and measurement methods. Furthermore, the most often used traditional equipment for measuring bitumen rheology, the dynamic shear rheometer (DSR) with parallel plate, is briefly discussed. An overview of the linear viscoelastic concept is also provided to help understand the viscoelastic behaviour of bitumen. The last five sections of the literature review before the summary discuss the effect of the following sample preparation and test circumstances phases on the rheological parameters obtained by DSR:

- Plate Geometry,
- Pre-heating time and temperature of bitumen,
- Sample Manufacturing,
- Storage condition of the manufactured sample,
- DSR temperature when mounting the sample.

1.1.1 Bitumen

The term "bitumen" is commonly used in Europe and is equivalent to "asphalt" or "asphalt binder" in the U.S.A. Outside North America, "asphalt" refers to mixes of bitumen and mineral particles. Bitumen is one of the oldest building and road engineering materials and was widely used in all early civilizations, including Babylonia, Mesopotamia, Sumeria, Chaldea, Mohenjo-Daro and Harappa, Phoenicia, China, and later, Greece and Rome (Abraham, 1918; Murali Krishnan and and Rajagopal, 2003; Boulangé et al., 2013). Bitumen's primary properties, including adhesivity, waterproofing, thermoplasticity, durability, ease of modification, reusability, and recyclability, make it a suitable construction and engineering material. Around 120 million tonnes of bitumen were consumed globally in 2022 (IBEF, 2024). Approximately 85% of the bitumen produced worldwide is used to make asphalt mixtures for the pavement industry, which among others includes parking lots, airport runways, and roads.

Bitumen is defined as a "virtually non-volatile, adhesive and waterproofing material derived from crude petroleum, present in natural asphalt, which is completely or nearly completely soluble in toluene and very viscous or nearly solid at ambient temperatures" by the European specification (EN12597, 2024). It is composed mostly of hydrocarbon molecules with small amounts of heteroatoms, which can significantly affect bitumen characteristics. Heavy metals, in addition to heteroatoms, can exist in small contents. Bitumen is a complex material whose properties change depending on the crude oil source, production method, additives, and other chemical-physical treatments (Zakar, 1971; Halstead, 1984). The complicated chemical composition of bitumen makes precise identification and classification of all these forms difficult. The separation of bitumen elements based on polarity and solubility into a saturated, aromatic, resin, and asphaltene fraction (SARA) is a widely established analytical method (Corbett, 1969; Lesueur, 2009; ASTM-D4124, 2018). The ratio of resins to asphaltenes determines whether the bitumen is soluble (SOL) or gelatinous (GEL) (Figure 1) (Whiteoak et al., 1990). Aromatics, which comprise the bitumen's lowest molecular weight naphthenic aromatic compounds, represent the majority of the dispersion medium for the bitumen's body asphaltenes and impact its adhesion and ductile qualities, while saturates and resins influence its viscosity and flow (Halstead, 1984).

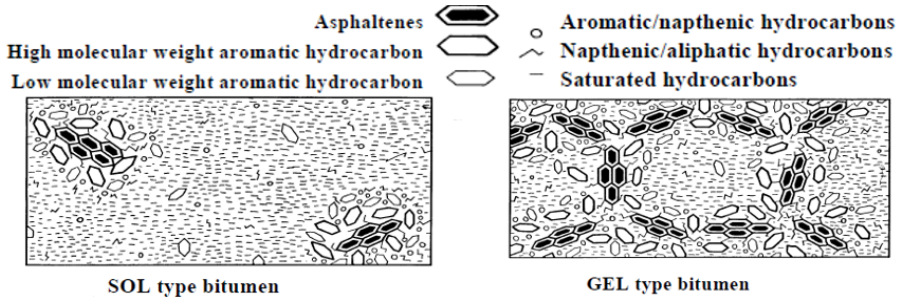

Figure 1. Schematic representation of SOL and GEL-type bitumen (Whiteoak et al., 1990).

1.1.2 DSR

Bitumen's viscoelastic behaviour is too complex to be represented by only traditional consistency metrics like penetration and softening points. Rheology is the study of material flow and deformation characteristics. In other words, bitumen rheology studies the relationship between stress and strain in bitumen. The necessity for complete bitumen characterization has long been recognized. The term dynamic shear rheometer (DSR) was used in the 1990s to describe rheometers used in the asphalt industry. A rheometer can be used to perform a variety of fundamental rheology experiments, including rotational, oscillatory, creep, and stress relaxation tests. Additionally, the viscoelastic characteristics can be determined. Rheometers can collect data such as torque, angular frequency, rotational speed, angular velocity, and frequency, which can then be processed and converted to rheological parameters such as shear rate, shear strain, and shear stress, to calculate complex shear modulus |G*| and phase angle δ, for instance. Plots can then be used to illustrate the calculated data. When a viscoelastic substance, such as bitumen, is stressed, some of the distortion is recovered, but some remains. Thus, it is critical to test within a non-destructive range of specimens at different temperatures and frequencies in oscillatory testing (small amplitude oscillatory shear). The phase angle is the angle at which the harmonic oscillating strain response lags behind the sinusoidal stress. The material's elastic and viscous response dictates the phase angle value. It is 0° for elastic materials and 90° for viscous materials. As a result, the phase angle of bitumen as a viscoelastic material ranges from 0° to 90°.

In the DSR test, bitumen is sandwiched between two parallel plates, which can be rotated at different frequencies (Goodrich, 1991). During DSR testing, the responding strain/stress is measured by applying a torque to a disc-shaped bituminous sample in response to the applied stress/strain. In the strain-controlled mode, a sinusoidal strain with constant amplitude is applied to the specimen, whereas in the stress-controlled mode, the specimen is exposed to a sinusoidal stress with constant amplitude. Figure 2 depicts oscillatory shear readings using a DSR test with a parallel plate system geometry.

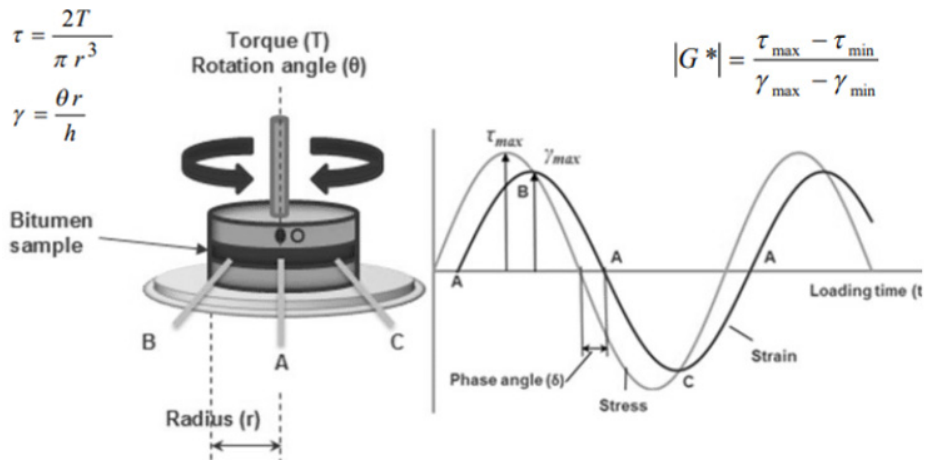

Figure 2. Dynamic shear measurements using parallel plate geometry (Mukandila et al., 2015).

The following equations are used for calculating strain and stress in this instrument on the edge of the plate (Stroup-Gardiner and Newcomb, 1995; Airey and Brown, 1998): where h is the gap between plates (mm), r is the plate radius (mm), T is the applied torque (N-m), and θ is the rotation angle (radians). The absolute complex modulus (G*) was measured based on shear strain (γ) and shear stress (τ). In the parallel plate geometry system, we have a non-uniform strain rate moving from r=0 in the centre to r=max in the periphery, and from h=0 in the bottom to h=max at the top. However, the parallel plate is suitable for testing the bituminous mixture containing particles up to 100 μm (10 times smaller than the gap height of 1 mm according to ISO 3219-2).

$\gamma = \theta\, r/\, h$

$\tau = 2T/\pi\, r^3$

$| G^*(\omega) | = \tau\, max/\gamma\, max$

1.1.3 Linear viscoelastic (LVE) region

Linear elasticity is the fundamental basic material model, where stress is proportional to strain (Hooke's law). However, when bitumen is dynamically tested as a viscoelastic material, two behaviour domains emerge: the linear domain and the non-linear domain (Boussad et al., 1996). Non-linearity responses of bitumen generally become minimal at strain amplitudes less than a particular limit (LVE limit), and the material behaviour can then be effectively represented by a linear viscoelastic approximation. Most bitumen behaviour is non-linear under large traffic loads or extreme environmental conditions (Bahia et al., 1999), where bitumen is exposed to large stress or strain. However, determining the linear limit

is important before doing oscillatory tests such as T-f-sweep tests, which test material over a wide range of temperatures and frequencies using well-established linear viscoelastic models.

Rheological properties can be obtained from the conventional frequency sweep at different temperatures according to EN 14770 or as suggested in several studies, with temperature ramping at a fixed frequency, which takes less time (Porot et al., 2020). Since time-temperature dependency is only valid in the linear region of behaviour, determining the linear limit is required to use the time-temperature superposition concept to interpret the results. The linear region can be found from a strain amplitude sweep test, in which the applied strain is increased during the test and then the linear region can be found by plotting complex modulus versus shear strain.

According to SHRP, the linear region can be defined as the point beyond which the measured value of complex modulus decreases to 95% of its maximum value. According to EN 14770 to remain in the linear range, the value of G′ and G″ must not differ by more than 5 % of the initial value over the stress or strain range chosen. The initial value can be taken as the intercept of a regression line fitted to the first measured values. It has been observed that testing within the strain range of 0.5% and 10% lies within the linear range for most of the binders, while for PMBs the range is much less (EN14770, 2012). Nevertheless, according to Rahimzadeh (2002), the LVE stress and strain limits were higher than the SHRP recommended stress and strain levels. There was no significant reduction of the linearity range for the modified bitumen, while the strain and stress LVE limits for the studied multigrade 35/50 bitumen were somewhat lower than those discovered for the other four studied bitumen (50 pen unmodified, EVA modified, and two SBS modified). Additionally observed, all the binders demonstrated dominant elastic behaviour in the first region, high frequency (low temperatures), with slight variances in the viscoelastic characteristics of the bitumen. At intermediate frequencies (temperature), the SBS PMBs began to exhibit viscoelastic variations from the other binders. This was especially apparent in the phase angle master curves, where the SBS polymers began to dramatically increase the elasticity of the modified binders. Except for the SBS PMBs, all bitumen began to lose elasticity and approach a viscous state at very low frequencies (high temperatures).

1.1.4 Plate geometry

According to a study (Scholz and Brown, 1996), using the DSR is a useful way to learn more about how bitumen behaves in thin films subjected (plate gap) to shear stresses. However, the bitumen film thickness coating aggregates in actual asphalt mixtures can range from a few microns to a few millimetres (Mack, 1957; Wu et al., 2020; Wu et al., 2021).

According to EN 14770, the operational ranges are as follows: at low temperature, a plate with a diameter of 8 mm and a gap size of 2 mm is preferred (suitable for stiffnesses |G*| in the range 100 kPa to 10 MPa), while at intermediate to high temperature, a 25 mm plate and a gap of 1 mm is preferred (suitable for stiffnesses in the range 1 kPa to 100 kPa). According to Airey et al. (2017) utilizing a 25 mm plate for a complex modulus larger than 100 kPa overestimates elastic response and underestimates bitumen stiffness.

In a different study, the effects of plate geometry and gap size were explored concerning two viscosity-graded neat bitumen VG10 and VG30, as well as two modified bitumen (VG10 + SBS and VG10 + EVA). Gap sizes of 1, 2, and 3 mm for plates with a 25 mm diameter and gap sizes of 1 and 2 mm for plates with an 8 mm diameter were investigated. At the higher test temperatures (40, 60, and 70 °C), a higher gap resulted in a lower complex modulus and phase angle, but the opposite was true at the lower test temperatures (10, 20, and 30 °C). According to the study, 8mm diameter plates generate higher values for phase angles at higher temperatures (Singh et al., 2016).

Liu et al. (2020) have also investigated how the size of the gap between the plates affects the results. The outcome shows that for the tested neat bitumen (penetration at 25 °C: 70.6 1/10 mm; ring and ball softening point: 47.6 °C), the complex modulus tends to decrease when the gap size reduces from 1mm to 10 µm. The modified bitumen (PG-76 + 4% SBS) showed the same trend but with a different sensitivity. It exhibits more viscous behaviour when the gap size is reduced from 250 to 50 m, in contrast to neat bitumen, which exhibits more elastic behaviour.

The effect of different gap sizes on two neat performance graded bitumen (PG58–28) from different sources, two elastomers modified (SBS), four plastomer modified bitumen, and two oxidized bitumen were all evaluated by (Zhai et al., 2000). It was discovered that the G* falls constantly when the gap size decreases from 1mm to 10 µm. The bitumen modified with elastomers was the most susceptible to changes in gap size, while the oxidized bitumen showed the least sensitivity to gap changes. However, for the majority of bitumen, the phase angle remains constant as the gap size varies.

Another study shows that based on the fitted master curves of the G* and δ at a reference temperature using the 2S2P1D (two springs, two parabolic elements, and one dashpot) model, similar rheological properties can be obtained with both the 1.75 mm and 3 mm gap size with 4 mm geometry for five distinct types of bitumen (50/70, 70/100, SBS modified, and short-term and long-term aged 70/100). However, the sample preparation procedure with the 3 mm gap appears to generate more consistent samples than the 1.75 mm sample preparation, leading to higher repeatability (Wang et al., 2019).

1.1.5 Pre-heating time and temperature of bitumen

Previous studies show that for the SBS-modified binder, the pouring or homogenisation temperature of the binder affects rheological tests more than storage time. The result of a test conducted at temperatures between 120 °C and 200 °C on two elastomer-modified samples (50/70 + 3.5% SBS and 70/100 + 5% SBS), shows that the G* increases by pouring temperature, and for lower pouring temperatures viscosity η* stabilises as frequency decreases from 10Hz toward 0.001Hz when tested at 50 °C (Soenen et al., 2005). Also, another study shows the influence of pouring temperature and oven setting duration for sample manufacturing before testing on the rheological properties of bitumen. It investigates a pure performance graded bitumen PG 64-22 and two PMBs PG 70–22 and PG 76-22 in original, and after short and long-time ageing processes at temperatures of 143 °C and 185 °C for a duration of 1/2, 2 and 4 h. result indicate an increase in the G* by an increase in pouring temperature for all ageing condition for almost all the tested material. Phase angle showed more dependency on heating duration than temperature compared to the G*. The study recommends 2 hours of oven heating at 143 °C for sample manufacturing, taking into account the sample's short-term ageing index and absolute decline in complex viscosity (Dessouky et al., 2011). Furthermore, Büchner et al. (2020) revealed that most of the 20 European road asphalt laboratories that took part in an interlaboratory study heated pure bitumen, 50/70 (penetration at 25 °C: 64 1/10 mm; ring and ball softening point: 51.3 °C), and polymer-modified bitumen 25/55-55 (penetration at 25 °C: 46 1/10 mm; ring and ball softening point: 58.0 °C) between 90 °C and 180 °C for the manufacturing of samples for DSR testing. A heating temperature of about 150 °C was used by the majority of participants. However, only a small number of participants chose to vary the heating temperature based on the type of binder, choosing a slightly lower temperature for the neat bitumen than the polymer modified. In a different study, an oven heating temperature of approximately the softening point temperature plus 100 °C is applied to all of the distinct types of studied bitumen (unmodified, elastomer, and plastomer modified)(Airey et al., 2017).

Previous bitumen sample preparation in EN 12594 (2014) states that modified bitumen heating within 180-200 °C may be needed, but it should not be heated above 200 °C, and heating unaged neat bitumen to 100 °C above softening point temperatures should be avoided. EN 14770 (2012) specifies a temperature of (85±5) °C above the softening point but not higher than 180 °C for neat bitumen. According to the previous version of mentioned standards, the duration of melting, homogenising, and moulding should not exceed 135 min, but reheating time differs between a maximum of 30, 60, or 120 min depending on the mass of sub-samples. Limits in the recently released EN 12594 (2024) have been modified to provide more exact conditions for heating time and temperatures and guarantee compliance with the most recent release of EN 14770 (2023) in clause 7.2. Current bitumen

sample preparation specifies the maximum heating temperature of (85±5) °C above the softening point, and for modified bitumen (190±5) °C regardless of the softening point. The heating duration for sub-samples weighing less than 50 g should be limited to 15 minutes, according to the most recent version.

1.1.6 Specimen manufacturing

According to EN 14770 (2012), specimens can be manufactured in 3 ways, poured into moulds or sheets, directly onto plates, and applied vials (Figure 3). Using a vial is not recommended for polymer-modified binders, which can be due to the potential risk of molecule shape change under shear load when it is squeezed out from the vial. A previous study shows that the repeatability of the hot pour onto plate method is slightly higher than the repeatability of using a mould (silicone) and weighing methods, which involves pouring a pre-weighted amount of hot bitumen directly onto a plate without trimming before testing. The G* obtained by silicone mould is slightly higher, which follows with direct hot pour method and weighing method (Airey et al., 2017). However, directly onto plates and vials, methods are removed from the latest version of EN 14770 (2023).

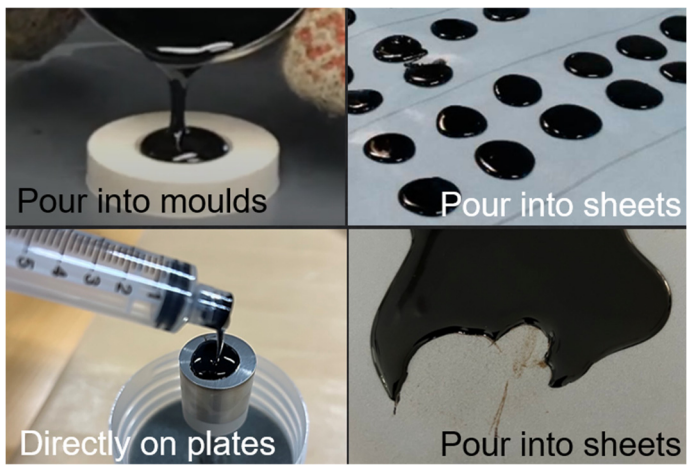

Figure 3. Sample manufacturing methods.

1.1.7 Storage condition of the manufactured specimen

Previous studies reveal that the waiting time at room temperature between the bitumen sample casting and the start of the test procedure does not have a significant impact on the test result for pure bitumen and styrene-butadiene-styrene (SBS)

modified binder (Soenen et al., 2006). However, for waxy bitumen and special polymer-modified binders, different interpretations can be represented, which demonstrates the importance of reaching bitumen's full equilibrium when considering slow isothermal crystallisation during storage for polymer-modified binders. For instance, for the plastomer-modified bitumen, ethylene-vinyl acetate (EVA), about 6° increase is observed for the phase angle (δ) as frequency decreases from 10Hz toward 0.1Hz over a maximum of 24 hours delay. However, no effect was observed for modulus (Eckmann et al., 2012). Another study shows that the complex viscosity ($\eta^* = G^*(\omega)/\omega$) changes more than a decade at 0.001 Hz for the EVA-modified binder (B70/100+5 % EVA). This influence is also observed in the phase angle, which decreases at 0.001 Hz over the waiting time drastically (Soenen et al., 2006).

According to EN 14770 (2012), the minimum storage periods before specimen de-moulding and testing were 2 h for neat bitumen, 12 h for PMB, and no more than 3 days regardless of bitumen type. However, the most recent version of EN 14770 (2023) specifies a minimum storage time of 30 min, 12 h for modified bitumen that exhibits crystallisation processes, and a maximum of 2 weeks.

1.1.8 DSR temperature when mounting the specimen

When placing a test sample onto the DSR a high temperature of the parallel plates is, to some extent, essential for making secure bonding between binder and plate, especially true for viscous binders like polymer-modified binders. However, an upper limit needs to be chosen carefully to avoid ageing the sample before testing. A study shows that, for the tested plastomer-modified binder, the bonding at either high (80 °C) or low (30 °C) temperatures does not have a significant impact on the measured stiffness modulus |G*|. However, lower phase angles have been observed for the sample that was bonded at a higher temperature. It was believed that there may have been other factors at play in addition to the higher bonding temperature, such as the initial reheating and the extended interval between bonding and testing for the specimen mounted at 80 °C. (Eckmann et al., 2012). Airey et al. (2017) theorize that the slightly higher G* for the moulded sample method compared to the hot pour method may be brought on by differing temperatures applied when samples are mounted onto the DSR. Bitumen is viscous and above its softening point in the hot pure method, but elastic and at room temperature in the silicone mould method, which can expose the sample to internal stress when it is pressed between the plates before testing. However, it appeared that the tested neat bitumen with a lower softening point compared to the SBS-modified bitumen had a smaller effect which can be due to its more viscous behaviour at room temperature when placed in the DSR. Specimen mounting temperatures applied by participants of an interlaboratory test for bitumen type 50/70 with softening points of 51.3 °C and 25/55–55 with softening points of 58.0 °C showed significant deviations between different

participants ranging from 10 °C to 90 °C with a slightly higher temperature selected for the PMB when the T-f-sweep tests were performed at a temperature range between –30 °C to 0 °C (Büchner et al., 2020). However, the study did not investigate the consequences of this variation in bonding temperature.

According to the standard EN 14770 (2012), the temperature of both the upper and lower plate of the rheometer needs to be set to a maximum of the binder's softening point, namely plus (20 ± 5) °C, or at (90 ± 5) °C, whichever is the lower, for at least 30 min to facilitate acceptable bonding of the test sample to the plates. Also, it is understood that a manufactured specimen can be placed in a refrigerator for a maximum of 30 min at about 5 °C before the de-moulding and bonding of the sample material to the DSR device. However, the most recent version of EN 14770 (2023) specifies the bonding temperature of 5 °C to 20 °C above the softening point and keeps it at least for 5 min after reaching the selected temperature.

1.1.9 Filler

An asphalt mixture consists of aggregates, bitumen, and additives, exhibiting viscoelastic behaviour influenced by the properties of each constituent material. Fillers, which enhance the adhesion between mixture components, are defined as fine particles that pass through a 0.063 mm sieve (EN1097-7, 2022). Fillers can be sourced from crushed natural rocks, industrial by-products, or waste materials (Chen et al., 2022). It improves the adhesion properties of the bituminous mastic that depends on the physicochemical properties of the filler (Wang et al., 2018), filler's morphology, composition, friction between particles, behaviour under moisture and temperature, among others (Liu et al., 2018a). It also improves the mechanical response of the asphalt mixture to traffic and changes in temperature (Guo et al., 2017; Miró et al., 2017). The surface energy, chemical reaction, molecular orientation, and mechanical contact are the four mechanisms that have been adopted to explain the interaction between bitumen mastic and mineral aggregate (Wasilewska et al., 2017; Liu et al., 2018b; Mohammed et al., 2018; Yi et al., 2018; Huang et al., 2021; E et al., 2023).

While the properties of filler-bitumen are crucial for the development of mastic as a binder, research in this area is relatively sparse compared to studies focusing solely on bitumen modification. This is despite the fact that mastic plays a significant role in the adhesion of aggregates (Micaelo et al., 2017). The destresses in asphalt mixtures, which arise from failures at the filler-bitumen interface, are largely attributed to the characteristics of the filler particles (Veytskin et al., 2015).

There are no standardized tests specified for mastic testing. The delta ring and ball difference method mentioned in EN 13179-1:2013 is seldom used (at least in Sweden) to measure the increase in the softening point of a bitumen-filler aggregate

mixture with a volumetric content of F/B (37.5 / 62.5) compared to the softening point of the bitumen alone.

The dynamic mechanical analysis of the interaction is one of the most promising approaches which studies the interfacial behaviour indirectly and is based on the rheology property of mastic. Guo et al. (2017) proposed an interface interaction parameter based on the classical LVE theory model and the modified Palierne emulsion model. It was found that the proposed indicator can represent the interaction between bitumen and filler exactly (Rochlani et al., 2021a). The C interaction parameter of Guo et al. (2017) is also employed in this research to evaluate the interaction between bitumen and different fillers rather than only $\Delta T_{R\&B}$ for the stiffening impact of fillers.

1.2 Summary of the findings of the literature review

Different phases of preparation and conditioning of samples on DSR testing were investigated in different studies. Frequency sweep tests were performed in different ranges of temperatures and strain levels to measure the complex modulus and phase angle to describe the rheological behaviour of bitumen under different conditions.

Testing within the LVE regime of the material is essential to model the bitumen rheological behaviour. The LVE limit for all bituminous increases with test temperature, though with varying degrees of temperature dependence. Using an inappropriate plate diameter can also over or underestimate the elastic and stiffness response of the bitumen. Thus, to prevent measuring under non-linearity conditions and over or underestimating the rheological parameters, it is required to determine the LVE range and take the complex modulus value into account when selecting plate geometry (100 kPa – 10 MPa for PP08 and 1 kPa – 100 kPa limit for PP25) for all planned test temperatures. Conclusions about the effect of gap size on bitumen rheological properties among research were contradictory, which could be attributed to material and test condition dependency. According to the findings of the studies, modified bitumen is more susceptible to gap change than unmodified and aged bitumen. However, the complex shear modulus appeared more sensitive to gap size variation than the phase angle. Complex modules were shown to increase as gap size increased, except for the tested material at higher temperatures. Therefore, it is crucial to maintain the standard recommended gap size of 2 mm with PP08 and 1 mm with PP25 to avoid gap size dependency on outcomes. Sample manufacturing methods can be generally divided into three ways. The results showed that the mould and weighing mould methods produced slightly higher and lower G* values than the hot pour method and that the repeatability of each method varied only slightly. The effect of pouring temperature and oven setting period on sample fabrication demonstrates that higher temperatures can increase G*.

However, interlaboratory research indicates that operators use a diverse range of temperatures, highlighting the need for deeper research with different types of materials in the subject. In contrast to plastomer-modified bitumen, the waiting time between bitumen sample casting and the start of the test method does not have a major impact on the test outcome for neat and SBS-modified bitumen. Nevertheless, viscoelasticity appears to be more susceptible to storage time than stiffness. In the case of bonding temperature, the DSR plates' temperature when mounting the samples appears to have no major impact on stiffness modulus G*, but rather on phase angle. A slightly higher G* was observed for the moulded specimen than with the hot pure method, which was mounted onto DSR at a lower temperature than the hot pure approach.

1.3 Identified research gap and problem

One reason for the lack of study on the impact of measurement technique with DSR in practice is that in many European countries, penetration-based bitumen specification is more common than performance-based specification based on DSR test results for the asphalt industry, despite research interest in DSR testing to facilitate and accelerate this transition (Zhu et al., 2021). In testing bituminous binders with DSR several factors could affect the measurements of the rheological properties. For example, several studies show the importance of having the same thermal treatment to achieve an acceptable precision on the complex modulus, phase angle, and SHRP parameter (G*/sin δ) when testing in low frequency and for polymer-modified bitumens (PMBs) during the sample preparation and testing phase (Mouillet et al., 2004; Soenen et al., 2005; Eckmann et al., 2012). The effect of different plate diameters and the gap size between the plates have been presented in earlier studies. It was shown that a higher gap size leads to a decreased value of the complex modulus and phase angle at higher temperatures (Carswell et al., 1998; Singh et al., 2016; Liu et al., 2020). Another study presented differing values from DSR tests using three different sample preparation methods (Airey et al., 2002a). Some studies demonstrate that the sensitivity of the equipment to measure torque (Divya and Krishnan, 2018), and the limit of linear viscoelasticity (Airey et al., 2002b), should be considered to obtain a consistent result from DSR testing. The testing of polymer-modified bitumens using a DSR normally leads to greater variation in the result compared to testing of unmodified bitumen (Airey and Hunter, 2003). The morphology of the PMB increases the challenge of limiting the variation in the testing (Airey, 2003; Soenen et al., 2008; Zhu et al., 2017). The European Standard for DSR determination of the rheological parameters of bitumen and bituminous binders EN 14770 released in 2012 allows a broad interpretation, various test circumstances, and sample preparation methods such as temperature and duration selection and optional trimming, by different laboratories, making it

challenging to achieve good consistency in results. The recent release of EN 14770 in 2023 has improved some details on heating temperature and duration, specimen storage time, and bonding temperature as mentioned in earlier sub-sections, an even better precision may be achievable with stricter instruction for instance when it comes to trimming or the range limits. However, past studies were limited in either the size or scope of their data; they focused only on one factor per study and are often performed in one laboratory making it difficult to study the precision of the studied factor. The studies that evaluate multiple factors simultaneously with their potential interaction effects between the factors at a laboratory-controlled condition, as well as the inclusion of the data on interpretations of the current EN (practices) from different asphalt laboratories to identify the steps that may need to be more strictly defined are lacking. Filling this gap can help improve the current standard in the future version and highlight the importance of operators following them closely to enhance consistency in the DSR test results before specifications based on DSR test results become a requirement from the Swedish Transport Administration among others for the asphalt industry nationally and internationally.

Furthermore, while there are numerous standards for bitumen testing, there are no standards in Europe for mastics (Rochlani et al., 2021b), or tests that can adequately predict the performance of filler mixed with bitumen (Grabowski and Wilanowicz, 2008). Even now, as technology advances, the behaviour of mastic is overlooked, and the applicability of Superpave methods (Lagos-Varas et al., 2020) and the Time-temperature superposition principle (Tan and Guo, 2013) may need to be investigated.

2 Aim and Research Questions

This PhD research aims to assess the methods for testing bitumen with a DSR in the LVE region and develop a simple instruction that can describe DSR testing of bitumen with an acceptable degree of precision especially for the beginner. This project will assist in achieving the aim of Svenska Byggbranschens Utvecklingsfond and guidelines by creating better conditions for entrepreneurs and the industry to ensure sample preparation and test procedure conformance among laboratories rather than following their interpretation of EN 14770. The first goal is to review the existing sample preparation and conditioning methods for testing the rheological properties of bitumen and their potential impact on measured data with DSR according to existing method EN 14770. The precision of the DSR testing will also be evaluated. The second goal is to determine how three selected conditioning and sample preparation phases can affect complex modulus and phase angle. The third goal is to investigate the effect of technique variations on measured parameters with DSR when modified bitumen is involved. The final goal is to test the rheological properties of bitumen mixed with fillers called mastic with DSR applying the suitable practices following the findings of previous studies in this research project and comparing results with traditional tests such as softening point and Penetration.

2.1 Research Questions

The research questions (RQs) listed below are addressed in this thesis. The motivation for each research question and how they complement each other to achieve the goals of this PhD research are then described.

Ultimately, these research questions (RQ1–RQ4) will provide some guidance on conducting the tests for better result consistency and suggestions for future work that could be developed based on this research. This effort is critical to complete before the Swedish Transport Administration, like many other countries, requires the asphalt industry to follow DSR test results-based specifications.

2.1.1 Research Question I (RQ1):

What factors need to be considered when testing bitumen with DSR to achieve a reliable result?

This research question is based on the findings of the literature review that show the different phases of DSR testing affect the measured parameters, however, to find which phases are more critical all are investigated in one study (study I). This leads to scrutinising utilized practices, techniques, and EN 14770:2012 interpretations in sample preparation and test setup when testing with DSR. This is to increase our understanding of various factors that need to be considered when investigating the rheological properties of the bituminous binders to achieve a method (protocol) that leads to reliable results. This screening is achievable through investigation of data from wide-ranging RR tests over three years conducted within the European asphalt laboratories, and a review of the existing literature. Answering this research question will help to uncover the importance of different phases of measuring the rheological properties of bitumen with DSR using the existing EN method. This, in turn, identifies areas that may still be unclear in the EN method and suggests some directions for future research.

2.1.2 Research Question II (RQ2):

How do the selected factors (heating temperature for manufacturing sample, bonding temperature, and trimming) affect the measured rheological parameters of unmodified bitumen with DSR?

This research question is based on the findings of Study I and seeks to determine the effect of three selected factors by quantifying their impact on rheological parameters |G*| and δ Two factors heating temperature (HT) for sample manufacturing and bonding temperature (BT) were selected after quantifying the effect of a list of factors from multiple datasets derived from RR tests studied before this in study I. The third-factor radial trimming operation of the sample was of interest since trimming exposes the sample to an ignorable intervention and no information was available in the analysed dataset. Quantifying the impact of the studied factors varying between two levels will reveal the relationship between the factors and outcomes (|G*| and δ), facilitating the selection of a suitable level for studied factors aside from the importance of the factors for enhanced result consistency. Thus, a two-level, three-factor experimental design is performed to solve the research question, which involves an interpretable and statistical model to gain insights into the underlying relationship between studied factors the oven setting temperature (HT), bonding temperature (BT) to the rheometer, and trimming operation (Trim) on measured rheological parameters |G*| and δ.

2.1.3 Research Question III (RQ3):

How do heating temperature for the manufacturing sample, bonding temperature, and trimming affect modified bitumen's measured rheological parameters with DSR?

The motivation behind this research question is based on the findings of Study I and Study II, which show how the chosen stages of testing with DSR affect outcomes. The aim of RQ3 is similar to RQ2, but it involves modified bitumen. To be precise, study III aims to answer RQ3 and will incorporate relevant input variables identified from RQ1 and RQ2 to design the experimental work. The results will be reported according to EN 14770:2023 with parameters TX, a temperature at which |G*| equals certain values ($T_{|G^*|}$) and their respective phase angles δ_{TX} aside from |G*| and δ following EN 14770:2012 which is applied in RQ1 and RQ2.

The inclusion of modified bitumen in study III was critical to this thesis work because the idea of transitioning from traditional tests such as softening point (ring and ball method) to DSR tests, which simulate the reality better in the case of temperature and load variation, becomes more critical as demand for modified bitumen increases due to climate and traffic load changes. This research question (RQ3) seeks to answer how the three following factors affect the rheological parameters with DSR according to EN 14770:2023 in the case of neat and modified bitumen: (1) the pre-heating temperature (HT) for manufacturing specimens in a mould, (2) the bonding temperature (BT) at which the specimen bonds onto the DSR, and (3) the radial trimming (Trim) operation of the specimen. These factors were selected based on a prior screening of data from a set of interlaboratory tests among European laboratories in Study I to answer RQ1. To answer the RQ1, Study I investigate the equipment brand, specimen manufacturing technique, storage duration of specimens, pre-heating temperature and duration for manufacturing specimens, the temperature at which the specimen bonds to the DSR, equilibrium duration, and linear viscoelastic range. Its findings demonstrated that, compared to other steps, the bonding temperature (BT) had a small but significant impact on more tested conditions. Additionally, the pre-heating temperature (HT) of bitumen used to manufacture the specimen must be carefully selected. Furthermore, the radial trimming (Trim) of excess material, which exposes the specimen to a large intervention was of interest due to its significant effect on outcomes discovered in study II performed to answer RQ2.

2.1.4 Research Question IV (RQ4):

How do the rheological properties of mastic (bitumen mixed with filler) measured with DSR relate to the type and content of fillers, and can these results be validated using the physical properties of mastic obtained from traditional tests?

The reason for RQ4 is to evaluate results from DSR when bitumen is modified with a filler and tested according to findings of the earlier studies in this thesis and compare them with results from traditional tests such as penetration and softening point (ring and ball method). This research question is designed to unveil how the rheological behaviour of mastic (bitumen mixed with filler) with varying filler content and geometrical and physical properties can be correlated with the obtained rheological parameter of mastic using DSR. The results of the DSR test will be reported according to the current standard method EN 14770:2023 and the inputs from earlier research questions (RQ1–RQ3) will be applied to perform the DSR tests.

2.2 Structure of this thesis

The objectives were reached through 4 studies. Figure 4 illustrates a schematic framework of the PhD project.

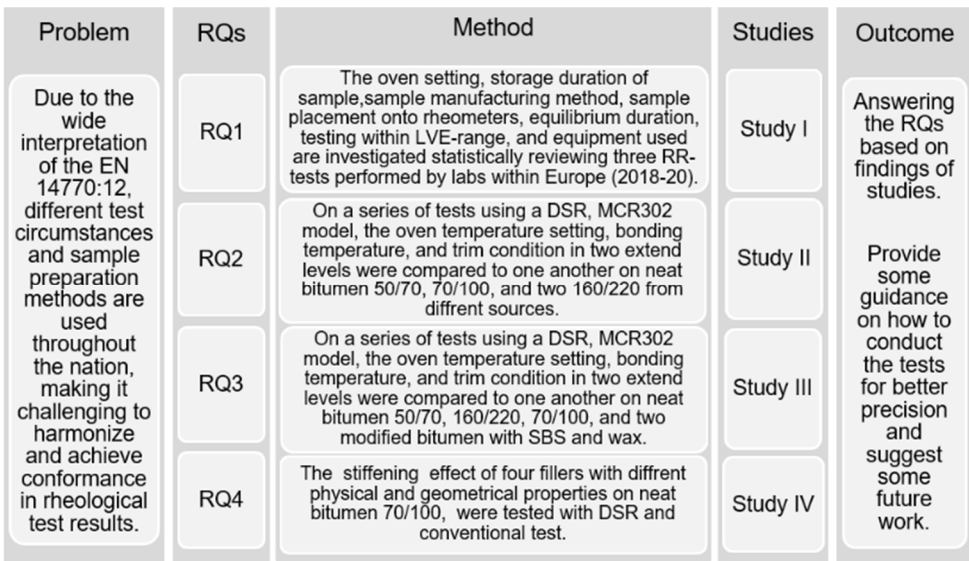

Figure 4. Schematic illustration of the context of the PhD work.

The research began with a review of the literature on bitumen rheological testing methods with a DSR. The aim was to illustrate the potential effect of sample preparation and conditioning procedures on the results. Database searches were undertaken to gain a thorough perspective of sample preparation for the DSR

testing. Web of Science and Scopus were utilized to find articles of interest, and the database search was updated in November 2022 to include more current references. Since some broad terms, such as "dynamic shear rheometer" might be relevant to numerous fields, not just bitumen, the first search result numbers were more than 2000 papers. The following terms—bitumen/asphalt, complex modulus/complex shear modulus, sample preparation/specimen preparation, pouring temperature, gap size, and bonding temperature—were combined and added to reduce the number of hits. Later, the screening method was used to filter the results further. Based on this technique and the elimination of duplicate records, the number of relevant papers was decreased and made more pertinent; a substantial proportion of studies that did not explore the impact of sample preparation procedures were excluded. Additionally, citation searching was applied to the retrieved papers to identify further studies from Google Scholar.

In Study I the data from the different steps of sample preparation methods were derived from three interlaboratory round-robin (RR) tests sponsored by Eurobitumen France, Routes de France, and Cerema Ouest with participants from European laboratories. The tested materials were penetration-graded neat bitumen 20/30 in 2018 and polymer-modified bitumen 45/80-55 in 2019 and 2020. The tests were conducted after short-term ageing in a rolling thin film oven (RTFOT) according to EN 12607-1 (2014) in 2018–2019, and without ageing i.e., no RTFOT nor PAV in 2020. The precision analysis is expressed using the repeatability standard deviation (S_r), reproducibility standard deviation (S_R), repeatability coefficient of variation (CV-r), and reproducibility coefficient of variation (CV-R). The Microsoft Excel and R software (CoreTeam, 2013) were used to prepare and perform the statistical analyses on data from all test combinations and materials to explore the underlying impacts on G* and δ caused by variations in participant practices.

In Study II, a two-level three-factor factorial design experiment was carried out to evaluate the following factors in two extended levels, low (−) and high (+): (1) the oven temperature setting, (2) bonding temperature, and (3) trimming operation. An Anton Paar DSR, MCR302 model at Lund University was used to conduct all the T-f-sweep tests on four penetration-graded neat (unmodified) bitumen types of 50/70, 70/100, and 160/220 from two different suppliers. The DSR's setup and procedure for testing are described, along with how the data gathered by the RheoCompass software will be modelled using the 2 Spring-2 Parabolic-1 Dashpot (2S2P1D) model using MATLAB® program.

Study III, like Study II investigates the influences of three critical specimen preparation parameters (1) the pre-heating temperature (HT) for manufacturing the specimen, (2) the bonding temperature (BT) onto the rheometer, and (3) the trimming (Trim) operation for preparing the specimen after bonding on DSR test outcomes. An Anton Paar DSR, MCR302 with RheoCompass software was used to

collect the rheological properties of five materials in an oscillatory-type testing mode which is statistically analyzed with software.

This study, however, contains two types of modified bitumen (70/100+4% SBS and 70/100+4% wax) in addition to penetration-graded neat (unmodified) bitumen types (50/70, 160/220, and 70/100). Kraton D1192, a linear styrene-butadiene-styrene (SBS), and Sasobit, a long-chain aliphatic hydrocarbon synthetic prill form (wax), are the commonly utilized additives for bitumen modification around the world as well as the results reported according to the updated version of EN 14770:2012 i.e., EN 14770:2023; the characteristic temperatures of bitumen's specific stiffness TX with corresponding phase angle δ_{TX} aside from the complex shear modulus |G*| and phase angle δ. In addition, a repeatability evaluation of the test results was conducted.

In Study IV the physical and mechanical behaviour of mastics prepared with a penetration-graded neat bitumen 70/100, three types of mineral fillers from various quarries in Sweden as quartz diorite (D), quartz-rich granite (Q), and monzogranite (G), and an additive filler (industrial product) at three different filler-to-binder (F/B) content ratios of 40%, 50%, and 60% are investigated. The relationship of geometrical and physical properties of filler such as grading (Particle size distribution), grain shape, density (SG), specific surface areas (SSA), and Rigden voids (RV) with the physical and mechanical behaviour of mastic also studied applying traditional tests the penetration and softening point ($T_{R\&B}$), as well as temperature-frequency-sweeps (T-f-Sweep) test using a DSR. Ultimately the effects such as stiffening strength of the geometrical and physical features of various fillers along with the filler F/B content ratios on mastic are tried to be validated with bitumen to filler interaction degree (C) based on DSR test results, softening point differences from bitumen after adding filers ($\Delta T_{R\&B}$), and the hardness-related property change (ΔPEN).

3 Methods and Materials

In the following sections, methods and materials for all four studies are presented shortly.

3.1 Study I

Study I aims to answer Research Question I (RQ1): What factors need to be considered when testing bitumen with DSR to achieve a reliable result?

Figure 5 shows a schematic structure of Study I. The various practices and interpretations of EN 14770:2012 used by participants in three round-robin tests are statistically investigated.

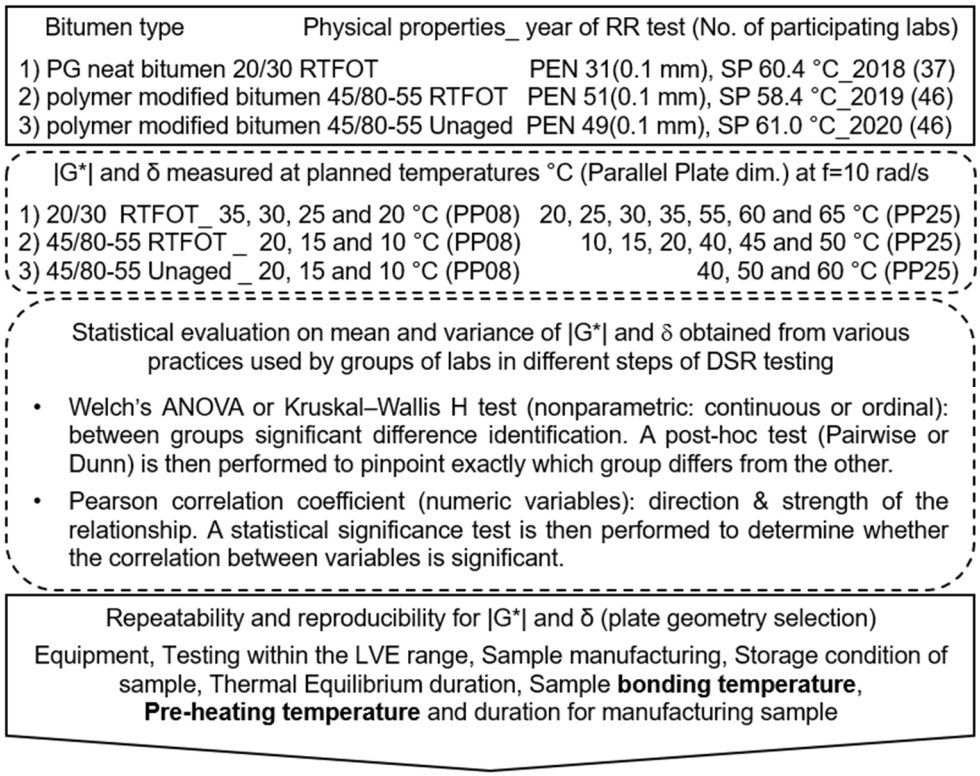

Figure 5. Schematic structure of Study I.

3.1.1 Materials and data collection

This study is based on data from three European round-robin tests (RR tests) carried out in 2018 with 37 laboratories participating, which increased to 46 in 2019 and 2020. The tests were performed on the penetration-graded bitumen 20/30 in 2018, as per EN 12591 (2009), and the polymer-modified bitumen PMB 45/80-55 in 2019 and 2020, as per EN 14023 (2010). The tests were conducted after short-term ageing in a rolling thin film oven (RTFOT) according to EN 12607-1 (2014) in 2018–2019 and on an original binder without ageing i.e., no RTFOT nor PAV in 2020. Tests were performed according to the RR test instruction at the planned temperatures and f= 10 rad/s (1.59 Hz). The laboratories conducted two independent repeats for each test combination at pre-defined test temperatures.

3.1.2 Statistical analysis

The variation in the preparation of the bituminous binders for sample manufacturing method, storage time of sample, bonding temperature of sample onto rheometer, thermal equilibrium duration at different testing conditions, testing within the viscoelastic linear range, and the brand of equipment used by participants are investigated. The processing of data and statistical analysis is done according to ISO 5725-2 (2002). The repeatability standard deviation (S_r), reproducibility standard deviation (S_R), repeatability coefficient of variation (CV-r), and reproducibility coefficient of variation (CV-R) are used to express the precision analysis. According to ISO 5725-6 (2001), the difference between results obtained in the same or alternate laboratory is significant, if it is greater than the repeatability limit ($r = 1.96 \times \sqrt{2}\ S_r$) or the reproducibility limit ($R = 1.96 \times \sqrt{2}\ S_R$), respectively.

Underlying effects on outcomes due to variation in practices applied by participants were investigated. The used practices counted as a category. Means and variances of G* and δ from different categories compared with each other using R software (CoreTeam, 2013) to determine if categories significantly affected the outcomes. To determine which statistical test, Welch's ANOVA or Kruskal-Wallis (H-test), should be used Zimmerman's guideline (2011) was used. When results indicate a statistically significant mean difference between the group's means, multiple comparisons post hoc tests (Pairwise tests or Dunn's test) are used to pinpoint the precise groups with significant differences. For all performed statistical tests, the 5% significance level is used. A Pearson correlation test is performed to quantify the direction and strength of the relationship (Correlation Coefficient: r) in the case of numeric variables, followed by a statistical significance test to determine whether the correlation between variables is significant.

3.2 Study II

Study II aims to answer Research Question II (RQ2): How do the selected factors (heating temperature for manufacturing sample, bonding temperature, and trimming) affect the measured rheological parameters of modified bitumen with DSR?

Figure 6 shows a schematic structure of Study II. A two-level three-factor factorial design experiment was conducted to find the effect of the oven heating temperature for the manufacturing sample (HT), the temperature at which the sample bonds onto the equipment (BT), and the radial trimming state of the manufactured sample on measured data by DSR. Factors are studied at low (–) and high (+) levels. The tests

were performed on the penetration-graded bitumen 50/70, 70/100, and 160/220 from two sources.

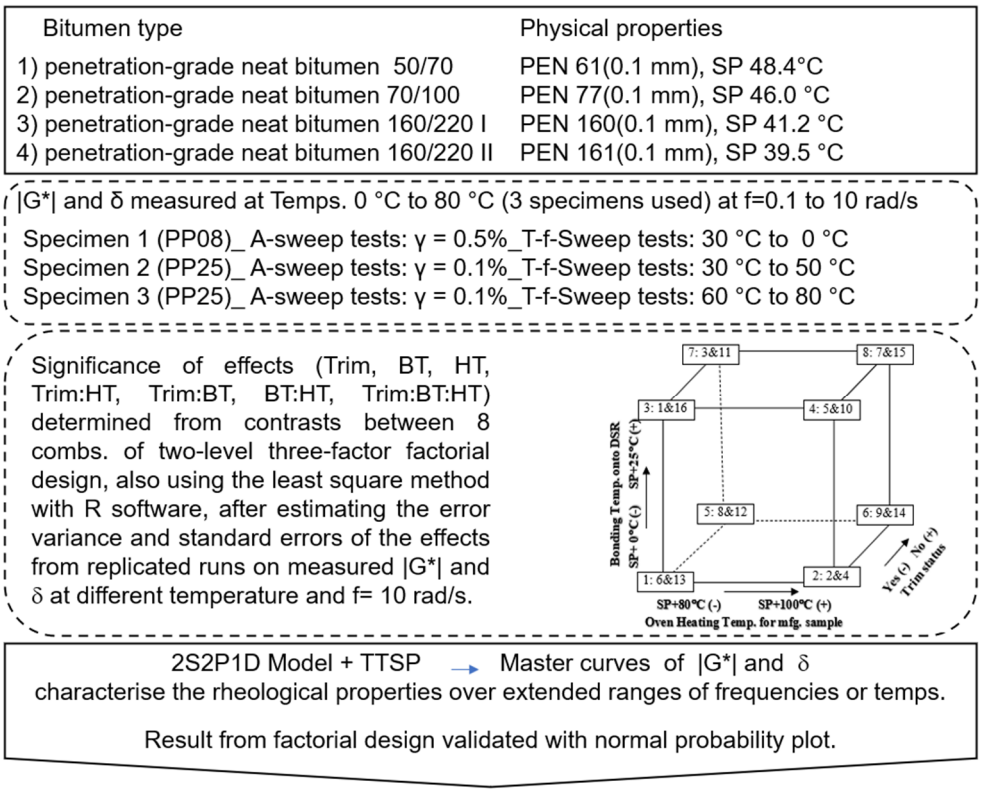

Figure 6. Schematic structure of Study II.

3.2.1 Testing plan: Strain and frequency sweep test

An Anton Paar MCR302 DSR with RheoCompass software was used for measuring complex shear modulus (G*) and phase angle (δ) in an oscillatory-type testing mode using 8 mm and 25 mm parallel plate testing geometries. The storage modulus (G′) and the loss modulus (G″) can be represented as |G*|cos(δ) and |G*|sin(δ), respectively. As per the current standard (EN14770), the LVE region is a range of strain up to which the value of G′ and G″ differ by less than 5% of the initial value over the chosen shear strain range. The strain A-sweep test was performed at all the tested temperatures and materials. The strain amplitude limits for 8 mm and 25 mm geometries were selected at 0.1% (0.001 mm/mm) and 0.5%, respectively, where the shear modulus is relatively independent of shear stress.

The T-f-sweep tests were performed for each of the 8 conditions set (runs) and material. Each T-f-sweep involved 3 samples. For instance, one in the temperature range of 30 °C to 0 °C using a parallel plate with a diameter of 8mm (PP08) and gap height of 2 mm, and the two others, in the range of 30 °C to 50 °C and 60 °C to 80 °C using a parallel plate with a diameter of 25mm (PP25) and a 1 mm gap height. The same operator performed 48 T-f-sweeps per material, with two repeats, for each tested bitumen over the 8 runs. A frequency range of 0.1 to 10 Hz was used to collect 10 points from the logarithmic ramp pattern for each constant temperature. Note, that data only from the high and lower end of the frequency ranges were investigated. The tests were performed at intervals of 10 °C by allowing the material to remain at the test temperature for 15 min within the tolerance of ±0.2 °C. Consequently, T-f-sweep per sample took about 2.5 hours.

3.2.2 Preparation of DSR and specimen

The samples were heated at planned temperatures (SP+80 °C and SP+100 °C) for 20 min or 40 min depending on the size of the container 100 or 200 gr. The specific amount of heated bitumen was poured into silicone moulds after stirring and homogenization. The samples were stored at room temperature without being exposed to light. It was kept in refrigerator for 5 min at 5 °C temperature just before de-moulding. The sample storage time was maintained between 1 to 10 hours; the first specimens were stored for 1 hour, the second for about 4 hours, and the third for a maximum of 10 hours at room temperature. Zero gaps were carried out after waiting 10 min at the mid-point of the planned test temperature range. At the planned bonding temperature (SP+0 °C and SP+25 °C), in the trimming method, the sample was loaded onto the lower plate of the DSR. The upper plate was then gradually lowered to a gap of 1.05 mm for PP25 and 2.1 mm for PP08. After 60 sec the excess material was removed from the radial surface of the samples with a heated spatula. Trimming was done in several steps, wiping away the bitumen residue each time, and avoiding trimming with a too-warm spatula. At least the test gap was set to 1 mm and 2 mm. Meanwhile, for samples without trimming, the upper plate was removed from the rheometer (this is possible for Anton Paar instruments) and was centralized in the upper plate. Then gradually lower the upper plate toward the lower plate to reach a bulge around the periphery of the plates at the final gap of 1 mm and 2 mm for PP25 and PP08 respectively. To eliminate trimming, the exact amount of sample material is calculated to have the same amount tested in both methods. For 50/70 it was 0.53 g (PP25) and 0.11g (PP08), for 70/100 was 0.53 g (PP25) and 0.11g (PP08), for 160/220_I was 0.52 g (PP25) and 0.11g (PP08), and for 160/220_II was 0.52 g (PP25) and 0.11g (PP08). For the specimen, with trimming a slightly larger amount of material was used. The normal force-controlled mode compensated for the specimen's possible shrinkage at lower temperatures by

adjusting the gap to keep the normal force zero. This would be more critical if the temperature range were wider.

3.2.3 Statistical analysis

The significant parameters were determined manually from contrast coefficients (Table 1), also with a statistical analysis tool, R software to perform ANOVA tests after the main and interaction effects, and their standard errors were calculated. The main effect is the difference between the average outcomes of the factor at two defined levels, for instance, BT(G^*) = ($\bar{G}^*_{BT+1} - \bar{G}^*_{BT-1}$). A two-way interaction, for instance, BT:HT can be defined as the mean difference between the effects of bonding temperature (BT) and heating temperature (HT) at both levels. There is also an interaction effect between three factors, defined as the mean difference between the effects of three factors at the same levels (Box et al., 1978).

Table 1. Combination of a two-level three-factor factorial design with two replicates.

8 Combs.	Randomized Run Order	Contrast Coefficients for Main and Interaction Effects						
		Trim	BT	HT	Trim.BT	Trim.HT	BT.HT	Trim.BT.HT
1	6 and 13	(−1)	(−1)	(−1)	(+1)	(+1)	(+1)	(−1)
2	2 and 4	(+1)	(−1)	(−1)	(−1)	(−1)	(+1)	(+1)
3	1 and 16	(−1)	(+1)	(−1)	(−1)	(+1)	(−1)	(+1)
4	5 and 10	(+1)	(+1)	(−1)	(+1)	(−1)	(−1)	(−1)
5	8 and 12	(−1)	(−1)	(+1)	(+1)	(−1)	(−1)	(+1)
6	9 and 14	(+1)	(−1)	(+1)	(−1)	(+1)	(−1)	(−1)
7	3 and 11	(−1)	(+1)	(+1)	(−1)	(−1)	(+1)	(−1)
8	7 and 15	(+1)	(+1)	(+1)	(+1)	(+1)	(+1)	(+1)

The standard error of an effect (main or interaction), *SE* is the square root of the average over the estimated variance of 8 observations for an effect, which is the difference between the average of two levels according to Equation 1. A significant value of t distribution with 8 degrees of freedom (DF) at the 5% level (α=0.05) is 2.3; thus the 95% confidence interval for the estimated effects is given by Pr ($|t_{0.05,8}|>2.3$).

$$\text{SE (effect)} = \sqrt{\text{Var(effect)}} = \sqrt{\left(\frac{1}{8}+\frac{1}{8}\right)\cdot\left(\sum_{n=1}^{n=8}\frac{diff_n^2}{2}\right)/n)} \qquad (1)$$

The $|G^*|_i$ is a modelled outcome of the *i:th* combination at a specific temperature and frequency. The a_i are the coefficients obtained using the contrast between combinations, which are considered twice, due to the calculated effects yielding

changes of two units along each axis from (−) to (+). The a_i also can be estimated using the least square method in the R software package.

$$|G^*|_{i(i:1-8)} = (\sum_{i=1}^{i=8} G^* / n) + (a_1/2).Trim_i + (a_2/2).BT_i + (a_3/2).HT_i + (a_4/2).Trim_i \cdot HT_i + (a_5/2).Trim_i \cdot BT_i + (a_6/2).BT_i \cdot HT_i + (a_7/2).Trim_i \cdot BT_i \cdot HT_i$$

Figure 7 displays a normal probability of effect estimates at the 5% significance level for a specific temperature and frequency. All calculated effects are plotted against a straight line representing the normal distribution line. The outliers, indicated by squares, are thought to be the factors with the most governing parameters on the measured outcome (G*). The effects that are not statistically significant are typically distributed as a straight line with a mean equal to zero and variance σ, whereas the significant main effects and interactions have nonzero means and do not lie along the straight line (Daniel, 1959). In the example, Trim and HT are considered statistically significant.

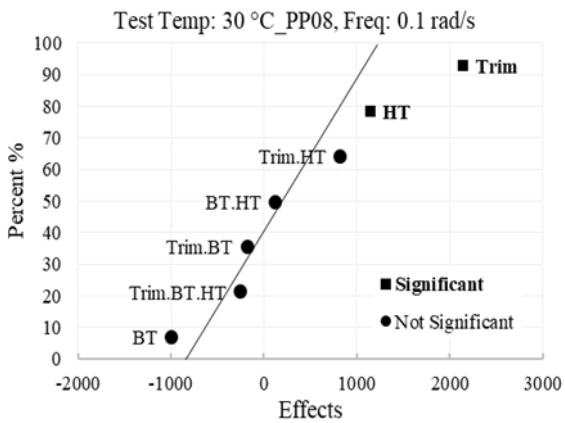

Figure 7. Normal probability of effect estimates at significance level of α=0.05.

3.2.4 Master Curve and 2S2P1D Model

Furthermore, the rheological test data were modelled using the 2 Spring-2 Parabolic-1 Dashpot (2S2P1D) model (Olard and Di Benedetto, 2003), and the time-temperature superposition principle (TTSP) (Delaporte et al., 2007) to construct complex modulus and phase angle master curves of the materials tested at an arbitrarily chosen reference temperature (15 °C). This model consists of seven

parameters and the predicted complex shear modulus |G*| can be obtained using Equation 2 (Benedetto et al., 2007).

The effect of the different combinations of factors under study (runs) is then investigated by comparing the differences of each observation (seven parameters) from the mean across the 8 runs to detect any statistically significant differences between the eight runs and parameters. The sensitivity of each parameter is judged according to the comparison of the correlation of variation (CV) in all runs.

$$G^*_{2S2P1D}(i\omega\tau) = G_0 + \frac{G_\infty - G_0}{1+\alpha(i\omega\tau)^{-k}+(i\omega\tau)^{-h}+(i\omega\beta\tau)^{-1}} \qquad (2)$$

2S2P1D model's seven parameters presented in Equation 2 are as follows: the $|G^*_{2S2P1D}|$ is the predicted dynamic shear modulus, G_0 is the static modulus when ω → zero (as G_0 for all bitumen is commonly close to zero, the seven parameters can be reduced to six), G_∞ is the glassy modulus when ω → infinite, ω is the angular frequency, i is the complex number ($i^2 = -1$), k and h are dimensionless parameters exponents with $0 < k < h < 1$, a is a shape-related constant parameter, β is a Newtonian viscosity-related constant parameter, and τ is temperature depended characteristic time. The William Landel and Ferry (WLF) equation was used to estimate $\tau = a_T(T_i)\,\tau_o$, where τ_o is computed at the reference temperature $\tau(T_{ref})$ and a shift factor $a_T(T_i)$ in the range of temperatures T_i measured in the laboratory (Ferry, 1980).

3.3 Study III

Study III aims to answer Research Question III (RQ3): How do heating temperature for the manufacturing sample, bonding temperature, and trimming affect modified bitumen's measured rheological parameters with DSR?

Figure 8 shows a schematic structure of Study III. In this study we are interested in further understanding how the three selected factors influence the measured TX and δ_{TX}, in addition to |G*| and δ for both neat and modified bitumen.

Bitumen type	Physical properties
1) penetration-grade neat bitumen 50/70	PEN 61 (0.1 mm), SP 46.8 °C
2) penetration-grade neat bitumen 160/220	PEN 160(0.1 mm), SP 41.2 °C
3) penetration-grade neat bitumen 70/100	PEN 85 (0.1 mm), SP 45.6 °C
4) polymer modified bitumen 70/100 + 4% SBS	PEN 39 (0.1 mm), SP 67.2 °C
5) polymer modified bitumen 70/100 + 4% wax	PEN 33 (0.1 mm), SP 79.0 °C

$|G^*|$, δ, $T_{|G^*|=15kPa}$ and $\delta_{T|G^*|=15kPa}$ measured at planned Temps at f=0.1, 10, 100 rad/s

Material	Specimen 1 (PP08) *TX*, δ_{TX} (at 5 MPa)	Specimen 2 (PP25) *TX*, δ_{TX} (at 15 kPa)	Specimen 3 (PP25) *TX*, δ_{TX} (at 1 kPa)
50/70	20 and 10 °C_ γ = 0.1%	50 and 60 °C_ γ = 0.5%	70 and 80 °C_ γ = 0.5%
160/220	10 and 0 °C_ γ = 0.1%	30 and 40 °C_ γ = 0.5%	50 and 60 °C_ γ = 0.5%
70/100	20 and 10 °C _ γ = 0.5%	45 and 55 °C_ γ = 0.5%	60 and 65 °C_ γ = 0.5%
70/100+ 4% SBS	20 and 10 °C_ γ = 0.1%	50 and 60 °C_ γ = 0.1%	70 and 75 °C_ γ = 0.1%
70/100+ 4% Wax	25 and 15 °C_ γ = 0.05%	65 and 75 °C_ γ = 0.05%	80 and 85 °C_ γ = 0.05%

Analysis of variance to determine statistically significant differences between means of 8 combs. of two-level three-factor factorial design on measured $|G^*|$, δ, $T_{|G^*|=15kPa}$, $\delta_{T|G^*|=15kPa}$

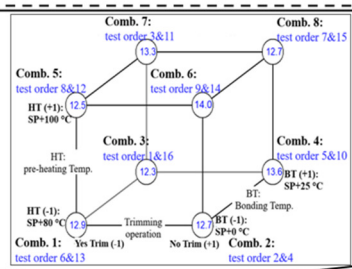

Significance of effects:
Trim
BT
HT
Trim:HT
Trim:BT
BT:HT
Trim:BT:HT

Figure 8. Schematic structure of Study III; properties of materials, testing plan, and expected outcome.

The temperature TX and the related phase angle δ_{TX} of $|G^*|$ at 5 MPa, 15 kPa are the new parameters for the expression of results according to EN 14770:2023. The $T|G^*|=1$ kPa represents the EN' recommended upper limit temperature suitable for measuring with PP25. The tests were performed on the penetration-grade neat bitumen 50/70, 70/100, and 160/220 from two different sources, as well as two polymer-modified bitumen, 70/100+ 4% SBS and 70/100+ 4% wax. The 70/100 samples were mixed by weight of 23% of the 160/220 and 77% of the 50/70 for each set of 8 conditions (combinations) separately.

Similar to Study II a two-level three-factor factorial experiment was designed to find the effect of the three phases of sample preparation and conditioning such as oven heating temperature for the manufacturing sample (HT), the temperature at which the sample bonds onto the equipment (BT), and the radial trimming state of manufactured sample on measured data by DSR.

3.3.1 Testing plan: Strain and frequency sweep test

An Anton Paar MCR302 DSR with RheoCompass software was used to measure the rheological parameters according to the plan shown in Figure 9. A logarithmic interpolation on measured |G*| and δ is conducted to obtain values of temperature TX and the related phase angle δ_{TX} for values of |G*| at 5 MPa, 15 kPa, and 1 kPa. The strain A-sweep test was performed at all the tested temperatures and materials and a range between 0.1% (0.001 mm/mm) and 0.05% was selected. The T-f-sweep tests were performed by the same operator for each of the eight combinations and material with two repeats. Each T-f-sweep involved 3 samples, each tested at frequencies of 0.1, 10, and 100 rad/s and at two temperatures with no more than 10 °C apart from each other. One in the temperature below the softening point of the material using a PP08 and a gap height of 2 mm, one above, and one just close to the softening point of the material using a PP25 and a gap height of 1 mm. To ensure that the temperature in the test specimen did not deviate from the temperature recorded by the DSR, a thermal equilibration time of 15 minutes was employed, with a tolerance of ±0.2 °C.

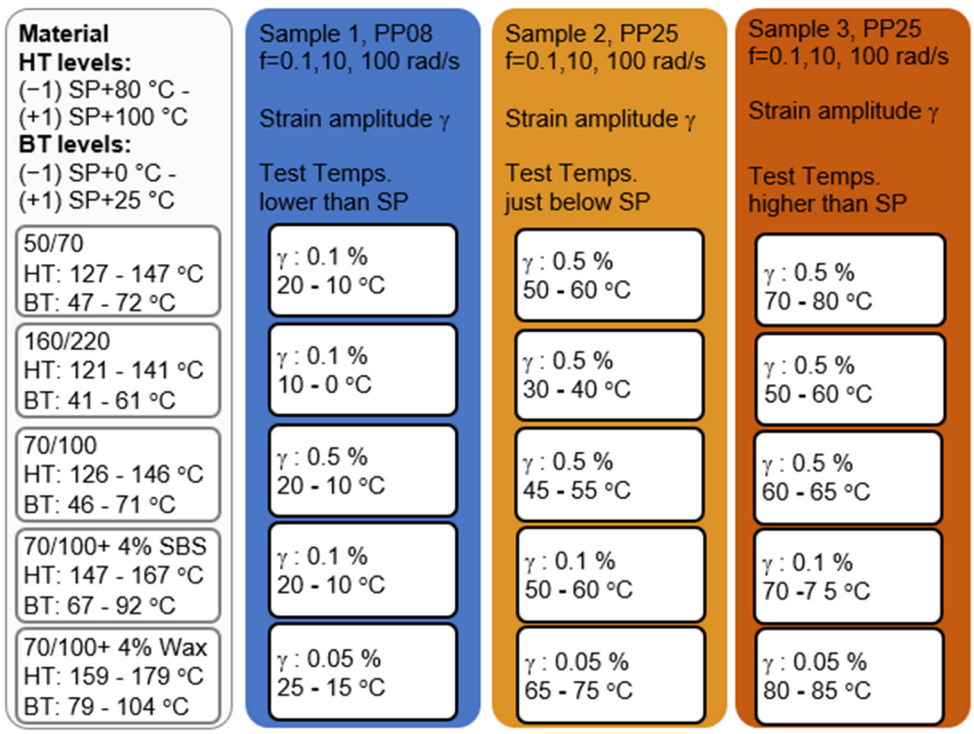

Figure 9. Schematic representation of the experimental plan.

3.3.2 Preparation of DSR and specimen

Specimens were manufactured in silicone mould after heating the material at the planned temperatures (SP+80 °C and SP+100 °C). For without trimming (high level +), the exact amount of bitumen material was calculated based on the volume of the specimen, resulting in a bulge around the periphery while testing. For 50/70 it was 0.53 g (PP25) and 0.11g (PP08), for 160/220 was 0.52 g (PP25) and 0.11g (PP08), for 70/100 was 0.53 g (PP25) and 0.11g (PP08), for 70/100+ 4% SBS was 0.52 g (PP25) and 0.11g (PP08), and for 70/100+ 4% wax was 0.52 g (PP25) and 0.11g (PP08). The amount of bitumen placed on DSR for preparing the specimen with trimming (low level –) was somewhat more than the without-trimming method. All the remaining phases of preparation and conditioning of the sample were constant and fixed according to EN 14770:2023. The specimens were stored at room temperature and covered with an opaque lid. The possible hardening effect was removed from the analysis using the same relative storage time for all tested specimens. Specimens 1, 2, and 3 were stored for a maximum of 2 hours, 10 hours, and 20 hours, respectively, and before testing specimens were removed from the mould after 5 min refrigeration at 5 °C temperature. Zero gaps were carried out after waiting 10 min at the mid-point of the planned testing temperatures. At the planned bonding temperature (SP+0 °C and SP+25 °C), in the case of the trimming method, the sample was loaded onto the lower plate of the DSR and the upper plate was then gradually lowered to a gap of 1.05 mm for PP25, and 2.1 mm for PP08, and after 60 second the excess material was removed from the radial surface of the samples with a heated, but not too hot spatula. Trimming was done in several steps, wiping away the bitumen residue each time. Finally, the test gap was set to 1 mm and 2 mm for testing. In the method without trimming, the weighed sample was carefully placed on the centre of the lower plate as much as possible. Then gradually lowered the upper plate toward the lower plate to reach the bulge around the periphery of the plates at the final gap of testing. The normal force-controlled mode which adjusts the gap to keep the normal force zero was activated for possible shrinking of the specimen at lower temperatures. However, this is not critical due to the narrow range of temperatures.

3.3.3 Statistical analysis

Statistical analyses on data that were generated for the characteristic values $T_{|G^*|=1\ kPa}$ and corresponding $\delta_{T|G^*|=1\ kPa}$ at high temperature, $T_{|G^*|=15\ kPa}$ and $\delta_{T|G^*|=15\ kPa}$ at intermediate temperature, $T_{|G^*|=5\ MPa}$ and $\delta_{T|G^*|=5\ MPa}$ at low temperature, as well as for measured $|G^*|$ and δ in different test setup combinations are performed. The factors that have a statistically significant impact on the outcomes of the tested materials were identified, where the *p*-values from the ANOVA test were less than the confidence limit ($\alpha = 0.05$). The main and interaction effects are estimated using the least square method in the statistical analysis tool R software (CoreTeam, 2013)

which can also be calculated from the contrasts between combinations in 2^3 factorial design (Box et al., 1978). The main effect is the difference between the average outcomes of the factor at two defined levels. The two-way interaction is the effect between two factors, for instance, HT:BT, which can be defined as the mean difference between the effects of heating temperature and bonding temperature at both levels. There is also an interaction effect between three factors, defined as the mean difference between the effects of three factors at the same levels.

The experiment results covering the eight different test combinations (1 to 8) with two repeats (1 and 2) used to estimate the repeatability *r* (2.77* S_r), for TX and δ_{TX}, |G*|, and δ measured with PP08 and PP25 as follows: The computed values of the repeatability standard deviation, denoted by S_r.

S_r (TX) = SQRT [Average (var ($TX1_1$ & $TX2_1$), ..., var ($TX1_8$ & $TX2_8$))]

S_r (δ_{TX}) = SQRT [Average (var ($\delta 1_{TX\,1}$ & $\delta 2_{TX\,1}$), ..., var ($\delta 1_{TX\,8}$ & $\delta 2_{TX\,8}$))]

S_r (|G*|) = SQRT [Average (var ($|G^*|1_1$ & $|G^*|2_1$), ..., var ($|G^*|1_8$ & $|G^*|2_8$))]

S_r (δ) = SQRT [Average (var ($\delta 1_1$ & $\delta 2_1$), ..., var ($\delta 1_8$ & $\delta 2_8$))]

3.4 Study IV

Study IV aims to answer Research Question IV (RQ4): How do the rheological properties of mastic (bitumen mixed with filler) measured with DSR relate to the type and content of fillers, and can these results be validated using the physical properties of mastic obtained from traditional tests?

Figure 10 shows the methodological framework of study IV for laboratory experiments to investigate the effect of different filler types and filler-to-bitumen (F/B) volumetric content ratio on the mastic properties.

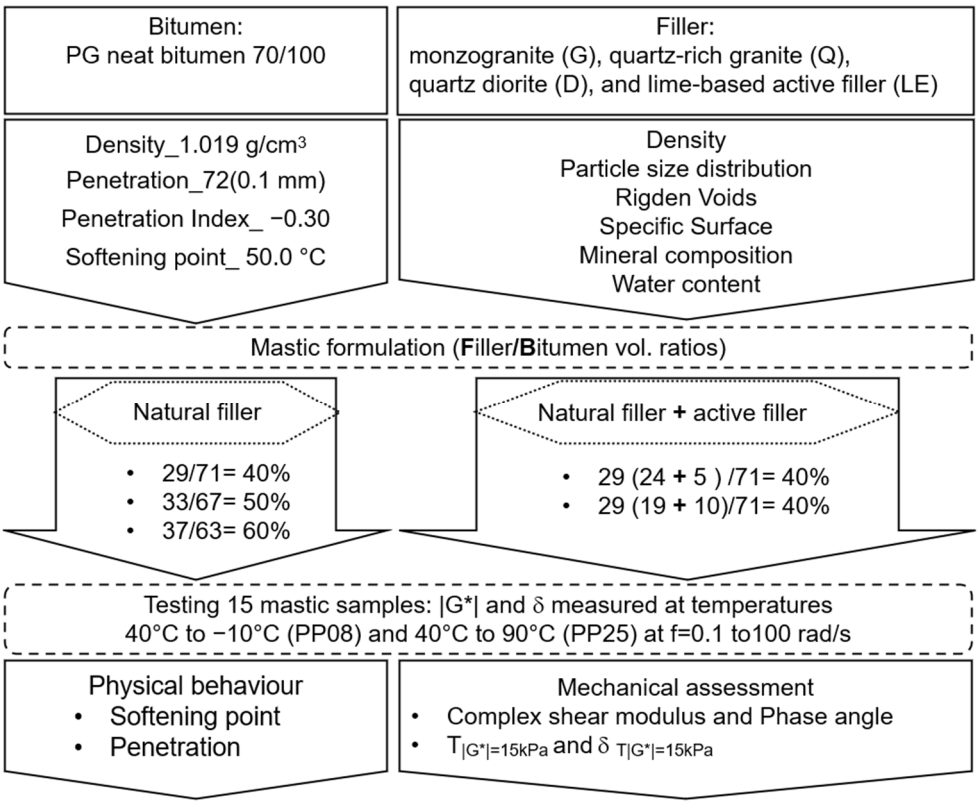

Figure 10. Schematic structure of Study IV.

A penetration-grad neat bitumen type of 70/100, three mineral filler types commonly used in Sweden obtained from crashed natural rocks, and an industrially manufactured lime-based active filler Nordkalk Terra E (LE) were selected to produce fifteen bitumen mastic types. Three volumetric content ratios (Vol. F/Vol. B) of 40%, 50%, and 60% are studied. These ratios are based on the F/B range of 1:1.0–1:1.5 by mass regulated by the Swedish Transport Administration (Trafikverket, 2020) to match the ratio range of a common dens-graded asphalt mixture in Sweden with a maximum aggregate size of 11 mm and a bitumen type 70/100 (i.e. ABT 11 70/100). The F/B of 60%, which exceeds the F/B range of 1:1.5 by mass was selected for corresponding the ratio for the delta ring and ball ($\Delta T_{R\&B}$) test in EN 13179-1. T-f-sweep tests were conducted at temperatures ranging from −10 °C and 90 °C, and frequencies ranging from 0.1 rad/s to 100 rad/s to measure the rheological parameters.

Figure 11 shows studied mineral fillers obtained from various quarries in Sweden are identified as quartz diorite (D), quartz-rich granite (Q), and monzogranite (G) using the QAP classification diagram (Streckeisen, 1976). The chemical

composition of the industrially manufactured lime-based active filler, Nordkalk Terra E is as follows: Calcium oxide (40%– 70 %), Silica (10%– 25 %), Aluminum oxide (0%– 15 %), Iron(III) oxide (< 2 %), Phosphorus pentoxide (< 1 %), with a pH-value greater than 12.

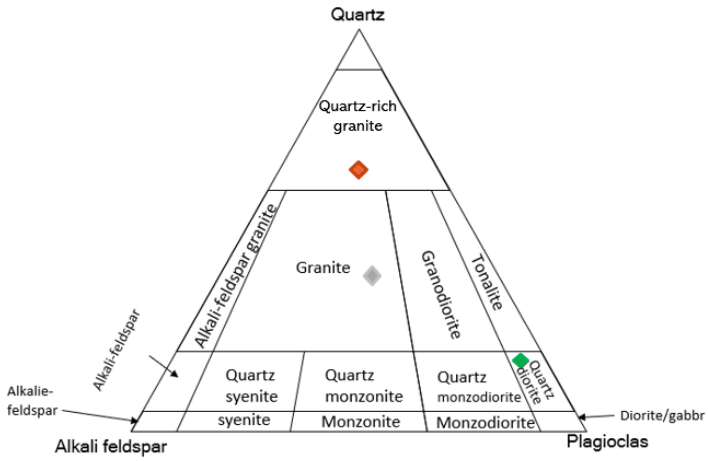

Figure 11. Compilation of rock type affiliation based on the calculated mineral composition of respective natural fillers. Gray rhombus: monzogranite (G), Red-brown rhombus: quartz-rich granite (Q) Green rhombus: quartz diorite (D).

3.4.1 Testing plan

An Anton Paar MCR302 DSR with RheoCompass software was used to measure the rheological parameters of the base bitumen (70/100) and the 15 different mastics and the base bitumen according to the plan shown in Table 2. These mastic mixes were examined by penetration test at 25°C (EN1426, 2015) as a hardness-related property change measurement by adding different fillers to the bitumen, the difference between the bitumen and mastic softening points ($\Delta T_{R\&B}$) (EN1427, 2015), and T-f-sweeps test using a DSR (EN14770, 2023). The T-f-Sweep tests were conducted at temperatures ranging from 40 °C to –10 °C applying PP08 and 40 °C to 90 °C applying PP25 with an interval of 10 °C, and frequencies ranging from 0.1 rad/s to 100 rad/s to measure the |G*|, δ, $T_{|G^*|=15kPa}$ and $\delta_{T|G^*|=15kPa}$. To remain in the LVE range, strain A-sweep tests were performed at each test temperature and were set at 0.1% (0.001 mm/mm) for PP08 and 1% for PP25.

For filler, the following geometrical and physical properties were determined: particle density (SG) using the pycnometer method (EN1097-7, 2022), particle size distribution and SSA were measured using a Laser Diffraction Sizer (Malvern' Mastersizer 3000) (ISO13320, 2009), mineral-petrographic composition and grain shape (morphology) were observed using an optical polarizing microscope (Nikon's ECLIPSE LV100N POL), void in dry compacted filler (Rigden

Voids) was obtained using the Rigden equipment (EN1097-4, 2008), and water content (EN1097-5, 2008). The SG was used to calculate the Rigden voids (RV) and volumetric ratios of the mastic mixture.

Table 2. Mastic formulation.

Mastic ID	Filler(s)/Bitumen Vol.% ratio	Filler(s)/Bitumen mass ratio
G29_40	29% monzogranite / 71% = 40%	50.9 / 49.1 = 1.04
G33_50	33% monzogranite / 67% = 50%	56.4 / 43.6 = 1.30
G37_60	37% monzogranite / 63% = 60%	60.9 / 39.1 = 1.55
Q29_40	29% quartz-rich granite / 71% = 40%	51.2 / 48.8 = 1.05
Q33_50	33% quartz-rich granite / 67% = 50%	56.7 / 43.3 = 1.31
Q37_60	37% quartz-rich granite / 63% = 60%	61.1 / 38.9 = 1.57
D29_40	29% quartz diorite / 71% = 40%	53.2 / 46.8 = 1.14
D33_50	33% quartz diorite / 67% = 50%	58.7 / 41.3 = 1.42
D37_60	37% quartz diorite / 63% = 60%	63.0 / 37.0 = 1.70
G24LE5_40	(24% monzogranite + 5% lime-based active filler) / 71 = 40%	51.3 / 48.7 = 1.05
Q24LE5_40	(24% quartz-rich granite + 5% lime-based active filler) / 71 = 40%	51.5 / 48.5 = 1.06
D24LE5_40	(24% quartz diorite + 5% lime-based active filler) / 71 = 40%	53.1 / 46.9 = 1.13
G19LE10_40	(19% monzogranite + 10% lime-based active filler) / 71 = 40%	51.6 / 48.4 = 1.07
Q19LE10_40	(19% quartz-rich granite + 10% lime-based active filler) / 71 =40%	51.8 / 48.2 = 1.07
D19LE10_40	(19% quartz diorite + 10% lime-based active filler) / 71 = 40%	53.0 / 47.0 = 1.13
Bitumen ID	Bitumen properties	
B70/100	PEN 72.0*10-1 mm, SP 50.0 °C, and specific gravity of 1.019 g/cm3	

3.4.2 Preparation of DSR and Specimen

100 g of Mastics were produced using bitumen type 70/100 and the corresponding weight of each filler based on their density in a mass ratio of filler-to-bitumen as given in Table 2. First, the bitumen was heated to 150 °C for 15 min to make it flowable. The required filler, preheated at 150 °C for 15 min, was then poured on top of the bitumen inside the container. The bitumen–filler mix was stored in the oven at 150 °C for max 20 min and mixed consistently before, during, and after the storage inside the oven using a metallic tool to ensure a homogenous mix before manufacturing samples for DSR, the delta ring and ball (softening point increment), and penetration tests. For DSR testing the samples were manufactured similarly to previous studies in this thesis i.e., in a silicone mould. However, all the samples are trimmed before testing, and a bounding temperature is set to the estimated softening point (R&B) of mastics plus 10 °C. The specific amount of heated bitumen (0.58 g

for PP25 and 0.12 g for PP08) was poured into the silicone mould after stirring and homogenization.

3.4.3 Master curve, and Bitumen–filler interaction parameter

The DSR parameters, complex shear modulus, and phase angle were modelled using the 2 Spring-2 Parabolic-1 Dashpot (2S2P1D) model mentioned in section 3.2.4. To visualize the behaviour of tested bitumen and mastics, master curves are plotted, which illustrate complex shear modulus and phase angle versus frequency for all tested temperatures.

Mastic characteristics are influenced not only by the properties and proportions of bitumen and filler but also by bitumen-to-filler physicochemical interaction. As part of the physicochemical interaction, polar groups of bitumen are selectively adsorbed onto the filler surface (Fritschy and Papirer, 1978; Clopotel and Bahia, 2013). To evaluate the bitumen-filler interaction, numerous studies have been conducted. The following approach—which is based on the LVE theory model and Palierne emulsion model—was chosen because it was shown to accurately depict the interaction (Rochlani et al., 2021a). In this study, Equation 3 (Guo et al., 2017) is applied to determine the interaction degree (C) at three different volumetric F/B ratios of (29/71), (33/67), and (37/63), over a wide range of temperatures (−10 °C to 90 °C) and frequency of 10 rad/s (1.59 Hz). The complex shear modulus of bitumen and mastic is represented by $|G^*_{mastic}|$ and $|G^*_{bitumen}|$. The filler volume fraction (V_{filler} / $V_{filler + bitumen}$) is denoted by φ. A greater C value implies a stronger bitumen–filler interaction.

$$\frac{|G^*_{mastic}|}{|G^*_{bitumen}|} = \frac{1+1.5\,\varphi\,C}{1-\varphi\,C} \qquad (3)$$

4 Results

In the following sections, the results of the 4 studies are presented shortly.

4.1 Study I: Sample preparation techniques on DSR testing: round-robin tests on bitumen

The results of Study I are presented here briefly; the full paper describing Study I is in Appendix III.

4.1.1 Precision

The reproducibility of 10% for the complex shear modulus and 5% for the phase angle are the recommended values in EN 14770:2012 based on the Rilem TC 180-PEB work (Sybilski et al., 2004). The repeatability for G* and d was determined to be 5% and 1% for paving grade bitumen and 8% and 2% for polymer-modified bitumen from a study by Eckmann et al. (2008). The coefficient of variation under repeatability conditions (COVr) and the coefficient of variation under reproducibility conditions (COVR) for each of the testing combinations and sample material are calculated at a frequency of 1.59 Hz (10 rad/s).

It is found that reproducibility values vary between 7% and 19.6% and the repeatability values are within a range of 2%– 11.8% for |G*| (Figure 12.a), and 0. 2%– 3.4% for δ. However, eliminating the PP25 data at low test temperatures of 10 to 20 °C and the PP08 data at high temperatures of 25 to 35 °C improves the precision significantly. Nevertheless, the unaged 45/80-55 obtains the best precision, followed by RTFO conditioned 45/80-55 at higher testing temperatures and 20/30 at lower testing temperatures. For the phase angle, the coefficient of variation under reproducibility conditions meets the criteria given in EN 14770: 2012 for all the results, except at temperatures as low as 10 °C and 15 °C for RTFO conditioned 45/80-55 and 20 °C for 20/30 in PP25 geometry. For the phase angle, a reverse relationship can be noticed between the coefficient of variation and temperature, also mentioned by Büchner J. et al. (2020) for smaller parallel plate geometry. On the contrary, another interlaboratory study with a smaller number of participants using the same type of bitumen, but with different Pen and SP values,

shows a wider spread of data around the mean for phase angles than the complex shear modulus (Błażejowski et al., 2016). To prevent temperature reliance for δ, the repeatability limit (r) and reproducibility limit (R) related to the arithmetic mean value are expressed in absolute value as shown in Figure 12.b, which will remain constant regardless of temperature. Ignoring the extreme values due to the selection of unsuitable plate geometry or a low number of involved laboratories, unaged 45/80-55 achieves the highest precision with a limit of r=1° and R=3°. There has been an overall improvement in the collected data precision over the three years of the round-robin tests, which may be attributed to round-robin instruction experience and the removal of the influence of various individual practices on the RTFOT technique performed by each participating laboratory from the most recent year, where tests were performed on unaged bitumen.

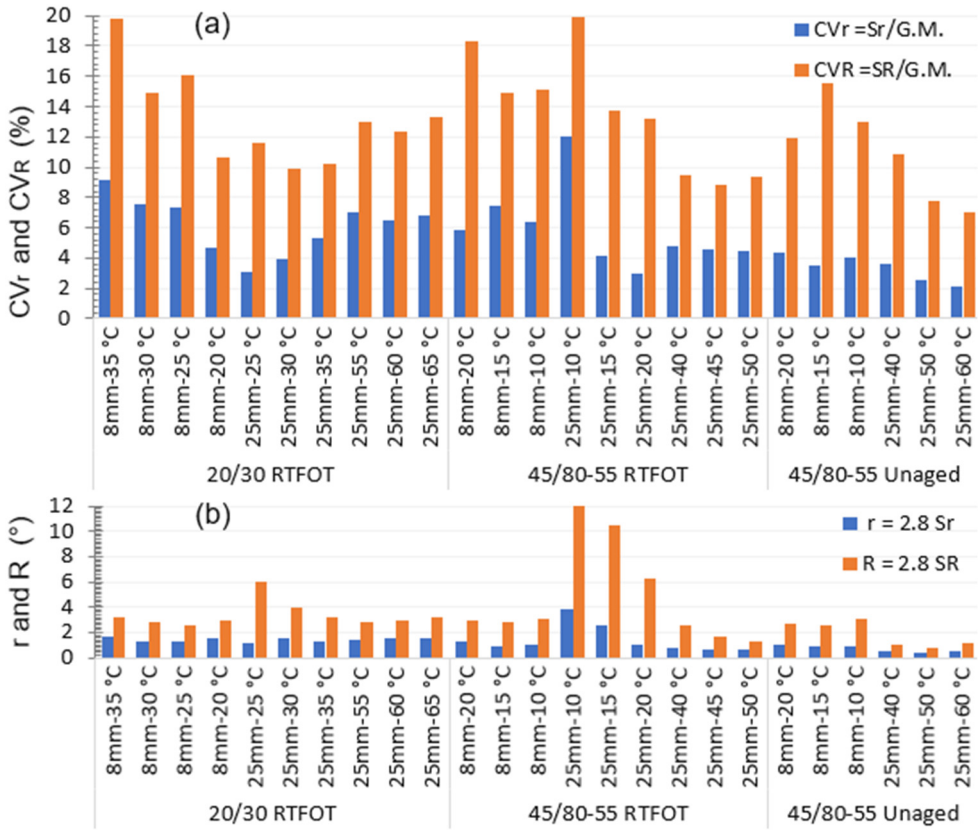

Figure 12. Coefficient of variation under repeatability conditions related to the geometric mean value (CVr), and coefficient of variation under reproducibility conditions related to the geometric mean value (CVR) for G*(a).Standard deviation under repeatability conditions (S_r) and standard deviation under reproducibility conditions (S_R) for δ (b).

The |G*| and δ obtained from 8 mm and 25 mm parallel plates at overlap temperatures were examined. The values of |G*| and δ deviate from the mean of |G*| and δ at the overlap temperatures by less than 6% and 0.6°, respectively, which is significantly better than the recommended values of 15% for |G*| and 3° for δ.

4.1.2 Testing within the viscoelastic linear range

For participants with better precision, only two to three laboratories in the 2019 and 2020 round tests reported that they had not studied the viscoelastic linear range of the sample material. They may have chosen suitable shear strains or stresses based on their experiences with the material and used device. Stress-controlled mode was used by five laboratories in 2018 and two laboratories in 2020, while most of the laboratories applied strain-controlled mode. Some participants varied strain amplitude as a function of temperature, while others applied strain as a function of plate dimension.

4.1.3 Equipment

Most laboratories used various models of Anton Paar manufactured rheometers (MCR 101, 102, 301, 302, 501, 502, 702, smart pave 102/301, and EC-Twist 502). Malvern Panalytical rheometers represented six models (Kinexus DSR, DSR+, Pro, Pro+, Ultra+, and KNX) as the second most used brand. The Discovery HR 2 and AR1000 models were produced by TA Instruments and the Haake Mars 2 and 3 models were produced by Thermo Scientific, respectively are the second to last used brand. The Bohlin brand model DSR2 is used only by one lab. Results indicate that laboratories with better precision used Anton Paar devices the most.

When comparing the Malvern and Anton Paar brands, the Malvern resulted in a higher G* when applying PP025 and a lower G* with PP08. However, the differences are only significant in the two test conditions listed here: for unaged 45/80-55 at PP08- 20 °C and PP08- 15 °C. For δ, the Malvern brand resulted in a higher value than Anton Paar for all test conditions except for testing at 40 °C and 50 °C with PP25 for unaged 45/80-55. The differences, however, are not significant.

4.1.4 Specimen manufacturing

Figure 13 shows the most frequently used method during the round-robin test between 2018 and 2020. The trend for using silicone mould is increasing by the year, which can be the result of a larger amount of Anton Paar equipment among participant laboratories, which offer silicone mould. Nevertheless, only a few laboratories mentioned their mould supplier. One laboratory each year used the hot pouring onto the plate method for the 25 mm plate dimension. Statistical tests were

used to examine the differences in the G* and d based on the sample manufacturing method used by participants. The term "other-mfg." refers to manufacturing methods other than sheet and silicone mould. The sheet manufacturing method resulted in a higher G*, and a lower d on average than mould manufacturing method for all test conditions with no significant differences between the two methods. There are, however, statistically significant differences ($p < 0.05$) between other-mfg. and sheet, as well as between other-mfg. and mould at a few testing conditions.

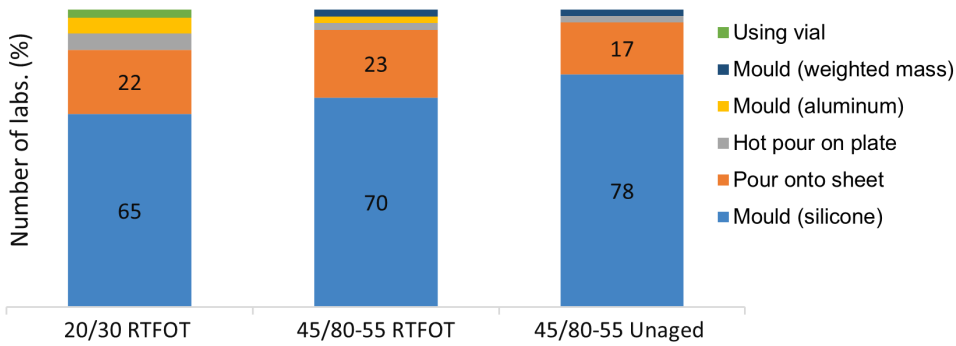

Figure 13. Sample manufacturing methods used by number [%] of laboratories.

4.1.5 Pre-heating setup for manufacturing specimen

In this study only in the 2020 round-robin test are DSR samples directly manufactured after heating, while in 2017, 2018 and 2019 round-robin tests undergo short-term ageing and samples manufacturing in the three following different ways:

Case 1: without additional heating

Case 2: cooling slightly and reheating to a defined temperature and duration

Case 3: cooled and stored for later reheating to a defined temperature and duration.

Case 2 is the least preferred method applied by 14%– 21% of laboratories. The average heating temperature in this case is less than the other two cases. For pure bitumen 20/30, the participants with better precision exceeded the EN's recommended upper limit range while others followed it strictly. In the case of PMB in both conditions, aged and unaged, almost the same range of temperature (155–185 °C) is used by more than 80% of participants regardless of their result precision. The outcome presents a tighter range of temperatures within the range limits of EN, which leads to satisfactory test results. The heating duration preferences noticeably differ between labs. for all materials, except for the unaged 45/80-55. An oven sitting duration between 60 to 90 min for pure bitumen, and no longer than 60 min for PMB regardless of ageing condition, is chosen by the majority of labs with better precision. Results also indicate, for these labs., that heating temperature decreases

as oven sitting duration increases. The storage and reheating duration results are widely distributed in case 3, which makes drawing a general conclusion difficult. Differing from case 1, the heating temperature increases in case 3, and the reheating duration and storage duration also increase for labs. with better precision. For all the cases and sample materials, labs. with better precision prefer a slightly higher heating temperature than others on average. The COV for the time duration is much higher than the heating temperature.

For RTFOT 20/30, the G* shows a statistically significant moderately negative relationship with heating temperature, while the correlation for δ is positive. However, for RTFOT 45 /55-80, G* and δ were found to be insignificantly negatively correlated with heating temperature for sample manufacturing. The unaged 45/55-80, on the other hand, has a different tendency compared to aged one at higher test temperatures (PP25), which may be attributed to its stronger relationship (greater r) to heating duration rather than temperature in comparison to other materials.

For manufacturing samples of pure bitumen 20/30, approximately 25% of laboratories exceed the temperature of 160 °C. However, for the PMB in both aged and unaged conditions, approximately 30% of laboratories use temperatures lower than 160 °C, yielding more accurate results in terms of coefficient of variation and standard deviation for G* and δ, respectively, when compared to laboratories using temperatures higher than 160 °C. These comparisons show that the upper limit for pure bitumen (145–160 °C) is likewise appropriate for the PMB. It should be noted that the softening points of all tested materials are near one another.

Contrary to aged 20/30 and 45/55-80, for unaged 45/55-80 the heating duration decreases from 58 min to 50 min when the heating temperature increases from lower than 160 °C to higher than 160 °C. Nevertheless, the differences are insignificant for all test conditions and materials, except for the δ at PP25- 60 °C for unaged 45/55-80.

4.1.6 Storage time of the manufactured specimen

The average sample storage time for laboratories is very widely distributed, especially for the first two years of the round-robin tests and for pure bitumen compared to modified bitumen. In all the rounds, the labs. with better precision have a slightly shorter waiting time on average after removing the extreme values. A relatively higher storage time is obtained for 20/30 compared to other materials, due to two laboratories having a time delay as high as 7 and 14 days. However, both mentioned laboratories generate data with good precision and have used similar sample manufacturing methods (mould), with two different brands of equipment a heating temperature as high as 160 °C and 150 °C, and duration of up to 70 min and

60 min, both of which are close to the average of the corresponding round (157 °C and 69 min).

According to EN 14770 (2012), the maximum delay recommended is 72 hours regardless of the type of bitumen, with a minimum storage duration of 2 and 12 hours for pure and polymer-modified bitumen, respectively. Nevertheless, labs with better precision prefer to wait for less than 2 hours for pure bitumen and at least 12 hours for PMB. The three days of waiting time was exceeded with no significant effect on results.

The statistical tests were conducted to examine the differences in results by the three categories of waiting time applied by laboratories: waiting time shorter than 2 hours in case of unmodified bitumen and 12 hours for PMB, medium waiting time between 2 and 72 hours, and waiting time equal or longer than 72 hours.

In most test conditions, a long waiting time resulted in a higher G*, and a lower δ compared to the short waiting time. However, there are statistically significant differences only for 45/80-55 in unaged conditions as follows: for the G* at test condition PP08- 20 °C between long waiting time and medium, and at 50 °C and 60 °C with PP25, between the long and short waiting time. For the δ, a significant difference was found only at PP25- 65 °C.

4.1.7 Specimen bonding temperature

The result shows that only 19%– 30% of labs with better precision prefer to place the sample in a refrigerator before de-moulding, which can be due to the former knowledge and experience of the operators about the material. For neat bitumen, the chosen temperature range for bonding bitumen follows the recommended upper limit, while PMB exceeds the limit.

The bonding temperature used for the modified bitumen is slightly higher. The duration of the bonding sample is wildly varied for all sample materials However, it does not exceed 30 min except for one laboratory for bitumen 20/30, which is delayed by 45 min. An average of around 15.2 min for pure bitumen and around 12.6 min for modified bitumen are preferred for better precision.

Regardless of the precision of the participant's reported results, a slightly higher bonding temperature is chosen for the modified bitumen than pure bitumen, regardless of their softening point. The duration of the bonding sample is wildly varied for all sample materials (1– 30 min); only one laboratory for bitumen 20/30, is delayed by 45 min. Labs prefer an average duration of around 16 min for neat bitumen and around 13 min for modified bitumen. Pearson’s correlation test shows a positive relationship between the G* and bonding duration for 20/30 and a negative relationship for 45/55-80 regardless of ageing condition. However, this is significant at 40 °C and PP25 for RTFO aged 45/55-80.

Based on Pearson's correlation test results, there are negative relationships between the bonding temperature used by participants and the G* for RTFO-aged bitumen, which are significant. However, for unaged bitumen, the bonding temperature positively correlated with the G* across test conditions, although this impact peaked statistically at PP25- 40 °C. This effect might be brought on by the ageing of fresh bitumen at higher bonding temperatures. The result of the correlation test between the δ and bonding temperature indicates a positive relationship at test temperatures between 40 °C to 65 °C for all the materials. However, the relationship between these variables is negative, for 45/55-80 at test temperatures between 10 to 20 °C. For the δ similarly to G*, for most test conditions, the larger coefficient of correlation is indicated with bonding temperature rather than bonding duration.

Additionally, a statistical test was conducted to examine the differences in G* by three bonding temperature spans used by laboratories. The chosen temperature spans are lower than the SP of the tested materials (25– 55 °C), around SP (55– 75 °C), and higher than SP (80– 90 °C). For both RTFO-aged bitumen, the G* value is higher for a bonding temperature lower than the softening point (25– 55 °C), compared to the higher softening point (80– 90 °C) for almost all test conditions. Significant differences (p-value < 0.05) were found among half of the test conditions, indicating the need to maintain unambiguous upper and maybe lower bonding temperature limits.

It should be noted that this result is based on data from RR tests that were performed before the release of the latest version of EN 14770 in 2023. The bonding temperature was updated as 5 °C to 20 °C above the softening point in EN 14770:2023. The softening point plus (20 ± 5) °C, or at (90 ± 5) °C whichever is the lower was specified as the bonding temperature in the previous version EN 14770:2012.

4.2 Study II: Effects of various DSR testing methods on the measured rheological properties of bitumen

The results of Study III are presented here briefly; the full paper describing Study II is in Appendix III.

4.2.1 Evaluation of studied factors; affecting factors

The effects and standard errors of the selected factors were calculated at frequencies of 0.1 rad/s and 10 rad/s at temperatures between 0 °C to 80 °C for 50/70 and 70/100, and 0 °C to 70 °C for 160/220. Results show that the complex modulus is more sensitive to the variation in studied factors than the phase angle. Almost the same

pattern is observed in terms of the significance of effects comparing the lower and higher tested frequencies. The bonding temperature is the most evident factor affecting G* and δ followed by oven heating temperature contrariwise in the case of the 160/220_I. As the two bonding temperature levels are not very high, the higher G* and lower δ cannot attributed to ageing but better adhesion between the bitumen and plates in temperature slightly above the softening point. The variation in oven heating temperature strongly affected the results of the 160/220_I contrary to all other materials. The master curve of this bitumen also showed a weak overlapping on shifted temperature, which may hint that it had a different natural chemical component. Comparing the bounding temperature effect at a frequency of 10 rad/s and the first tested temperatures of the 3 samples used for the T-f-sweep tests indicates that, the bonding temperature effect is not significant at the higher tested temperature for both G* and δ. Trimming the sample tested at lower temperatures of 0 °C to 30 °C for all tested materials tends to significantly increase the δ and decrease the G*, which indicates higher sensitivity of PP08 to trimming. Higher G* in without trimming can be due to more amount of excess material left on the plate's periphery compared to the trimmed one. The BT has a negative relationship with measured G* at medium test temperatures for 70/100 and almost on all the evaluated temperatures for 50/70 and 160/220_II.

In 2-way interaction, for G*, Trim:BT has the strongest effect on all materials and temperatures except for 160/220 at lower temperatures where Trim:HT affects more. For δ, the most effective two-way interaction was Trim:BT for 70/100 and 160/220_II. For 160/220_I the Trim:HT, and for 50/70 the BT:HT is the least important factor for δ. However, the interaction effect Trim:BT may only be relevant at the first temperatures measured after bitumen is loaded onto the plates. Except for 160220_I, HT does not generally have a statistically significant impact on the results, unless it interacts with other parameters. This may be attributed to the fact that the range of oven heating temperature (SP+80 and SP+100°C) in this study is very small. According to the findings, the parameters under investigation have varied degrees of influence on G* and δ.

The bar chart shows the percentage contribution of the effects to outcomes |G*| (Figure 14) and δ (Figure 15) at f= 10 rad/s which is calculated by dividing each effect by the total of all effects in a set of tests, to compare and estimate the share of the variation that could be attributable to a particular factor across the tested materials. It observed that outcomes from higher test temperatures tend to be more susceptible to fluctuations in test conditions (different effects). The three-way interaction has the most contribution share for bitumen type 160/220_II. The BT and HT have the most contributions for 160/220_I, and Trim:BT is the most contributor to 70/100. For 50/70 the main effects (Trim, BT, and HT) appear to have the most contribution.

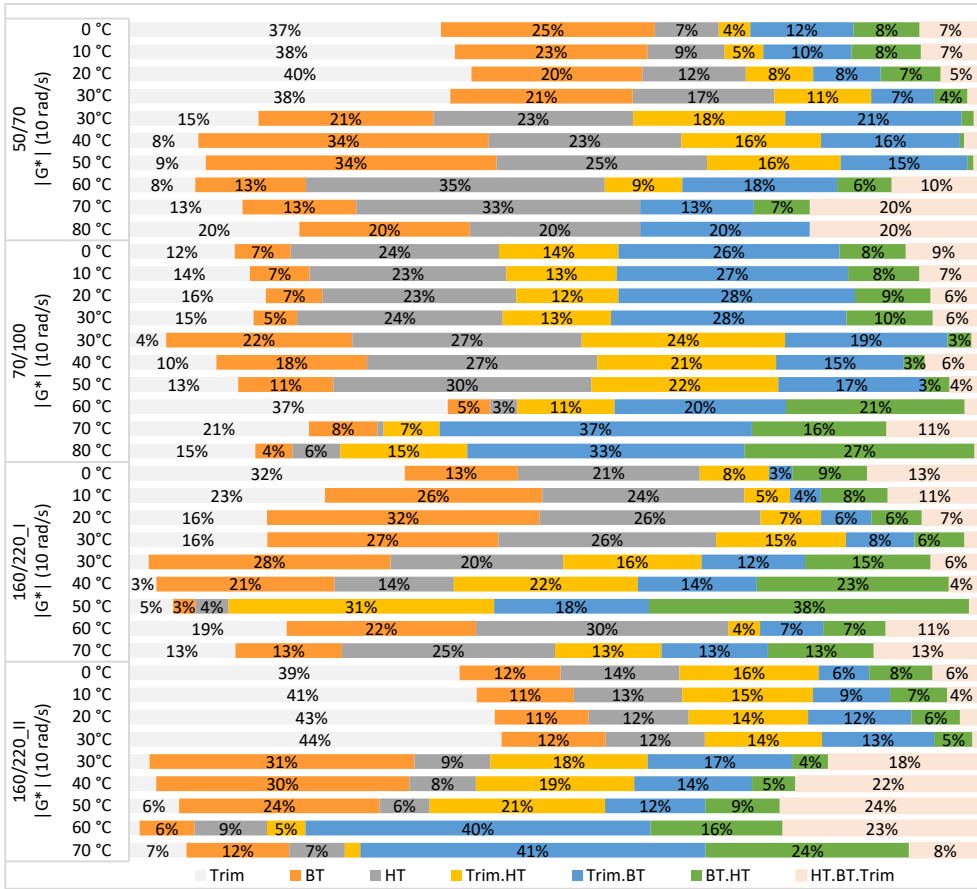

Figure 14. The percentage contribution of effects to the variation in |G*| at tested temperatures and materials.

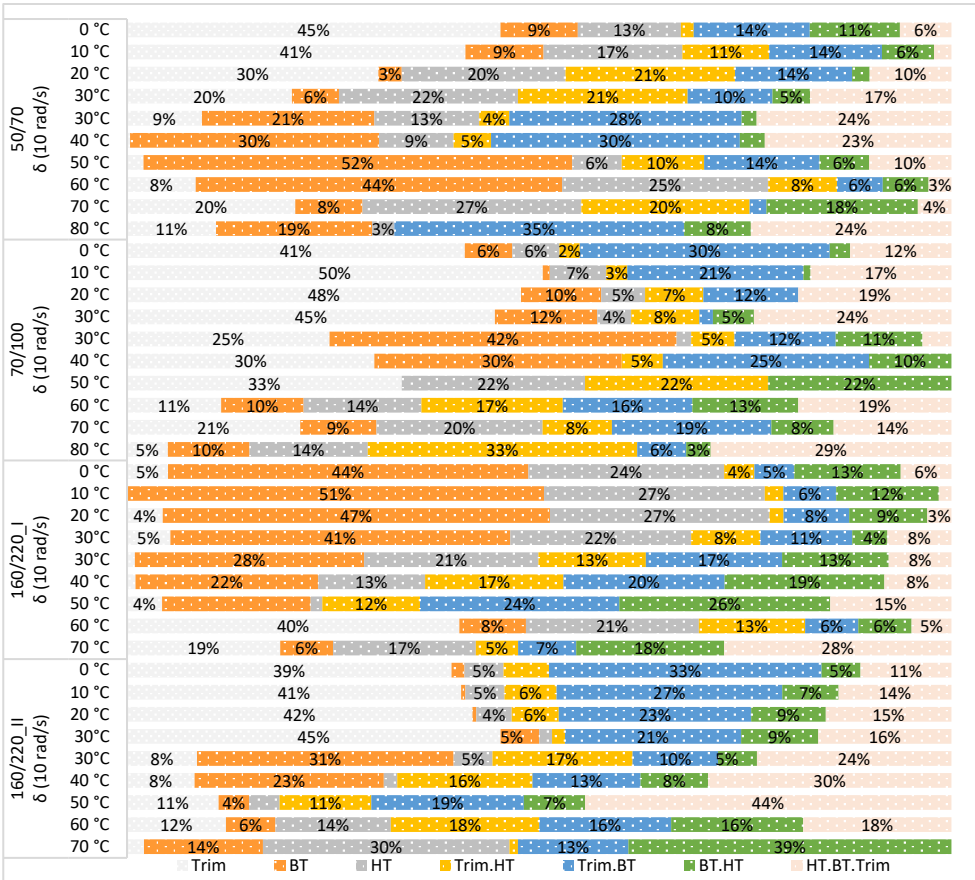

Figure 15. The percentage contribution of effects to the variation in δ at tested temperatures and materials.

4.2.2 Evaluation of rheological behaviour (2S2P1D Model)

The observed pattern in complex modulus master curves, phase angle master curves, and black diagrams (complex shear modulus versus phase angle) plots suggests that tests with three different components at two tested levels provide nearly similar results. According to the 2S2P1D model, the significant differences observed between different runs are not between two extreme sets of conditions i.e., 1 and 8, 2 and 7, 4 and 5, or 3 and 6 in standard run order, except for 160/220_I. The 160/220_I showed significant differences between two runs of 3 and 6; significantly higher β, α, and G∞ when the sample was manufactured at a lower temperature, bonded onto DSR at a higher temperature, and trimmed compared to the opposite conditions. Paper III, appendix III, displays statistically significant variations between eight runs for 2S2P1D parameters (G_∞, k, h, α, τ, β, log τ) across all investigated materials.

4.3 Study III: Assessing the effect of specimen preparation methods on DSR test results of bitumen using factorial design analysis

The results of Study III are presented here briefly; the full paper describing Study III is in Appendix III.

4.3.1 Repeatability evaluation of test result

Tables 3 and 4 show the calculated Mean and repeatability for measured outcomes (G*, δ, TX and δ_{TX}) with DSR from 8 test combinations. The repeatability of wax-modified bitumen was significantly affected by test conditions. The neat bitumen showed a smaller range of variation for r than modified ones.

Table **3.** Estimated Mean and repeatability for TX (°C) and δTX (°).

Material	$T_{\|G^*\|=5\ MPa}$		$T_{\|G^*\|=15\ kPa}$		$T_{\|G^*\|=1\ kPa}$		$\delta_{T\|G^*\|=5MPa}$		$\delta_{T\|G^*\|=15kPa}$		$\delta_{T\|G^*\|=1\ kPa}$	
	Mean °C	r °C	Mean °C	r °C	Mean °C	r °C	Mean (°)	r (°)	Mean (°)	r (°)	Mean (°)	r (°)
50/70	15.5	0.8	50.3	0.8	70.3	0.8	46.2	0.9	73.9	0.3	83.7	0.4
160/220	7.5	2.1	39.7	0.7	57.3	1.5	41.8	3.1	71.2	0.8	81.8	0.7
70/100	13	1.7	48.2	0.4	61.1	0.5	45.9	1.7	73.8	0.4	83.8	0.3
70/100+4%SBS	14.4	1.3	55.3	0.8	79.3	0.6	42.9	1.5	65.4	1	81.1	2.1
70/100+4%Wax	23.2	3.4	70.9	1.9	84.2	1.9	33.9	2.8	42.8	4.9	56.8	2

Table 4. Estimated Mean and repeatability for |G*| (%) and δ (°).

Material	Mean kPa	r %	Mean kPa	r %	Mean kPa	r %	Mean (°)	r (°)	Mean (°)	r (°)	Mean (°)	r (°)
50/70	**@ 20 °C**		**@ 50 °C**		**@ 70 °C**		**@ 20 °C**		**@ 50 °C**		**@ 70 °C**	
	2434.1	14	15.8	12	1	9	50.7	1.2	73.7	0.4	83.6	0.2
160/220	**@ 10 °C**		**@ 30 °C**		**@ 50 °C**		**@ 10 °C**		**@ 30 °C**		**@ 50 °C**	
	3544.7	25	73.7	21	2.9	12	43.8	3.5	63.4	2.9	78.1	0.7
70/100	**@ 20 °C**		**@ 45 °C**		**@ 60 °C**		**@ 20 °C**		**@ 45 °C**		**@ 60 °C**	
	1638.8	31	23.5	6	2.9	5	52.5	0.7	71.9	0.5	80.5	0.2
70/100 +4%SBS	**@ 20 °C**		**@ 50 °C**		**@ 70 °C**		**@ 20 °C**		**@ 50 °C**		**@ 70 °C**	
	2169.4	18	27.3	9	2.7	6	47.7	1.0	61.3	1.1	76.3	1.4
70/100 +4%Wax	**@ 25 °C**		**@ 65 °C**		**@ 80 °C**		**@ 25 °C**		**@ 65 °C**		**@ 80 °C**	
	4143.2	34	54.9	20	2	21	34.8	2.8	36.6	4.3	52.6	2.2

4.3.2 Evaluation of studied factors; affecting factors

According to the results, TX has 42 statistically significant effects, whereas δ_{TX} has 26. However, comparing the SE reveals that the outcome phase angles (δ_{TX} and δ) for modified bitumen vary more than they do for unmodified ones, with ranges of (0.3– 0.63°) and (0.18– 0.88°), respectively. This shows that modified bitumen is more sensitive to variations in testing settings than unmodified bitumen. The chosen levels for the studied factors are quite near to each other, hence very few significant impacts were expected. Nonetheless, TX may be a better option for result expression than |G*| because it is derived from two distinct data points, which could explain the higher consistency across tested materials.

The results show that, when PP08 was used, the $T_{|G^*| = 5\ MPa}$ values increased significantly in the specimen preparation technique without trimming compared to the specimen with trimming. When specimens are not trimmed, the measured |G*| values arise also. Except for bitumen 70/100 and 70/100+4%SBS, there was no significant difference in $T_{|G^*| = 15\ kPa}$ and $T_{|G^*| = 1\ kPa}$ values between the trimming and non-trimming techniques when PP25 was used for the testing. Trimming the specimen in the case of SBS-modified bitumen was difficult, even in the case of PP25, which is easier than PP08 due to the greater diameter and lower height of the specimen. The bitumen was rubberized, and a small amount of bitumen was pulled out or an excess amount of barely noticeable bitumen stuck around the outside perimeter of the DSR plates during trimming while attempting to avoid overheating the spatula for trimming. Interestingly, low, and high bonding temperatures alone did not influence TX values, but when combined with trimming, the effect became statistically significant; higher TX values were recorded when the specimen was bonded in SP+25 °C and not trimmed. HT and BT appeared to have greater effects than the trimming state on measured outcomes when tested at intermediate and higher temperatures with PP25. According to the coefficient of the main effect BT, increasing the bonding temperature from SP (low level) to SP+25 °C (high level) decreased the measured values of $\delta_{T|G^*| = 5\ MPa}$ and $\delta_{T|G^*| = 15\ kPa}$ for almost all of the tested materials. This means higher elastic behaviour of the bitumen could be concluded when bonded at a higher temperature than at a lower temperature. For all tested materials, the effect of HT appeared to be minimal on $\delta_{T|G^*| = 5\ MPa}$. As for the wax-modified bitumen, HT had a substantial impact on the measured δ at higher test temperatures, resulting in a lower $\delta_{T|G^*| = 1\ kPa}$ value with a higher heating temperature SP+100 °C compared to the lower heating temperature SP+80 °C. The increased viscous behaviour at higher test temperatures cannot be attributed to the ageing of bitumen because the material was not subjected to extremely high temperatures or an extended duration of heating.

Appendix II shows a 3D visualisation of G* for tested bitumen under the three variables examined in this study at frequencies of 0.1, 10, and 100 rad/s, and the three temperatures (lower than SP, about SP, and greater than SP of tested

materials). Across all tested frequencies, the tested material exhibits a similar pattern.

The bar chart shows the percentage contribution of the effects to outcomes |G*| and δ (Figure 16), and TX and δ_{TX} (Figure 17), calculated by dividing each effect by the sum of all 7 effects in a set of tests. This allows us to compare and estimate the share of the variation that could be attributable to a particular effect across the tested materials. The importance of effects is not independent of the type of bitumen, according to the ranking of their contribution to outcomes. However, the results observed at higher test temperatures tend to be more susceptible to fluctuations in test conditions, particularly for modified bitumen. Even though the three main effects are expected to account for a large portion of the variation, interactions between the components also appeared statistically significant, particularly in the case of SBS-modified bitumen for TX and δ_{TX} values. The three-way interaction contributed most bitumen type 70/100 among others.

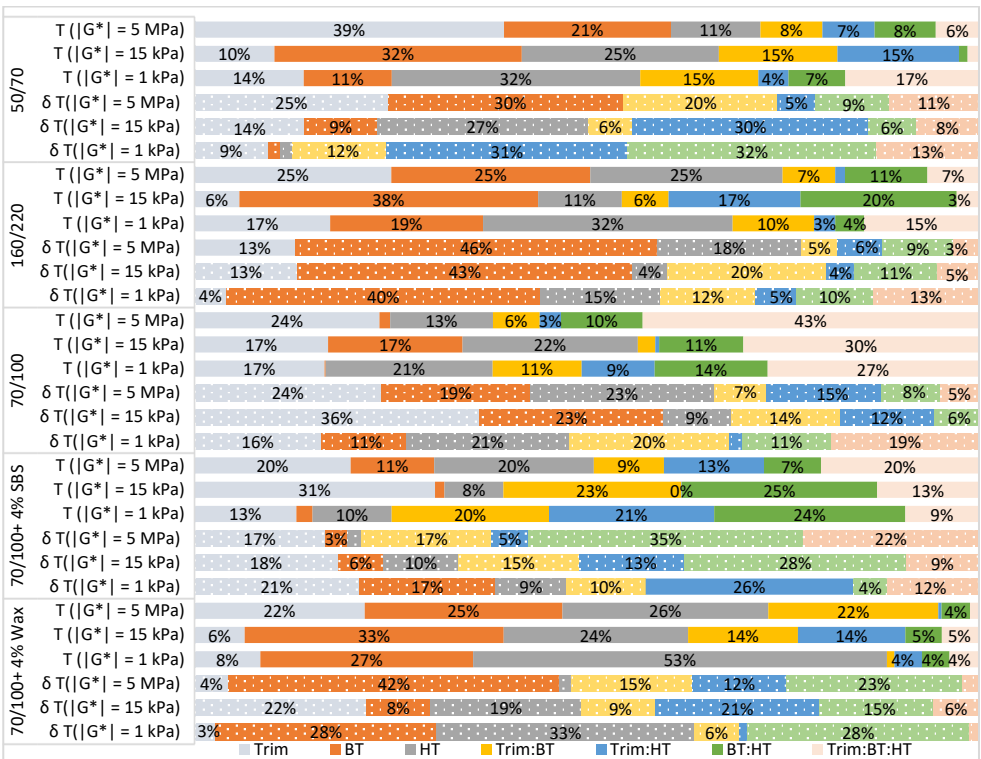

Figure 16. The stacked bar chart shows the percentage contribution of effects to the variation in TX (sold-filled) and δ_{TX} (pattern-filled) at tested temperatures and materials.

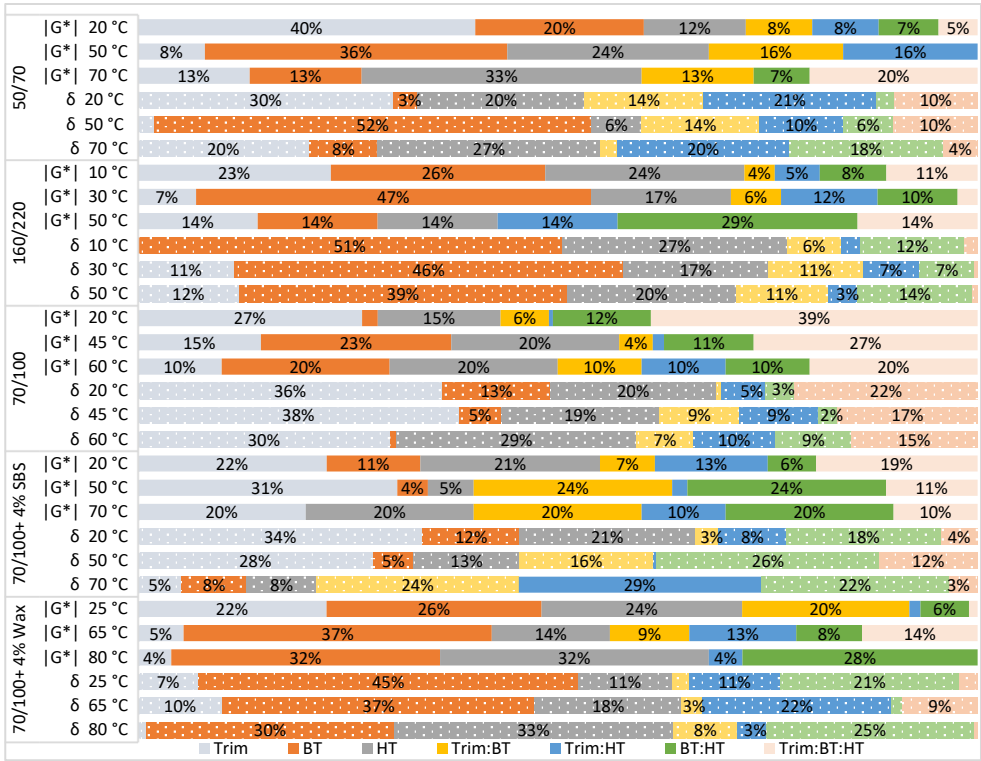

Figure 17. The stacked bar chart shows the percentage contribution of effects to the variation in |G*| (sold-filled) and δ (pattern-filled) at tested temperatures and materials.

4.4 Study IV: Examination of rheological properties of mastic with different types of filler

The results of Study IV are presented here briefly; the full paper describing Study IV is in Appendix III.

4.4.1 Filler properties

The studied fillers obtained from various quarries in Sweden are identified as quartz diorite (D), quartz-rich granite (Q), and monzogranite (G). Table 5 shows the physical properties of the studied fillers. The monzogranite (G) has the largest SSA and the quartz diorite (D) has the lowest SSA. However, the monzogranite (G) has the lowest RV and the quartz diorite (D) has the largest RV. This confirms voids in compacted filler (RV) may be explained by other factors besides SSA, such as

particle shape, size, surface structure, and particle size distribution (Dan et al., 2014; Antunes et al., 2015). The RV result indicates that fillers will have almost comparable stiffening effects in the following order: quartz diorite (D), quartz-rich granite (Q), and monzogranite (G).

Table 5. Properties of fillers.

Filler type (ID)	Specific surface area (m^2/g) ISO 13320: 2020	Rigden voids (%) EN 1097-4	Water content (%) EN 1097-5	Particle density (Mg/m^3) EN 1097-7
monzogranite (G)	0.500	38	0.18	2.64
quartz-rich granite (Q)	0.408	39	0.12	2.67
quartz diorite (D)	0.252	40	0.09	2.89
lime-based active filler Terra E (LE)	Not available	65	1.13	2.85

Figure 18 shows a plane-polarized light microscopic image of studied mineral fillers in grayscale. A summary of the microscopic image analysis of the minerals' shape of fillers is presented in Table 6. The grain shape will contribute to the quality of the interlocking system in mastic (Antunes et al., 2015), e.g., an angular cubic form can lead to good interlocking. The mineral component of filler can also affect the filler's stiffening strength (Cosme et al., 2016). For instance, quartz-rich granite (Q) contains small quantities of iron which can contribute to the hardening of mastic.

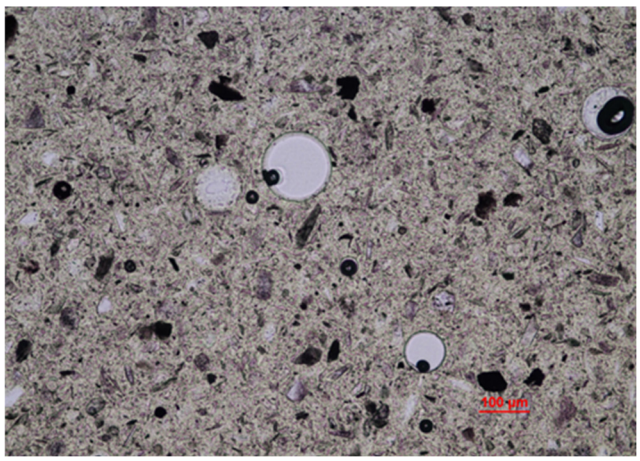

monzogranite (G)

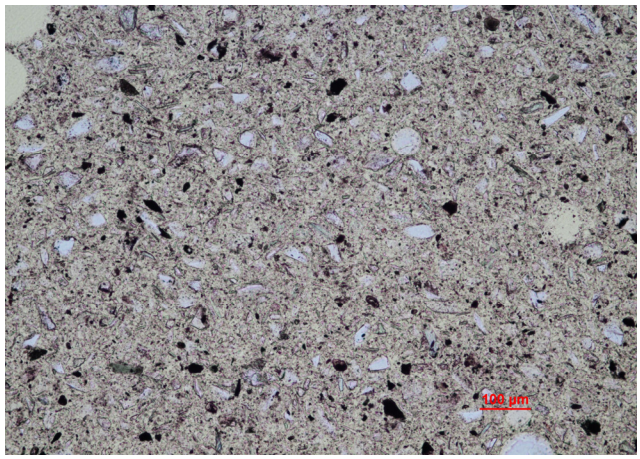

quartz-rich granite (Q)

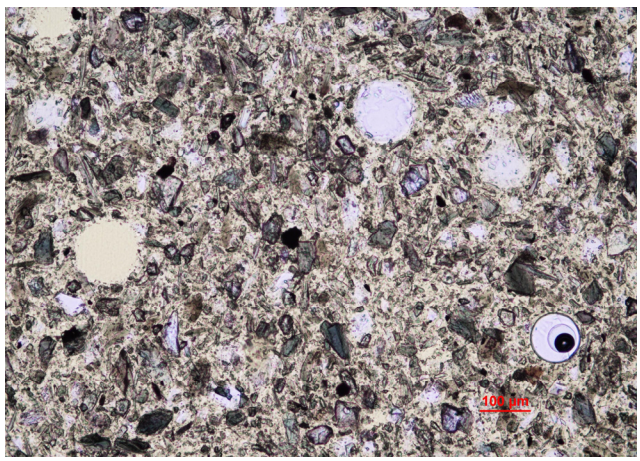

quartz diorite (D)

Figure 18. A black-and-white view of materials magnified by approximately 100 X; a distinct tabular grain structure of D; the light white and grey-white quartz and feldspar grains predominated in the Q's grains; and the "opaque minerals" (nearly black) are prevalent in Q and G.

Table 6. The microscopic image analysis summary.

Filler Type	Observed grain shapes
monzogranite	partly angular, often elongated and not cubic, rectangular and short-length
quartz-rich granite	partly angular, elongated and somewhat flaky, partially angular cubic forms
quartz diorite	tabular form, some cubic grains, elongated, rectangular, and more angular

Table 7 displays the results of grain size studies based on a random sample of about 100 grains per filler, and the estimated volume fractions of minerals based on analysis of roughly 500 grains. The monzogranite (G) has the most elongated grains of quartz and feldspar denoted in bold. In contrast to monzogranite (G), quartz-rich granite (Q) and quartz diorite (D) feature extraordinarily long, narrow mica grains, as indicated in bold. This most likely impacted the grain size (total mean) substantially. The quartz diorite (D) has the highest aspect ratio (3.91), i.e., the largest proportion of long narrow grains can be assumed to occur in this filler, which is followed by the quartz diorite (D) with 3.52, and the monzogranite (G) with 2.96.

Table 7. Aspect ratio (Length/Width) and the estimated volume fractions of minerals for corresponding filler type. The greatest aspect ratio per mineral and the dominant mineral are denoted in bold.

Filler type (ID)	monzogranite (G)		quartz-rich granite (Q)		quartz diorite (D)	
Mineral	L/W avg.	Mineral Vol.%	L/W avg.	Mineral Vol.%	L/W avg.	Mineral Vol.%
Quartz	**4.3**	32.0	2.9	**58.0**	2.4	7.0
Feldspar	2.3	**52.0**	1.7	32.0	2.2	32.0
Mica, biotite/muscovite	2.6	10.6	**8.2**	4.9	**6.8**	8.0
Amphibole/pyroxene	-	1.7	-	0.0	2.3	**50.0**
Opaque minerals	-	2.7	-	4.1	-	1.8
Miscellaneous	-	0.6	-	0.5	-	0.8
Total mean value	2.96	100 %	3.52	100 %	3.91	100 %

Figure 19 presents the volume-weighted particle size distributions measured using the Malvern Laser Diffraction Sizer. In cumulative and frequency distribution plots the Dv(50) is the volume-weighted median. The D[4,3] represents the volume-weighted mean diameter of particles and the Span indicates the dispersion width of the particle size distribution. The consistency of particle size uniformity increases with decreasing the Span value. The monzogranite (G) has the highest content of finer particles (<0.02 mm), while the quartz diorite (D) has the highest content of coarser particles (>0.02 mm). Brown et al. (1997) stated that the percentage of mineral filler smaller than 0.02 mm has no bearing on the stiffening of the mastic. Shao et al. (2005) observed bitumen mastics' effect on pavement performance is more dependent on average particle size and density than on the percentage of particles smaller than 0.02 mm and the mineral composition. The quartz diorite (D)

has the lowest span value (2.45) among studied mineral fillers indicating that it includes more particles of very similar size, as well as the largest grain based on microscopic morphological analysis, resulting in larger porosity, i.e., the highest RV (40%). The monzogranite (G) has the largest span value (3.20) and highest content of finer particles which led to a dense graded filler with the lowest RV (38%).

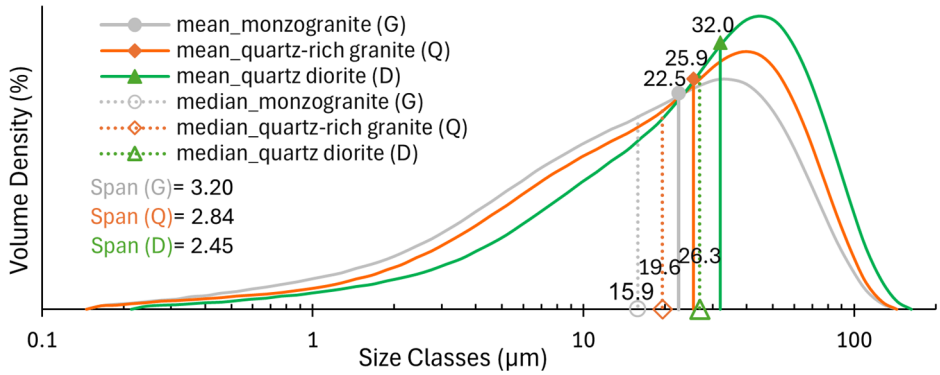

Figure 19. Volume-weighted particle size distributions.

4.4.2 Physical behaviour of Mastics

Figure 20.a illustrates the $\Delta T_{R\&B}$, assessment of the stiffening rate change by adding the fillers to the tested bitumen. The $\Delta T_{R\&B}$ increases rapidly for the monzogranite (G) after F/B of 50% (13.0 to 20.2 °C), while for the quartz diorite (D) it increases slower after F/B of 50% (18.4 to 27.2 °C). This can indicate a decreasing bitumen filler bond for the quartz diorite (D) by increasing the dosage of filler, which can be due to its larger particles that begin to come close to each other without having enough bitumen left to cover them and bond them to each other with more bitumen adsorbed in the surface of the fillers due to the higher RV of the quartz diorite (D). This also can be an effect of particle size. For monzogranite (G) more bitumen is needed to cover the higher SSA, while for quartz diorite (D) with lower SSA, there will be an excess of bitumen, however, the larger and more oblate-shaped grains are less prone to move, thus contradicting that there is more bitumen in the free volume. Figure 20.b shows the result of the hardness-related property change by adding the different fillers to the tested bitumen with a penetration value of 72 (0.1mm). The monzogranite (G) showed the lowest and the quartz diorite (D) highest stiffening (hardening) effects according to the penetration test results. The penetration values decrease more rapidly for the monzogranite (G) by F/B ratio increases compared to the other two. Since mastics with monzogranite (G) tend to have more particles (finer particles) than with the other two fillers, the needle can pass through it with more difficulty during the test.

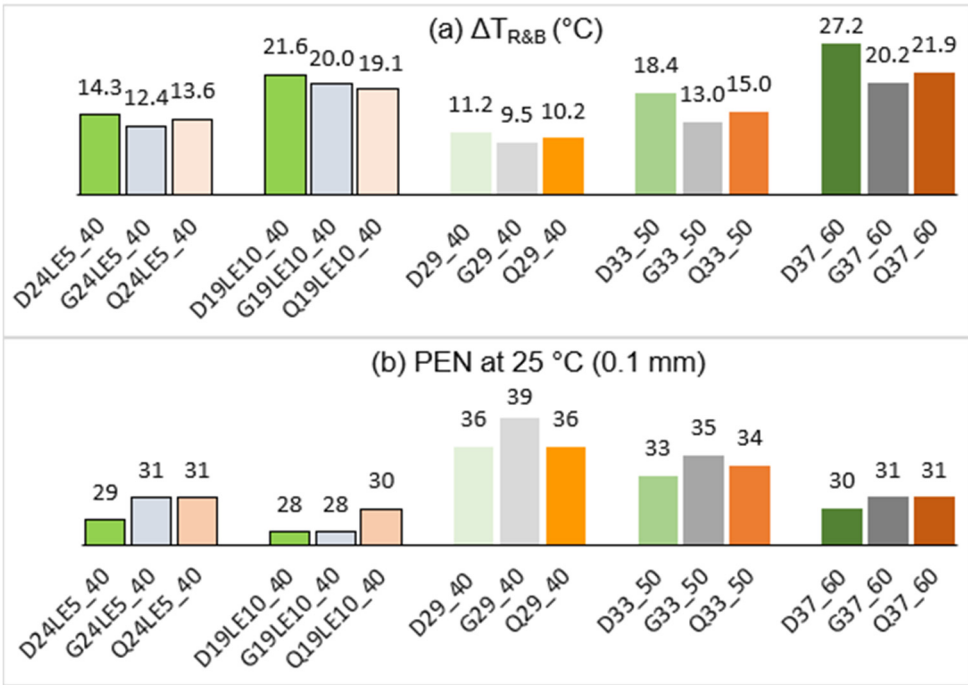

Figure 20. Illustration of mastics stiffening rate change by adding the fillers to base bitumen with an SP of 50 °C; Softening point test differences (a) and hardness-related property according to the PEN test.

The $\Delta T_{R\&B}$ (softening point) results do not completely agree with penetration results regarding the degrees of stiffness of fillers relative to each other. For instance, comparatively lower $\Delta T_{R\&B}$ (softening point) than expected were measured for Q29_40 (50+10.2 °C) compared to D29_40 (50+11.2 °C), and for G37_60 (50+20.2 °C) compared to Q37_60 (50+21.9 °C) considering the penetration test results. This slightly lower softening point can be explained by the fact that these mastic particles tend to separate from bitumen more easily because of the possible agglomeration between particles due to their higher finer particle content. For mastic with active filler LE, weaker physical-chemical interactions, allow the steel ball to cross the asphalt mastic more easily. These also could be because the mastics contain fillers with a greater volume of finer particles and specific surface areas that need to be coated with bitumen, which induces the formation of a bitumen mastic with lower resistance to the passage of the steel ball during the R&B test (Bastidas-Martínez et al., 2021).

Figure 21 illustrates the softening point against PEN. The stiffening effect increases with an increase in the F/B ratio. The increase in softening point and the decrease in the penetration values when fillers were partially replaced with LE at the F/B of 40%, was expected due to the physical-chemical interactions with the bitumen. However, the stiffening effect of the LE varies with the filler type and content of

the LE. At 5% content of LE, the mastic including the quartz-rich granite (Q) has stiffened drastically, however, at 10% content of LE the mastic containing the monzogranite (G) has stiffened significantly compared to other fillers.

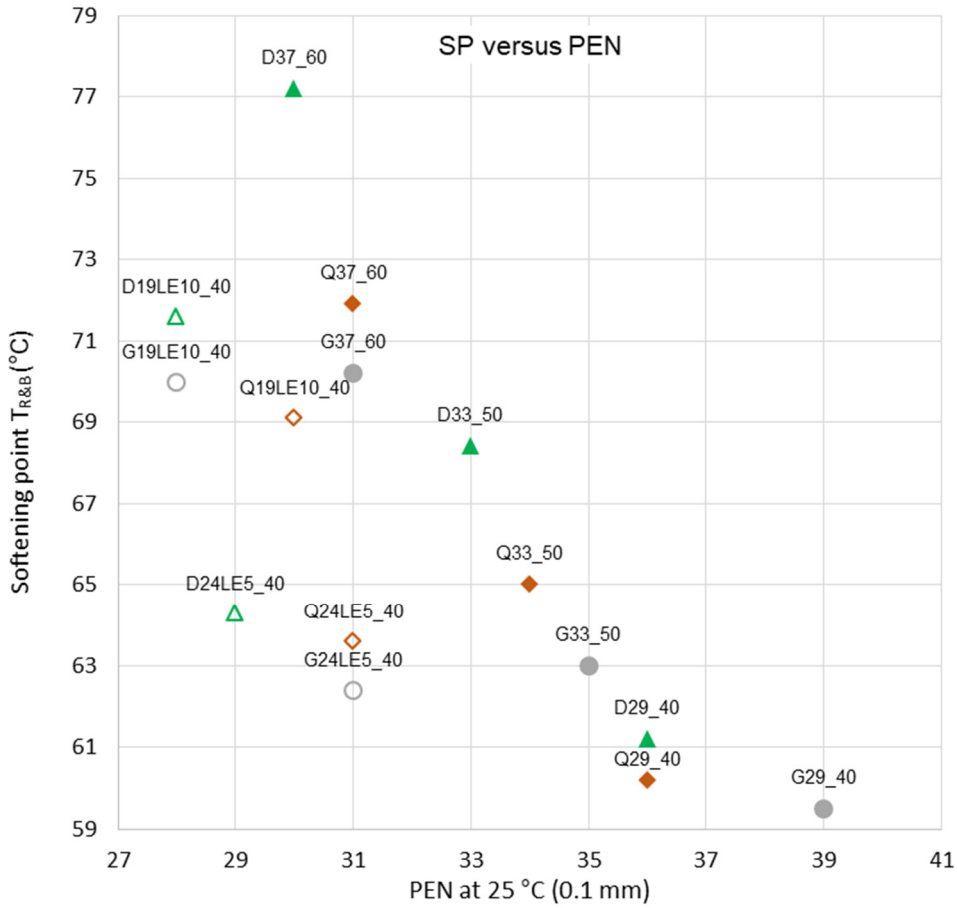

Figure 21. Plot of softening point ($T_{R\&B}$) against PEN at 25 °C.

4.4.3 Rheological behaviour of Mastics

Figure 22 illustrates the collected data and master curves for (a) the complex shear modulus and (b) the phase angle. At the F/B of 40%, the D29_40 (D40) has a slightly higher |G*| than the other fillers in the absence of LE, but all three overlap. At the F/B of 40% with 5%LE, the Q+LE has a higher |G*| than the other. At the F/B of 40% with 10%LE a similar tendency is observed when fillers are substituted with 5% LE, nevertheless, with 10%LE the Q+LE has a notably greater stiffening impact than the other two combinations across all frequencies (low to high). The partial

replacement of fillers with LE leads to further stiffening of the mastic for all three types, noticeable by the upward shift of the curves. A material's viscous and elastic properties are measured by the δ, which ranges from 0° for perfectly elastic materials to 90° for completely viscous materials. A slightly greater decrease in the phase angle for the Q+LE is observed compared to the D+LE and G+LE at frequencies between 10^{-4} and 10^{2}, i.e., the Q+LE has slightly more elastic behaviour. However, the master curves of phase angles at F/B of 40% for the three types of filler Q29_40, D29_40, and G29_40 overlap. The partial replacement of fillers with LE leads to the further elastic behaviour of the mastic for all three types, noticeable by the downward shift of the phase angle curves. At the F/B of 50%, the three fillers' stiffening curves are close to each other but have changed the ranking based on their |G*| values across the frequencies. The quartz-rich granite (Q) has a larger variation in viscous behaviour (phase angle curves) over frequencies than other fillers at the F/B of 50%. At the F/B of 60%, the observed ranking is almost similar to the F/B of 40% with a stiffer response. At lower frequencies for the quartz diorite (D) a slight upward shift in the |G*| master curve, and for quartz-rich granite (Q) a stronger viscous behaviour (upward shifts in the δ master curve) can be observed.

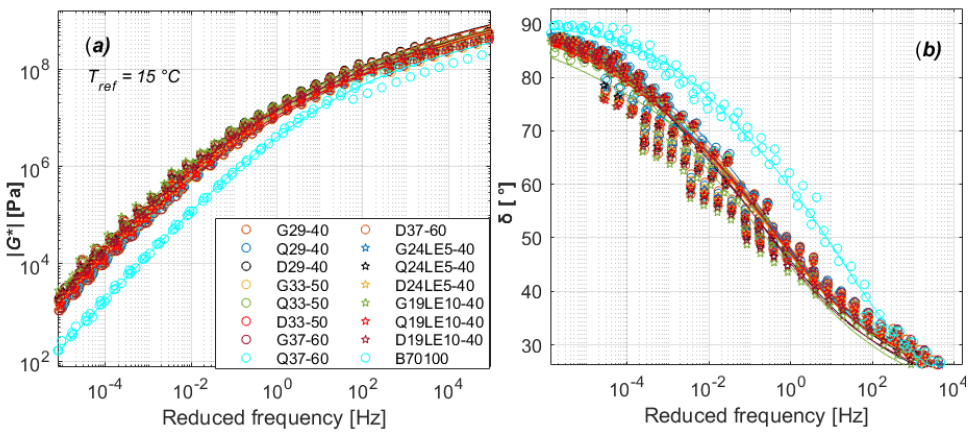

Figure 22. Measured rheological parameters and master curves;|G*| (a), δ (b).

Overall, the results presented in Figure 22 indicate that adding more filler leads to a greater stiffening effect, with all stiffness master curves shifting upwards and phase angle master curves shifting downward. For phase angle master curves, there are a few obvious differences in ranking pattern throughout the presented frequencies especially in the absence of LE, showing that the phase angle attribute is impacted more by the F/B than the filler type. Furthermore, the master curves in each F/B content overlap well, especially for 40% and 50% with a variation of about ± 3°. The explanation for these differences in ranking could be ascribed to the bitumen-filler interaction and filler compatibility with the bitumen, which resulted in varying

viscoelasticity. Also, slightly greater variation between mastics is observed in lower frequencies than in higher ones due to the larger difference in viscoelasticity between bitumen and filler at higher temperatures (lower frequencies). The phase angle decreases at very low frequencies for all the mastics which can be attributed to measuring the filler with elastic behaviour rather than mastic at higher temperatures, where bitumen flows out of the gap.

Figure 23 illustrates the temperature (TX) where complex shear modulus |G*| equals 15kPa ($T_{|G^*|=15kPa}$) at 10 rad/sec, and the softening temperature from the ring and ball method. It is not expected the $T_{|G^*|=15kPa}$ would match the mastic softening point rather than a reasonable comparison of the stiffening strength of different fillers. The difference between $T_{R\&B}$ (50 °C) and $T_{|G^*|=15kPa}$ (48 °C) is 2 °C for the neat bitumen. This difference varies depending on filler type, for instance, at the F/B of 40%, the difference rises from 2.1 °C to 3.2 °C across the mastics, but it also increases with the F/B ratio increase. The ring and ball test considerably overestimates the stiffening strength of the quartz diorite (D) at F/B of 50% and 60%. Furthermore, at 10% LE content, the stiffening strength of fillers obtained from the two methods relative to each other is mismatched for the quartz-rich granite (Q). The ring and ball test underestimates the Q19LE10 stiffening strength compared to $T_{|G^*|=15kPa}$. The difference in the results from methods indicates a new level of |G*| depending on the F/B ratio is needed to estimate the softening point, which also can be attributed to the inability (insufficient accuracy) of the ring and ball test to determine the stiffening impact at higher F/B concentrations (50% and 60%) and mastics with active filler (10% LE).

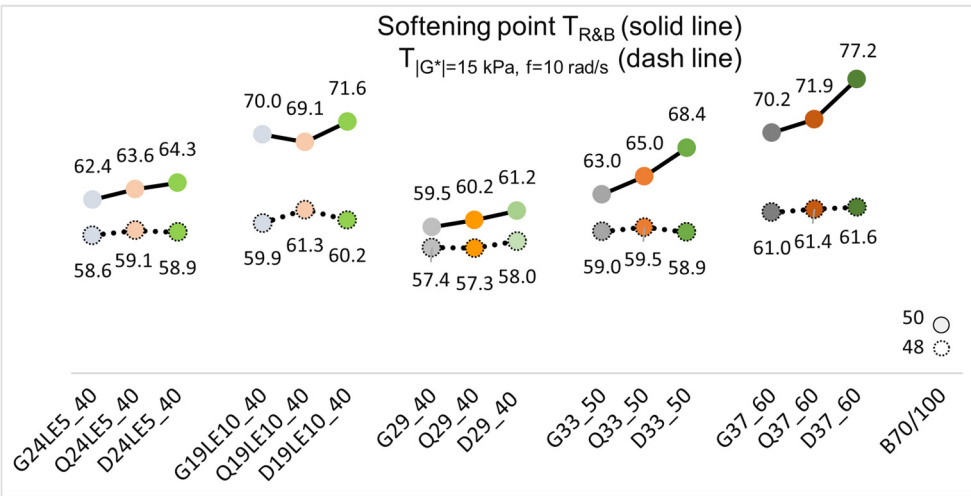

Figure 23. Comparison of physical and rheological parameters measured for mastics.

To resist rutting and deformation, the complex shear modulus elastic portion G′ should be large (larger G* and smaller δ). Therefore Superpave (SHRP) limits the rutting parameter to 1000 Pa (G*/sin δ ≥ 1.0 kPa) for unaged bitumen. However, 1 kPa is a low threshold for mastics and may require new higher levels, depending on the F/B ratio. The result indicates that the SHRP's upper-temperature limit increases with increasing the F/B content ratios. It increases from 79.0 to 83.6 °C for quartz diorite (D), from 78.5 to 82.9 °C for monzogranite (G), and from 79.1 to 83.9 °C for quartz-rich granite (Q). The mastics with filler type G containing a higher portion of finer particles are the least resistant to rutting among the studied mastics. This is consistent with a previous study (Muniandy et al., 2012), that mastic with medium to coarse particle size exhibited greater rutting resistance than mastic with fine particle size. The stiffening effect of increasing F/B from 40% to 60% is a continuous increase of T|G*|/sin δ for D, while for mastics including quartz-rich granite (Q) and monzogranite (G), it slows down a bit after F/B of 50% (φ=33%). This could be because the quartz diorite (D) contains comparatively larger particles, which exposes it to filler-to-filer contact at higher content, i.e., the quartz diorite (D) reaches the critical φ at a higher filler concentration. The mastics become even more rutting resistant when 5% and 10% of the fillers at the F/B of 40% are substituted with LE. The upper- temperature increases to a range from 80.9 °C to 81.6 °C for quartz diorite (D), 80.5 °C to 81.3 °C for monzogranite (G), and 80.7 °C to 82.2 °C for quartz-rich granite (Q) for 5% and 10% LE is presented.

4.4.4 Bitumen–filler interaction parameter analysis

Figures 24 show the numerically calculated interaction degrees C= $\frac{|G^*_{mastic}(\omega)|}{|G^*_{bitumen}(\omega)|}$, utilizing the complex shear modulus ratios at three different volumetric F/B of (29/71), (33/67), and (37/63), over a wide range of temperatures (−10 °C to 90 °C) and frequency of 10 rad/s and 0.1 rad/s. A logarithmic scale is chosen for interaction degree C to allow for the easy visualization of rates of change across temperatures.

The result shows that the C parameter increased by the F/B ratio for all filler types. The quartz diorite (D) has the highest and the monzogranite (G) has the lowest C values over almost all tested temperatures at the filler volume fraction (φ) of 29% and 37% (F/B of 40% and 60%). The quartz-rich granite (Q) at F/B of 50% interacts better with bitumen at lower temperatures and at F/B of 40% and 60% at higher temperatures. Across tested temperatures, the C values were also improved for all three mastics at the F/B of 40% (φ=29%) when it is partly replaced with LE, especially for mastics with quartz-rich granite (Q). This indicates that the interaction between bitumen and filler type Q+LE is stronger than filler types D+LE and G+LE. This could result from the higher SSA of the quartz-rich granite (Q) (0.408 m^2/g) than the quartz diorite (D) (0.252 m^2/g) for better adsorption of the bitumen, also in the case of fillers with similar SSA mastic containing LE forming a stronger bond

with quartz-rich granite (Q) than monzogranite (G) which can be due to the difference in the mineralogy (Table 7). The drastic improvement in the C value when replacing 5% LE with the quartz-rich granite (Q) in the mastics at F/B of 40% (φ=29%) can be attributed to a change in physico-chemical characteristics of the mastic modified with LE which resulted in an increased basic component when part of the quartz-rich granite (Q) which contains the highest amount of quartz and lowest was replaced with LE. This increase in the basic component made the mastic more favourable for acidic-natured quartz-rich granite (Q). The trend continues with replacing quartz-rich granite (Q) with 10% LE, where mastic displays an even higher basic component, and the acidic component is further reduced. This increase in the basic component and decrease in the acidic component makes the bitumen/mastic more favourable to forming a strong bond with the acidic-natured quartz-rich granite (Q). Similar conditions arise for monzogranite (G) at 10% LE content but are less obvious than for quartz-rich granite (Q) because monzogranite (G) is less acidic.

The temperature sensitivity of interaction degree C shows a more noticeable difference between fillers at the lower frequency of 0.1 rad/s (Figure 24.a). At low temperatures or higher frequency (10 rad/s), the fillers' ability to strengthen the complex modulus of the bitumen mastic becomes less pronounced, as the mineral filler exhibits elastic behaviour with a constant modulus, in contrast, the bitumen displays viscoelastic behaviour with a high modulus at low temperatures. Consequently, C demonstrates a speedy declining pattern with decreasing temperature (20 °C to −10 °C). While at high temperatures, the C values generally increase with increasing temperature (60 °C to 90 °C), due to the stiffness contrast between the filler and bitumen phases being highest, especially at high volume fractions, i.e. φ=37%, where the interaction of the particles stiffening effect also may happen. At intermediate temperatures (30 °C to 50 °C) the clear increasing trend disappears, this can be due to the more elastic nature of the bitumen just below its softening point (50.0 °C), which results in the generation of internal stress in the sample when sandwiched between the DSR plates and that make slightly higher G* of bitumen. The lowest temperature impact belongs to mastics with G, which has the smallest average grain radius compared to other fillers, facilitating more frequent particle contact with the same content. Consequently, when the F/B ratio was set at 40%, contacts between G particles might have occurred, leading to a higher C value for monzogranite (G) than quartz diorite (D) and quartz-rich granite (Q), especially at higher temperatures.

The stiffening effect's temperature and frequency dependency, and particle interaction effects at higher concentrations becoming more prominent agree with the previous studies (Faheem and Bahia, 2010; Hesami et al., 2012; Gusev, 2016; Wang et al., 2024). At temperatures between −10 °C and 60 °C, a similar pattern of bitumen-filler interaction was seen in another study (Rochlani et al., 2021b).

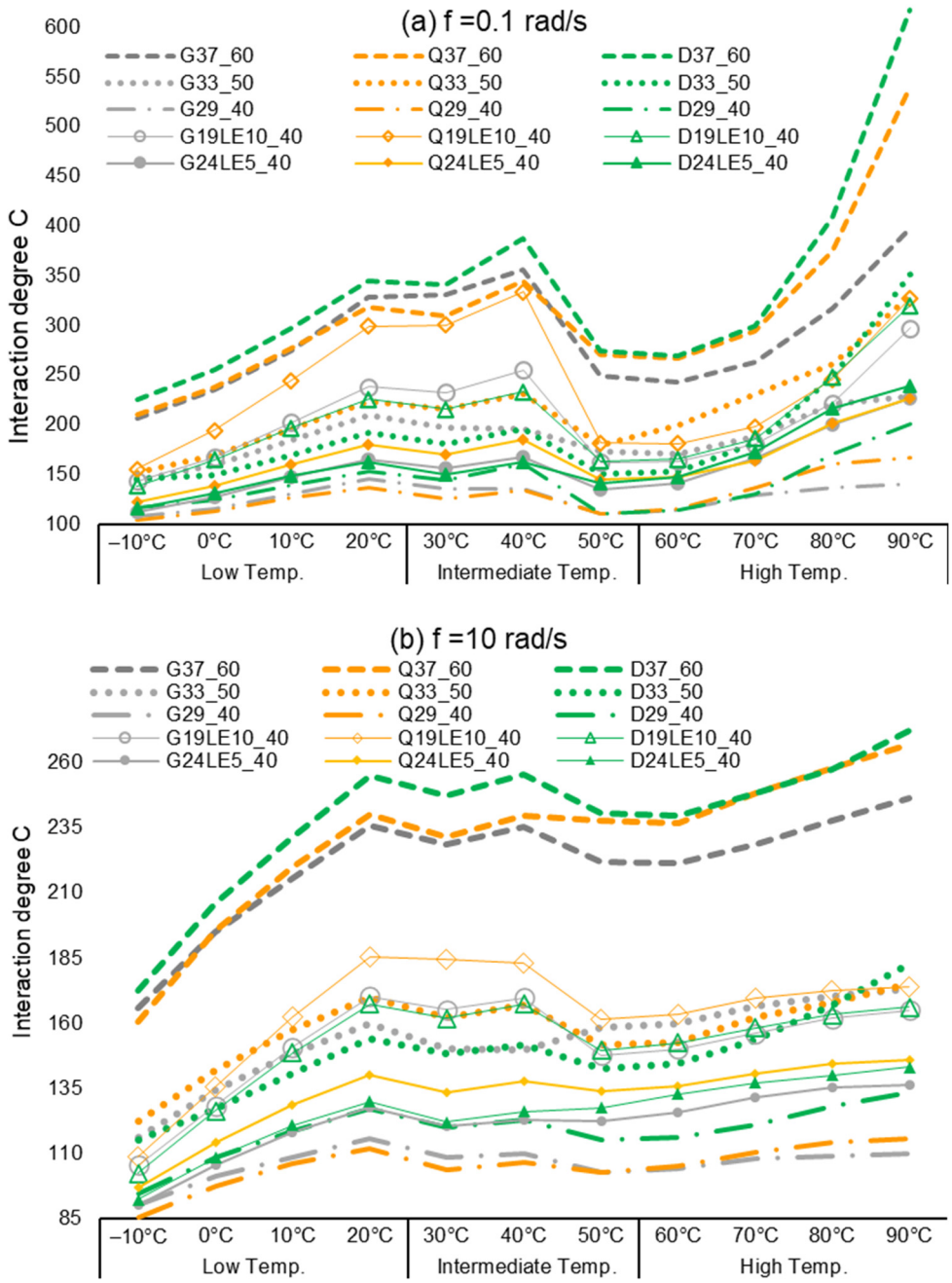

Figure 24. Calculated interaction degrees C at different temperatures and frequencies of 0.1 and 10 rad/s for tested mastics.

5 Answers to the research questions

5.1 The findings of Study I addressing RQ1

Study I identifies the effect of different steps in sample preparation and test setup on measured data complex shear modulus, |G*| and phase angle, d with DSR (Figure 25). Through the result of the round-robin tests conducted within the European asphalt laboratories and the existing research, we seek to answer this research question to help uncover the importance of different phases of measuring the rheological properties of bitumen with DSR following the existing EN method and some directions for future research. The materials under study are RTFO-aged neat bitumen 20/30, and PMB 45/80-55 in RTFO-aged and unaged conditions tested at a frequency of 10 rad/s (1.59 Hz) and temperatures ranging from 10 ℃ to 65 °C using a DSR per EN 14770:2012.

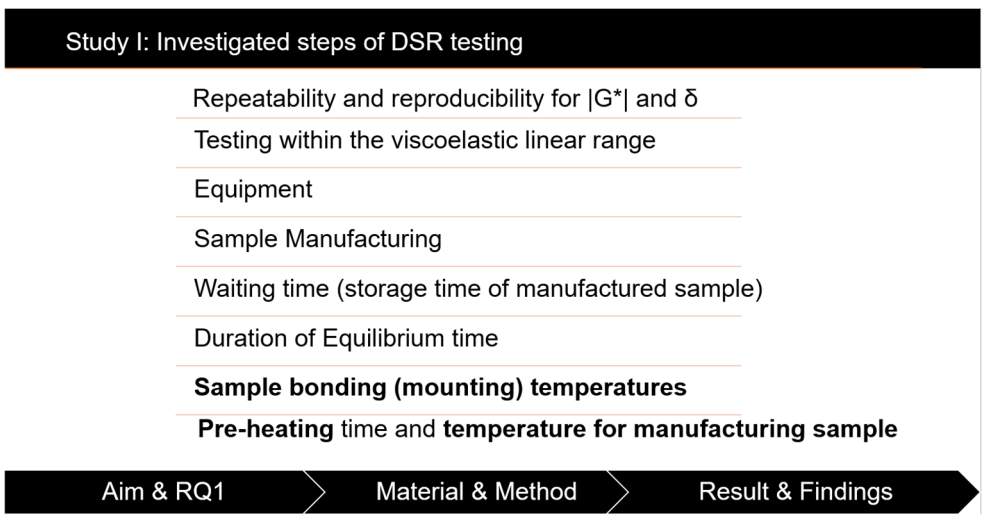

Figure 25. The investigated steps of sample preparation and test setup when applying a DSR.

Remarkable differences were identified in the preparation and conditioning of the sample through screening the practices. It is found that the repeatability coefficient of variation is within a range of CV-r=2%– 12% for |G*| and CV-r=0. 2%– 3.4% for δ. The reproducibility coefficient of variation is CV-R=7%– 20% for |G*| and

CV-R=0.4%– 20.2% for δ, which exceeds the EN 14770:12 recommended CV-R=10% for |G*| and CV-R=5% for δ. However, discarding the extreme values attributed to the selection of unsuitable plate geometry improves the precision range of |G*| significantly to a CV-r=2%– 8% and CV-R=7%– 16%, and a repeatability limit of r=2° and reproducibility limit of R=3° for δ which means a CV-R better than the criteria of 5% given in EN 14770: 2012. Testing in the shear strain range of 0.005 to 0.100, according to EN 14770:2012, falls within the LVE range for most binders, while the range is much smaller for PMBs. However, this range of linear viscoelastic behaviour may need to be determined for each geometry (test temperatures), to ensure measured complex shear modulus is independent of shear strain (or shear stress) across the testing temperatures. Nevertheless, in the round-robin tests, the LVE range of the sample was not inspected in only three laboratories. A closer examination of the methods utilized by participants reveals that the group with greater precision has not strictly followed all the preparation processes according to the existing method (EN 14770: 2012), such as waiting time, as well as much better repeatability than reproducibility results between laboratories can be due to differences in testing methodology rather than operator skill, which highlights the need for an easier to follow and interpretable method. An examination of equipment brand and sample manufacturing methods used by participants found that the measured G* was higher when the brand of Anton Paar and the sample manufactured by dropping bitumen on a sheet method were used, and applying the Malvern brand equipment and moulding method led to a higher δ. However, no significant differences were discovered across the two most used equipment brands and sample manufacturing methods. Furthermore, the measured δ is more sensitive to the manufacturing method than the G*. The long waiting time before testing the manufactured sample led to a higher G* and a lower δ value than the short waiting time, however, none of the studied bitumen would be significantly affected by waiting times of less than 2 hours or longer than 72 hours, which is outside the recommended range in EN 14770:2012. A statistically significant variation between different equilibrium timespans (5– 15 min and 15– 30 min) was detected only for unaged 45/80-55 at 40 °C. On the other hand, in most test conditions, the measured δ value increases along with the equilibrium time. 15 min temperature equilibrium time appears to be a suitable equilibrium duration, with results frequently falling between the upper and lower reported values regardless of equipment brand. Finally, the temperature at which the bitumen specimen bonds into DSR, and the sample manufacturing temperature showed significant associations with the outcomes in more test combinations than other sample preparation steps, according to the correlation tests. However, a sensitivity analysis, which examines each stage as the only variable in each experiment while holding all other conditions constant, is required to ascertain how much each phase of preparation and conditioning of the sample influences the outcome.

5.2 The findings of Study II addressing RQ2

To determine the effective factors for achieving better consistency in outcomes of DSR testing of bitumen, the impacts of a comprehensive set of factors on sample preparation and DSR setup were examined in Study I (Figure 26). Utilising statistical analysis, the relationships between these factors and the measured rheological parameters were captured. Significance tests were applied to identify variables to be investigated further while other factors were kept constant by factorial experimental design. A 2^3 experimental design matrix is carried out to answer the RQ2, whether and under what conditions does the perimeter trimming state (Trim) of the specimen on DSR testing—which was not investigated in Study I due to lack of data—, bonding temperature (BT) onto rheometer, and pre-heating temperature (HT) for manufacturing specimen significantly affect the measured parameter when these testing set-ups are varied. Verifications of the observed effects on complex shear modulus (G*) and phase angle (δ) were performed with two replications at various temperatures between 0 °C and 80 °C at a frequency of 10 rad/s (1.59 Hz). The tests were executed for 4 neat bitumen of types 50/70, 70/100, and 160/220 from two sources according to EN 14770:2012. The following presents the findings derived from the analyses.

The variation in HT strongly affected the results of 160/220_I contrary to all other studied materials. This may be attributed to the fact that the range of oven heating temperature (SP + 80 °C and SP + 100 °C) in this study is very small. Trimming the sample tested at lower temperatures from 0 °C to 30 °C for all tested material tends to significantly increase the δ and decrease the complex modulus, which indicates higher sensitivity of the smaller parallel plate (PP08) to trimming than the PP25. Increasing the factor BT from a lower to a higher value decreased the G* for practically all the temperatures tested for 50/70 and 160/220_II.

In 2-way interaction, in the case of G*, Trim:BT has the strongest effect on all the tested materials and temperatures except for the two softer bitumen 160/220 at lower temperatures, where Trim:HT affects more. For δ, the most effective 2-way interaction was Trim:BT for 70/100 and 160/220_II. The study showed that G* and δ have been affected by studied factors, the least for 70/100, followed by 50/70 and 160/220.

A simple visualisation of the measured rheological properties of the bitumen in the form of master curves seems to suggest that a different sample preparation method and the corresponding testing procedure used in this study do not lead to a significant effect on results overall. However, the large discrepancies across the eight runs do not reveal a consistent pattern among the materials, making it challenging to reach a broad conclusion. Additionally, the higher levels selected for HT and BT appear to have no ageing impacts on the materials. The occurrence of statistically significant differences was expected between those 2 extreme sets of

conditions, i.e., in the standard run orders 1 and 8, 2 and 7, 4 and 5, or 3 and 6. However, this significant difference was noticeable only for 160/220_I, between run orders 3 and 6, when the sample was manufactured at a lower temperature HT(−1), bonded onto DSR at a higher temperature BT(+1), and the sample is trimmed compared to the opposite conditions. The results of employing such a narrow range of variation in the sample preparation and conditioning procedures and observed variations in outcomes emphasise the importance of adhering to a more consistent test protocol to improve the repeatability of DSR testing on bitumen. Nonetheless, additional research with various types of modified bitumen may be required to confirm the findings (RQ3).

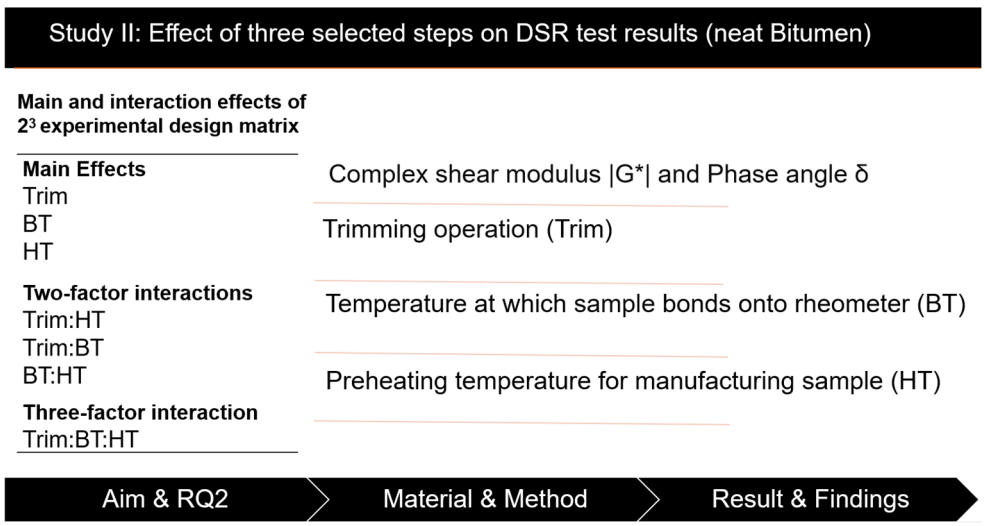

Figure 26. Impact of three specific factors on neat bitumen's DSR test results reported following EN 14770:2012.

5.3 The findings of Study III addressing RQ3

To answer the RQ3 Study III like Study II uses a 2-level 3-factor (2^3) factorial design (Figure 27). Given the influence of the radial trimming operation of the specimen after DSR plats are loaded with the specimen, the bonding temperature (BT) at which the specimen is bonded onto DSR plates, and the pre-heating temperature (HT) of bitumen to manufacture the specimens in a mould on the outcomes |G*|and δ, it is now of interest to further understand how these factors influence the measured TX and δ_{TX} aside from |G*| and δ for neat as well as modified bitumen. The temperature TX and the related phase angle δ_{TX} of complex shear modulus |G*| at 5 MPa, 15 kPa are the new parameters for the expression of results according to EN 14770:2023. the $T_{|G^*|=1\ kPa}$ represents the recommended upper limit temperature

suitable for measuring with DSR' 25 mm parallel plates. The materials under study are neat bitumen 50/70, 160/220, and 70/100, and PMBs, 70/100+ 4% SBS and 70/100+ 4% Wax tested at frequencies of 0.1, 10, and 100 rad/s (15.9 Hz) at different temperatures of lower, just below, and higher than SP of the selected materials using a DSR per EN 14770:2023. The following findings are drawn based on the laboratory experiments and statistical analyses:

- The effect of trimming operation (trimming vs. not trimming) of the specimen is significant when employing PP08, but not PP25. This could be because the PP25 specimen is easier to trim than the PP08 due to its larger diameter and lower height of the specimen.
- At higher test temperatures when using PP25, the HT and BT contribute more to the variation in the measured outcomes. Because PP25 has a larger surface area, it may be more sensitive to ensuring that the bonding temperature chosen is sufficient for the adhesion of the test specimen to the rheometer plates.
- Aside from the bitumen type 70/100 results, which appeared to be influenced by the individual batch of material used, unmodified binders are less susceptible to fluctuation in the studied parameters than modified ones. Three-way interaction Trim.BT.HT tends to contribute relatively little to the measured parameter variation.
- Interactions between two factors Trim.BT, Trim.HT, and BT.HT contributes more to the fluctuation in δ values than TX and |G*|.
- The variation in examined factors considerably influenced the repeatability based on data from wax-modified bitumen. However, considering the various testing settings used in this work, the estimated repeatability r precision for outcomes except for wax-modified bitumen is comparable to the values given in EN 14770:2023 and within repeatability criteria r. When data from wax-modified bitumen is ignored, the ranges for the variables r (TX), r (δ_{TX}), r (|G*|), and r (δ) are respectively 0.4– 2.1 °C, 0.3– 3.1°, 5– 31%, and 0.2– 3.5°.
- Overall, it is reasonable to conclude that variations in testing instructions can significantly impact DSR-recorded rheological parameters of bitumen. As a result, this study shows that clarifying the testing instructions and emphasising the need for operators to follow them closely can enhance consistency in the test results.

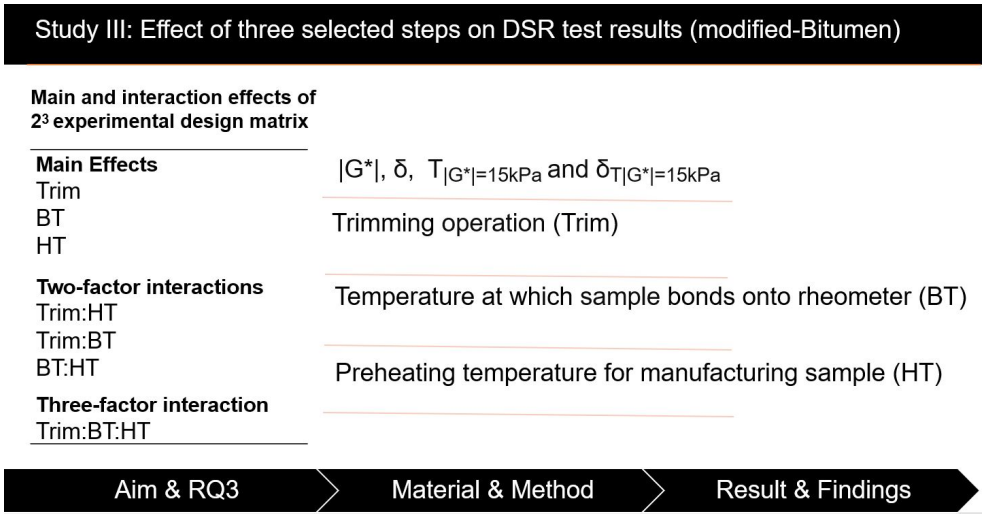

Figure 27. Impact of three specific factors on neat and modified bitumen's DSR test results reported following EN 14770:2023.

5.4 The findings of Study IV addressing RQ4

To answer RQ4 about how measured physical and mechanical properties can be related to the filler used in mastic (bitumen mixed with filler) laboratory experiments conducted (Figure 28) to investigate the properties of mastics prepared with a neat nominal bitumen 70/100, three types of mineral fillers (monzogranite, quartz diorite, and quartz-rich granite), and an industrially manufactured active filler Terra E (LE) at three different volumetric filler-to-bitumen (F/B) content ratios (40%, 50%, and 60%). The geometrical and physical properties of the studied fillers, such as particle density, particle size distribution, Rigden voids, specific surface area, and grain shape are also connected to the results from the traditional empirical methods of penetration and softening point ($T_{R\&B}$), as well as the DSR tested at temperatures between −10 °C and 90 °C with an interval of 10 °C at a frequency range of 0.1 to 100 rad/s (0.0159 to 15.9 Hz).

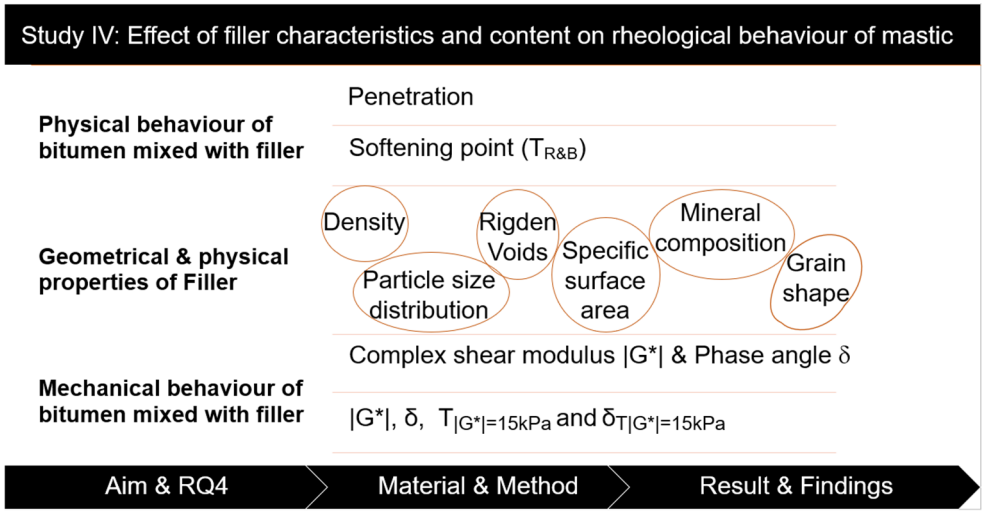

Figure 28. Rheological and physical assessment of mastics and their relationship with filler characteristics and content.

The results from SP and penetrations are consistent with DSR results to some extent. However, the DSR is required to monitor the behaviour of mastics containing fillers with varying properties over a broad temperature and frequency range. The following conclusions are drawn:

- In terms of stiffening effect, the amount of filler in mastic is more essential than the type of filler, since similar stiffening strength was observed for tested mineral fillers in mastics with the same F/B ratios.
- The relative stiffness of the mineral fillers to each other changes when they are replaced partially with LE. For instance, the quartz diorite (D) shows a slightly higher stiffening effect than quartz-rich granite (Q) at F/B of 40%, however by partial replacement of fillers by LE this rank is changed. This is due to the variation in interaction degree between the LE and different fillers (filler-to-filler), and the variation in interaction between different fillers and the bitumen (filler-to-bitumen).
- The observed differences in physical and geometrical properties of mineral fillers can explain their slightly different stiffening effect and performance. Overall, the stiffening effect increased with an increase in RV value. The SSA value is not consistent with RV and the stiffening effect of mineral fillers. However, the different particle size distribution and content of finer particles of the filler explains the variation in properties of mastics. For instance, for monzogranite (G) the lower softening point and resistance to rutting can be due to its higher content of finer particles, while the dense graded and larger average

particle size of quartz diorite (D) and quartz-rich granite (Q) contribute to a better rutting resistance and stronger stiffening effect.

- The monzogranite (G), with a higher content of finer particles and a broader particle size distribution, appears to be present in agglomerates, making it less elastic (higher fluidity) than quartz-rich granite (Q) and quartz diorite (D), which have more angular, coarser, and size uniformity among their particles, contributing to a better interlock with each other in mastic.

- A decreasing trend in the bitumen–filler interaction parameter (C) was observed with increasing temperature (frequency). This is due to the contrasting properties of fillers and bitumen, where fillers exhibit elastic behaviour with a constant modulus, and bitumen shows viscoelastic behaviour with an increasing complex modulus at higher temperatures (frequencies). The highest variation in C value among fillers occurs at temperatures just below the softening point of the bitumen used (30 °C to 50 °C), due to differences in the geometrical/physical properties (e.g. RV, particle size distribution) and their interaction ability with bitumen (stiffening power) when mastic begins to show fluidity. The C value also confirms that the active filler LE has an important contribution to the final behaviour of the mastic.

6 Discussion

This thesis aimed to assess the bitumen testing methods with DSR according to EN 14770. The first goal of this work is to review the existing sample preparation and conditioning methods and their potential impact on measured rheological parameters following EN 14770:2012. The precision of the DSR testing was also evaluated (RQ1). The second goal was to determine how the three conditioning and sample preparation phases affect the measured rheological parameters (RQ2). The third goal was to investigate the effect of the three testing technique variations when modified bitumen is involved (RQ3). The final goal was to test the properties of bitumen mixed with fillers with DSR applying the suitable practices found in previous studies and comparing results with traditional test results and their relationship with filler properties (RQ4).

It should be noted that the standard utilized for DSR determination of the rheological parameters of bitumen and bituminous binders has been revised from EN 14770:2012 to EN 14770:2023 during this PhD research (2020–2024). The revised version of the standard coincides with the conclusions of the first two studies published before the standard's release. The DSR test results that the author of this thesis submitted at the interlaboratory test (2023), which included over 70 European labs, were interestingly validated (approximate the mean values).

The main findings are as follows: the effect of the sample's trimming state is substantial on measured parameters at lower temperature tests when PP08 is applied. The BT and HT affect the outcomes more when applying PP25. The specified bonding temperature (BT) in EN needs to be closely followed or updated to a smaller interval, and more investigation on precise temperature setting (HT) can be done since it has a higher material type dependency among studied factors. The recommended BT range limits are changed from SP+15 °C and SP+25 °C in EN 14770:2012 to SP+5 °C and SP+20 °C in EN 14770:2023. However, a slightly wider range is chosen in this study which shows the consequence of deviation from EN and the importance of following the recommendations. The DSR gives a better prediction of behaviour of bitumen mixed with filler in reality as it simulates different loads and temperatures than only the SP and PEN tests. However, the bitumen test methods limit such as $T_{|G^*|=15kPa}$ and $G^*/\sin\delta \geq 1.0$ kPa among others can be studied to propose suitable levels for mastic test. Similarly, no guidelines are established for bitumen-filler DSR testing other than the existing method EN 14770.

The DSR manufacturer's guidelines can be followed to select a suitable test geometry depending on filler size similar to the modified bitumen.

The laboratory tests were carried out under controlled conditions to ensure that the acquired data was the result of intentional alterations in the procedure being studied. Also, data is collected, processed, and analysed in a very similar way when it is applicable to avoid possible errors in the designed experiment. Repeated measurements and using data from different operators and laboratories are necessary when working with method improvement which can be time-consuming and costly. However, small-scale experiments such as studies done during this PhD project can help to evaluate the effectiveness and applicability of the ideas for method improvement.

The validity of the results could be enhanced by including various types of neat and modified bitumen. Additionally, selecting fillers with properties significantly different from the common ones would facilitate a clearer investigation of the effects of filler properties. However, this approach would require more time.

7 Contribution of this thesis

This section describes the contributions of this PhD project. The project focused on investigating and expanding the knowledge of bituminous binder testing by a DSR, where there is a need for a common interpretation of the test method and a nationally uniform method of DSR testing within the industry to make it easier for the practitioner in the road construction industry to use better and more accurate technology in sample preparation and DSR setup. It would lead to consistent results across laboratories. The findings of studies conducted in this project agree with the updated version of EN 14770 in 2023. The author is not a member of the standardisation committee, but the findings have been discussed with initiated professionals. The laboratory work performed by the author of this thesis at Lund University was also validated by participating in the most recent RR test, conducted with over 70 participants from asphalt laboratories throughout Europe.

7.1 An easy-to-follow manual for DSR setup

The author of this thesis created an easy-to-follow guide for practitioners, see Appendix I. It explains how to use EN 14770 to collect data for instance in a T-f-sweep test. The collected data can be processed and used to build a master curve.

7.2 Spreading the findings to industry and academia

Research plays a vital role in education, enabling teachers like me to learn and generate new knowledge. This knowledge fosters continuous improvement in schools and bridges the gap between academia and industry, facilitating discussions on the practical implementation of research findings. By sharing research findings in my classrooms, I can keep future researchers and industry professionals informed, thereby enhancing collaboration between academia and industry. For instance, findings can be incorporated into upcoming master's thesis projects in partnership with the asphalt industry. Additionally, they will be shared with the industry through meetings, seminars, and contact persons involved in standardisation, promoting effective communication among parties involved in bitumen testing with DSR.

8 Conclusions

Data from three European round-robin tests and the conducted laboratory works by the author were analysed. I found the bonding and pre-heating temperature significantly affected the results among other steps when screening the RR data. It is also found discarding the data attributed to the selection of unsuitable plate geometry improves the precision range.

The factorial design analysis shows that the trimming state also significantly affects the measured parameters when PP08 is employed, regardless of bitumen type. I am convinced to promote result consistency trimming can be mandatory in the future version of EN. Also, the BT and HT affect the outcomes more when applying PP25.

The final laboratory experiments investigate the properties of mastics prepared with a neat bitumen, three mineral fillers, and an active filler at three volumetric filler-to-bitumen content ratios. The properties of the studied fillers are also connected to the results from the conventional tests of penetration (PEN) and softening point, as well as the DSR by performing T-f-sweep tests. I found results from the softening point and penetration are consistent with results from DSR, however, the DSR is required to monitor the behaviour of mastics containing fillers with varying properties over an extensive temperature and frequency range. The F/B content strongly affects the mastic behaviour. The relative strength of the mineral fillers to each other changes when they are replaced partially with an active filler. Overall, the stiffening effect increased with an increase in RV value. The SSA value is not consistent with RV and the stiffening effect of mineral fillers. However, the different particle size distribution and content of finer particles of the filler explains the variation in properties of mastics.

The findings highlight the importance of a clear standard and operators adhering to it closely to improve test result consistency. Organizing round-robin tests on relevant factors to be tested will substantially assist in incorporating these findings into the future version of EN 14770, easing the transition from traditional test-based requirements in the asphalt road industry to the DSR tests.

References

Aashto-T315 2022. *Determining the rheological properties of asphalt binder using a dynamic shear rheometer (DSR),* Washington, DC, American Association of State Highway and Transportation Officials.

Abraham, H. 1918. *Asphalts and allied substances: their occurrence, modes of production, uses in the arts and methods of testing*, D. van Nostrand.

Airey, G. & Brown, S. F. 1998. Rheological performance of aged polymer modified bitumens. *Journal of the Association of Asphalt Paving Technologists,* 67.

Airey, G., Hunter, A. & Rahimzadeh, B. The influence of geometry and sample preparation on dynamic shear rheometer testing. Proceedings of the 4th European Symposium on Performance of Bituminous and Hydraulic Materials in Pavements, Bitmat 4, 11-12 April 2002, Nottingham, Uk, 2002a.

Airey, G., Hunter, A. & Rahimzadeh, B. 2017. The influence of geometry and sample preparation on dynamic shear rheometer testing. *Performance of bituminous and hydraulic materials in pavements.* Routledge.

Airey, G. & Hunter, A. E. Dynamic mechanical testing of bitumen: sample preparation methods. Proceedings of the Institution of Civil Engineers-Transport, 2003. Thomas Telford Ltd, 85-92.

Airey, G., Rahimzadeh, B. & Collop, A. C. 2002b. Linear viscoelastic limits of bituminous binders. *Asphalt Paving technology,* 71**,** 89-115.

Airey, G. D. 2003. Rheological properties of styrene butadiene styrene polymer modified road bitumens. *Fuel,* 82**,** 1709-1719.

Alisov, A. 2017. *Typisierung von Bitumen mittels instationärer Oszillationsrheometrie*, ISBS, Institut für Straßenwesen, TU Braunschweig.

Anderson, D. A., Christensen, D. W., Bahia, H. U., Dongre, R., Sharma, M., Antle, C. E. & Button, J. 1994. Binder characterization and evaluation, volume 3: Physical characterization. *Strategic Highway Research Program, National Research Council, Washington, DC.*

Antunes, V., Freire, A., Quaresma, L. & Micaelo, R. 2015. Influence of the geometrical and physical properties of filler in the filler–bitumen interaction. *Construction and Building Materials,* 76**,** 322-329.

Astm-D4124 2018. *Standard test methods for separation of asphalt into four fractions*, ASTM International.

Astm-D7175 2023. *Standard test method for determining the rheological properties of asphalt binder using a dynamic shear rheometer,* West Conshohocken, PA, American Society for Testing and Materials.
Bahia, H. U., Zhai, H., Onnetti, K. & Kose, S. 1999. Non-linear viscoelastic and fatigue properties of asphalt binders. *Journal of the Association of Asphalt Paving Technologists,* 68.
Bastidas-Martínez, J. G., Rondón-Quintana, H. A. & Muniz De Farias, M. 2021. Behavior of asphalt mastics containing different materials as filler. *Canadian Journal of Civil Engineering,* 48**,** 347-355.
Benedetto, H. D., Delaporte, B. & Sauzéat, C. 2007. Three-dimensional linear behavior of bituminous materials: experiments and modeling. *International Journal of Geomechanics,* 7**,** 149-157.
Błażejowski, K., Wójcik-Wiśniewska, M., Olszacki, J. & Peciakowski, H. 2016. Interlaboratory tests of paving grade bitumen and polymer modified bitumen. *Measurement,* 50**,** 70.
Boulangé, L., Bonin, E. & Saubot, M. 2013. Physicochemical characterisations of the bitumen–aggregate interface to get a better understanding of stripping phenomena. *Road materials and pavement design,* 14**,** 384-403.
Boussad, N., Des Croix, P. & Dony, A. 1996. PREDICTION OF MIX MODULUS AND FATIGUE LAW FROM BINDER RHEOLOGICAL PROPERTIES (WITH DISCUSSION). *Journal of the Association of Asphalt Paving Technologists,* 65.
Box, G. E., Hunter, W. H. & Hunter, S. 1978. *Statistics for experimenters*, John Wiley and sons New York.
Brown, E., Haddock, J. E., Mallick, R. B. & Lynn, T. A. 1997. Development of a mixture design procedure for stone matrix asphalt.
Büchner, J., Wistuba, M. P., Dasek, O., Staschkiewicz, M., Soenen, H., Zofka, A. & Remmler, T. 2020. Interlaboratory study on low temperature asphalt binder testing using Dynamic Shear Rheometer with 4 mm diameter parallel plate geometry. *Road Materials and Pavement Design***,** 1-17.
Carswell, J., Claxton, M. & Green, P. Dynamic shear rheometers: making accurate measurements on bitumens. ARRB TRANSPORT RESEARCH LTD CONFERENCE, 19TH, 1998, SYDNEY, NEW SOUTH WALES, AUSTRALIA, 1998.
Chen, Y., Xu, S., Tebaldi, G. & Romeo, E. 2022. Role of mineral filler in asphalt mixture. *Road materials and pavement design,* 23**,** 247-286.
Clopotel, C. & Bahia, H. 2013. The effect of bitumen polar groups adsorption on mastics properties at low temperatures. *Road materials and pavement design,* 14**,** 38-51.
Corbett, L. W. 1969. Composition of asphalt based on generic fractionation, using solvent deasphaltening, elution-adsorption chromatography, and densimetric characterization. *Analytical Chemistry,* 41**,** 576-579.
Coreteam, R. 2013. R: A language and environment for statistical computing. R Foundation for Statistical Computing, Vienna, Austria. *http://www. R-project. org/*.

Cosme, R. L., Teixeira, J. E. S. L. & Calmon, J. L. 2016. Use of frequency sweep and MSCR tests to characterize asphalt mastics containing ornamental stone residues and LD steel slag. *Construction and Building Materials,* 122**,** 556-566.

Dan, L., Chuanfeng, Z., Yong, Q., Heng, B., Keyao, L. & Junfei, H. 2014. Analysing the effects of the mesoscopic characteristics of mineral powder fillers on the cohesive strength of asphalt mortars at low temperatures. *Construction and Building Materials,* 65**,** 330-337.

Daniel, C. 1959. Use of half-normal plots in interpreting factorial two-level experiments. *Technometrics,* 1**,** 311-341.

Delaporte, B., Di Benedetto, H., Chaverot, P. & Gauthier, G. 2007. Linear viscoelastic properties of bituminous materials: from binders to mastics (with discussion). *Journal of the Association of Asphalt Paving Technologists,* 76: 455 –494.

Dessouky, S., Reyes, C., Ilias, M., Contreras, D. & Papagiannakis, A. T. 2011. Effect of pre-heating duration and temperature conditioning on the rheological properties of bitumen. *Construction and Building Materials,* 25**,** 2785-2792.

Divya, P. & Krishnan, J. M. 2018. How to consistently collect rheological data for bitumen in a Dynamic Shear Rheometer. *SN Applied Sciences,* 1**,** 1-5.

Divya, P. & Krishnan, J. M. 2019. How to consistently collect rheological data for bitumen in a Dynamic Shear Rheometer? *SN Applied Sciences,* 1**,** 1-5.

E, G., Zhang, J., Shen, Q., Ji, P., Wang, J. & Xiao, Y. 2023. Influence of Filler Type and Rheological Properties of Asphalt Mastic on the Asphalt Mastic–Aggregate Interaction. *Materials,* 16**,** 574.

Eckmann, B., Chabert, D., Moglia, O., Largeaud, S., Descroix, P., Chailleux, E., Virginie, M., Soenen, H., Perez-Lepe, A., Nigen-Chaidron, S. & Lapalu, L. Complex modulus of bituminous binders. Results of the Round Robin Test of the GE1 working group (France). Proceedings 4th Eurasphalt & Eurobitume Congress, 2008 Copenhagen. 402-049.

Eckmann, B., Largeaud, S., Chabert, D., Durand, G., Robert, M., Van Rooijen, R., Chailleux, E., Mouillet, V., Soenen, H. & Clavel, N. Measuring the rheological properties of bituminous binders final results from the round robin test of the BNPÉ/P04/GE1 Working Group (France). 5th Eurasphalt & Eurobitume Congress, 2012. 12p.

EN1097-4 2008. *Tests for mechanical and physical properties of aggregates— Part 4: Determination of the voids of dry compacted filler,* Brussels Belgium, European Committee for Standardization (CEN).

EN1097-5 2008. *Tests for mechanical and physical properties of aggregates— Part 5: Determination of the water content by drying in a ventilated oven,* Brussels Belgium, European Committee for Standardization (CEN).

EN1097-7 2022. *Tests for mechanical and physical properties of aggregates— Part 7: Determination of the particle density of filler— Pyknometer method,* Brussels Belgium, European Committee for Standardization (CEN).

EN1426 2015. *Bitumen and bituminous binders— Determination of needle penetration,* Brussels Belgium, European Committee for Standardization (CEN).
EN12591 2009. *Bitumen and bituminous binders— specifications for paving grade bitumens,* Brussels Belgium, European Committee for Standardization (CEN).
EN12594 2024. *Bitumen and bituminous binders— Preparation of test samples,* Brussels Belgium, European Committee for Standardization (CEN).
EN12597 2024. *Bitumen and bituminous binders— Terminology,* Brussels Belgium,

European Committee for Standardization (CEN/TC 336).
EN12607-1 2014. *Bitumen and Bituminous binders— Determination of the resistance to hardening under influence of heat and air— Part 1: RTFOT METHOD,* Brussels Belgium, European Committee for Standardization (CEN).
EN14023 2010. *Bitumen and bituminous binders— Specification framework for polymer modified bitumens,* Brussels Belgium, European Committee for Standardization (CEN).
EN14770 2012. *Bitumen and bituminous binders— Determination of complex shear modulus and phase angle— Dynamic Shear Rheometer (DSR),* Brussels Belgium, European Committee for Standardization (CEN).
EN14770 2023. *Bitumen and bituminous binders— Determination of complex shear modulus and phase angle— Dynamic Shear Rheometer (DSR),* Brussels Belgium, European Committee for Standardization (CEN).
Faheem, A. F. & Bahia, H. U. 2010. Modelling of asphalt mastic in terms of filler-bitumen interaction. *Road Materials and Pavement Design,* 11**,** 281-303.
Ferry, J. D. 1980. *Viscoelastic properties of polymers*, John Wiley & Sons.
Fritschy, G. & Papirer, E. 1978. Interactions between a bitumen, its components and model fillers. *Fuel,* 57**,** 701-704.
Goodrich, J. L. 1991. Asphaltic binder rheology, asphalt concrete rheology and asphalt concrete mix properties (with discussion). *Journal of the Association of Asphalt Paving Technologists,* 60.
Grabowski, W. & Wilanowicz, J. 2008. The structure of mineral fillers and their stiffening properties in filler-bitumen mastics. *Materials and structures,* 41**,** 793-804.
Guo, M., Tan, Y., Hou, Y., Wang, L. & Wang, Y. 2017. Improvement of evaluation indicator of interfacial interaction between asphalt binder and mineral fillers. *Construction and Building Materials,* 151**,** 236-245.
Gusev, A. A. 2016. Controlled accuracy finite element estimates for the effective stiffness of composites with spherical inclusions. *International journal of solids and structures,* 80**,** 227-236.
Halstead, W. J. 1984. Relation of asphalt chemistry to physical properties and specifications. Virginia Transportation Research Council.
Hesami, E., Jelagin, D., Kringos, N. & Birgisson, B. 2012. An empirical framework for determining asphalt mastic viscosity as a function of

mineral filler concentration. *Construction and Building Materials,* 35**,** 23-29.
Huang, M., Zhang, H., Gao, Y. & Wang, L. 2021. Study of diffusion characteristics of asphalt–aggregate interface with molecular dynamics simulation. *International Journal of Pavement Engineering,* 22**,** 319-330.
Ibef. 2024. *International Bitumen Emulsion Federation* [Online]. Paris - France. Available: https://www.ibef.net/en/emulsions-2/key-figures/ [Accessed].
International Organization for Standardization 2001. *Accuracy (trueness and precision) of measurement methods and results — Part 6: Use in practice of accuracy values* (ISO 5725-6:1994/COR 1:2001).
Iso13320 2009. *Particle size analysis—Laser diffraction methods,* Switzerland, International Standard.
Lagos-Varas, M., Movilla-Quesada, D., Raposeiras, A., Arenas, J., Calzada-Pérez, M., Vega-Zamanillo, A. & Lastra-González, P. 2020. Influence of limestone filler on the rheological properties of bituminous mastics through susceptibility master curves. *Construction and Building Materials,* 231**,** 117126.
Laukkanen, O.-V. 2017. Small-diameter parallel plate rheometry: a simple technique for measuring rheological properties of glass-forming liquids in shear. *Rheologica Acta,* 56**,** 661-671.
Lesueur, D. 2009. The colloidal structure of bitumen: Consequences on the rheology and on the mechanisms of bitumen modification. *Advances in colloid and interface science,* 145**,** 42-82.
Liu, G., Yang, T., Li, J., Jia, Y., Zhao, Y. & Zhang, J. 2018a. Effects of ageing on rheological properties of asphalt materials and asphalt-filler interaction ability. *Construction and Building Materials,* 168**,** 501-511.
Liu, Q., Wu, J., Qu, X., Wang, C. & Oeser, M. 2020. Investigation of bitumen rheological properties measured at different rheometer gap sizes. *Construction and Building Materials,* 265**,** 120287.
Liu, X., Zhang, M., Shao, L. & Chen, Z. 2018b. Effect of volcanic ash filler on thermal viscoelastic property of SBS modified asphalt mastic. *Construction and Building Materials,* 190**,** 495-507.
Mack, C. 1957. Physical Properies of Asphalts in Thin Films. *Industrial & Engineering Chemistry,* 49**,** 422-427.
Micaelo, R., Guerra, A., Quaresma, L. & Cidade, M. 2017. Study of the effect of filler on the fatigue behaviour of bitumen-filler mastics under DSR testing. *Construction and Building Materials,* 155**,** 228-238.
Miró, R., Martínez, A. H., Pérez-Jiménez, F. E., Botella, R. & Álvarez, A. 2017. Effect of filler nature and content on the bituminous mastic behaviour under cyclic loads. *Construction and Building Materials,* 132**,** 33-42.
Mohammed, M., Parry, T., Thom, N. & Grenfell, J. 2018. Investigation into the bond strength of bitumen-fibre mastic. *Construction and building materials,* 190**,** 382-391.
Mouillet, V., Lapalu, L., Planche, J. & Durrieu, F. Rheological analysis of bitumens by dynamic shear rheometer: effect of the thermal history on the

results. PROCEEDINGS OF THE 3RD EURASPHALT AND EUROBITUME CONGRESS HELD VIENNA, MAY 2004, 2004.
Muniandy, R., Aburkaba, E., Yunus, R., Hamid, H. & Salihudin, H. 2012. Influence of mineral filler particle size and type on rheological and performance properties of SMA asphalt-filler mastics. *Asian Journal of Applied Sciences,* 5**,** 522-537.
Murali Krishnan And, J. & Rajagopal, K. 2003. Review of the uses and modeling of bitumen from ancient to modern times. *Appl. Mech. Rev.,* 56**,** 149-214.
Olard, F. & Di Benedetto, H. 2003. General "2S2P1D" Model and Relation Between the Linear Viscoelastic Behaviours of Bituminous Binders and Mixes. *Road Materials and Pavement Design,* 4**,** 185-224.
Petersen, J., Robertson, R., Branthaver, J., Harnsberger, P., Duvall, J., Kim, S., Anderson, D., Christiansen, D. & Bahia, H. 1994. Binder characterization and evaluation: Volume 1. *Rep. No. SHRP-A-367, Strategic Highway Research Program, National Research Council, Washington, DC*.
Porot, L., Büchner, J., Steinder, M., Damen, S., Hofko, B. & Wistuba, M. P. 2020. Comparison of different DSR protocols to characterise asphalt binders. *ISBM Rilem Symposium.* Lyon (online).
Rahimzadeh, B. 2002. *Linear and non-linear viscoelastic behaviour of binders and asphalts.* University of Nottingham Nottingham, UK.
Rochlani, M., Canon Falla, G., Wellner, F., Wang, D., Fan, Z. & Leischner, S. 2021a. Feasibility study of waste ceramic powder as a filler alternative for asphalt mastics using the DSR. *Road Materials and Pavement Design,* 22**,** 2591-2603.
Rochlani, M., Falla, G. C., Leischner, S. & Wellner, F. 2021b. Towards a unified performance based characterisation of bitumen and mastic using the DSR. *Road Materials and Pavement Design,* 22**,** S365-S382.
Scholz, T. V. & Brown, S. F. 1996. Rheological Characteristics of Bitumen in Contact with Mineral Aggregate (With Discussion). *Journal of the Association of Asphalt Paving Technologists,* 65.
Shao, X., Tan, Y. & Sun, L. 2005. Analysis on the relationship between several indexes of mineral filler and asphalt mortar. *J. Highway Transp. Res. Dev,* 22**,** 10-13.
Singh, B., Saboo, N. & Kumar, P. Effect of spindle diameter and plate gap on the rheological properties of asphalt binders. Functional Pavement Design: Proceedings of the 4th Chinese-European Workshop on Functional Pavement Design (4th CEW 2016, Delft, The Netherlands, 29 June-1 July 2016), 2016. CRC Press, 293.
Soenen, H., De Visscher, J., Vanelstraete, A. & Redelius, P. 2005. The influence of thermal history on binder rutting indicators. *Road materials and pavement design,* 6**,** 217-238.
Soenen, H., De Visscher, J., Vanelstraete, A. & Redelius, P. 2006. Influence of thermal history on rheological properties of various bitumen. *Rheologica Acta,* 45**,** 729-739.

Soenen, H., Lu, X. & Redelius, P. 2008. The morphology of bitumen-SBS blends by UV microscopy: an evaluation of preparation methods. *Road Materials and Pavement Design,* 9**,** 97-110.
Streckeisen, A. 1976. To each plutonic rock its proper name. *Earth-science reviews,* 12**,** 1-33.
Stroup-Gardiner, M. & Newcomb, D. 1995. Evaluation of rheological measurements for unmodified and modified asphalt cements. *Transportation research record***,** 72-81.
Sybilski, D., Vanelstraete, A. & Partl, M. 2004. Recommendation of RILEM TC 182-PEB on bending beam and rheometer measurements of bituminous binders. *Materials and structures,* 37**,** 539-546.
Tan, Y. & Guo, M. 2013. Study on the phase behavior of asphalt mastic. *Construction and Building Materials,* 47**,** 311-317.
Trafikverket 2020. TDOK 2013:0529 Bitumenbundna lager. Borlänge: The Swedish Transport Administration
Veytskin, Y., Bobko, C., Castorena, C. & Kim, Y. R. 2015. Nanoindentation investigation of asphalt binder and mastic cohesion. *Construction and Building Materials,* 100**,** 163-171.
Wang, D., Cannone Falchetto, A., Alisov, A., Schrader, J., Riccardi, C. & Wistuba, M. P. 2019. An alternative experimental method for measuring the low temperature rheological properties of asphalt binder by using 4mm parallel plates on dynamic shear rheometer. *Transportation Research Record,* 2673**,** 427-438.
Wang, J., Guo, M. & Tan, Y. 2018. Study on application of cement substituting mineral fillers in asphalt mixture. *International Journal of Transportation Science and Technology,* 7**,** 189-198.
Wang, Z., Jin, X., Sun, Y. & Wang, S. 2024. Micromechanics approach to calculate the adsorbed asphalt film thickness on mineral fillers and evaluate physiochemical interactions. *International Journal of Pavement Engineering,* 25**,** 2303670.
Wasilewska, M., Małaszkiewicz, D. & Ignatiuk, N. Evaluation of different mineral filler aggregates for asphalt mixtures. IOP Conference Series: Materials Science and Engineering, 2017. IOP Publishing, 022042.
Whiteoak, D., Read, J. & Hunter, R. N. 1990. *The shell bitumen handbook*, Thomas Telford.
Wu, J., Liu, Q., Yang, S., Oeser, M. & Ago, C. 2021. Study of migration and diffusion during the mixing process of asphalt mixtures with RAP. *Road Materials and Pavement Design,* 22**,** 1578-1593.
Wu, J., Wang, Y., Liu, Q., Wang, Y., Ago, C. & Oeser, M. 2020. Investigation on mechanical performance of porous asphalt mixtures treated with laboratory ageing and moisture actions. *Construction and Building Materials,* 238**,** 117694.
Yi, J., Pang, X., Feng, D., Pei, Z., Xu, M., Xie, S. & Huang, Y. 2018. Studies on surface energy of asphalt and aggregate at different scales and bonding

property of asphalt–aggregate system. *Road Materials and Pavement Design,* 19**,** 1102-1125.
Zakar, P. 1971. *Asphalt*, Chemical Publishing Company.
Zhai, H., Bahia, H. U. & Erickson, S. 2000. Effect of film thickness on rheological behavior of asphalt binders. *Transportation research record,* 1728**,** 7-14.
Zhu, J., Balieu, R., Lu, X. & Kringos, N. 2017. Numerical investigation on phase separation in polymer-modified bitumen: effect of thermal condition. *Journal of Materials Science,* 52**,** 6525-6541.
Zhu, J., Lu, X., Langfjell, M. & Gudmarsson, A. 2021. Quantitative relationship of fundamental rheological properties of bitumen with the empirical Ring and Ball softening point. *Road Materials and Pavement Design,* 22**,** S345-S364.
Zimmerman, D. W. 2011. A simple and effective decision rule for choosing a significance test to protect against non-normality. *British Journal of Mathematical and Statistical Psychology,* 64**,** 388-409.

Appendix I:

A step-by-step manual for DSR testing following EN 14770 for practicioners.

All data modification is done outside the Anton Paar MCR302 DSR software (RheoCompass). Three specimens, rather than one, can be used to ensure the zero-gap setup is valid across the tested temperature range, for example, if the test is run between –10 °C and 80 °C. The normal force should be set to 0N if the temperature range is larger. This isn't crucial if the range of temperatures tested per sample is limited. PP25 is recommended (EN14770:2023) for |G*| between 1kPa to 100 kPa (lower test temperatures) and PP08 for |G*| between 100 kPa to 10,000,000 kPa (higher test temperatures). When using PP25, be careful not to apply too low torque values, and when using PP08, avoid applying too high torque values. The particle size of the specimen should be ten times smaller than the gap size.

1. Turn on the air pressure, DSR, and cooler (set the cooler for the current spindle)

2. Start The rheometer software RheoCompass

3. Raise the drive shaft (spindle mount) to the high position

4. Couple the spindle with the drive shaft (the lines on the spindle and drive shaft face each other)

5. Start the test template and the control panel

6. Zero gap: set the temperature to mid-temperature of the intended test temperature range and conduct a zero gap immediately. Let the hood (Peltier) be down to achieve as uniform temperature as possible, wait 10 min, and do a second zero gap

7. Bonding sample: mount the sample on the lower plate at a suitable temperature to achieve a good bond, for instance, (softening point + 10) °C degrees

8. Trim: go to the trim position (a gap of 1.05 mm for PP25 and 2.1 mm for PP08) and carefully remove the excess binder from the periphery of the plates. Do this in several steps, and with great care to avoid inconsistency in collected data.

9. Start then gradually lower the upper plate toward the lower plate to reach a final gap of 1mm for PP25 and 2 mm for PP08; make sure a slight bulge around the periphery of the plates is made after this.

10. Test position: set the test temperature (the first planned test temperature) and as soon as the DSR approximately reaches the temperature set the test position and lower the hood, wait 10– 20 min at the planned temperature, and then start the test. The waiting time at test temperatures can be set to 15 min to avoid problems with temperature equilibrium issues for most of the DSRs.

11. After this waiting time an A-sweep (within a strain range of 0.01% to 100% for PP25 and 0.001% to 10% for PP08 per EN14770:2023) can be conducted to ensure testing within the LVE. When A-sweep has finished a waiting time of 3 min can be set before the frequency sweep test (usually between 0.1 Hz to 10 Hz) starts. In the RheoCompass the collected data is found under tap "Table" and the diagrams are found under "Diagram: G′ and G″". The A-sweep curves should always be observed to see whether anything seems strange or out of the ordinary, which can be due to instability in air pressure (for instance due to blockage in the compressor), there are excessive vibrations surrounding the DSR, the sample does not remain in the geometry, inadequate adhesion between the binder and plates, inhomogeneous sample, etc.

The A-sweep is dependent on preset temperature and frequency. It can be performed at ω= 10 rad/s (1.59 Hz) for different temperatures to obtain the suitable range. The LVE range can be determined manually (with a ruler), through a data table, or software. In RheoCompass the tolerance range of G′ deviation around the plateau value can be selected e.g., as ± 5% (EN14770:2023).

12. Saving the project file in RheoCompass: Choose the file containing all the tested intervals from the "Project - Data Browser" menu on the left, and make sure that the intervals listed under that file are also checked in. Note that the Table mode should be activated, not the Measurement or Black modes.

Project→ Home→ Import, Export→ Export selected item→ .csv file (.csv)

Close project→ RheoFinder→ Tests (select the test to be saved e.g. Project1)→ Home→ Import, Export→ Export selected item→ RHPTS file (.RhPts)

13. Cleaning of the plates: Raise the temperature to approximately 100 °C and use soft paper (serviette) to remove as much material as possible from both plates (upper and lower/button), after removing the upper plate from the drive shaft. Then lower the temperature to approximately 60 °C, apply a degreasing agent, and wipe the plates clean. Apply a small amount of alcohol to remove the fatty surface from the degreasing agent. Isopropanol is easily obtainable and works great.

Appendix II:

3D visualisation of G*(f= 0.1, 10, and 100 rad/s) under the three variables investigated for tested bitumen in Study III.

|G*| 50/70 at 20°C	HT 127°C	HT 127°C	HT 147°C	HT 147°C
BT 48°C_0.1 rad/s	137.2	156.0	136.6	167.7
BT 73°C_0.1 rad/s	127.8	139.8	131.1	159.5
BT 48°C_10 rad/s	2309.8	2684.1	2324.3	2753.2
BT 73°C_10 rad/s	2187.6	2352.2	2243.5	2617.9
BT 48°C_100 rad/s	4371.1	5018.3	4408.2	4950.1
BT 73°C_100 rad/s	4224.2	4362.7	4204.0	4873.5
|G*| 50/70 at 50°C	HT 127°C	HT 127°C	HT 147°C	HT 147°C
BT 48°C_0.1 rad/s	0.26	0.25	0.26	0.26
BT 73°C_0.1 rad/s	0.27	0.27	0.28	0.29
BT 48°C_10 rad/s	15.56	14.54	15.76	15.56
BT 73°C_10 rad/s	16.01	15.78	16.28	16.81
BT 48°C_100 rad/s	46.78	43.65	47.48	45.50
BT 73°C_100 rad/s	48.66	46.47	48.84	49.34
|G*| 50/70 at 70°C	HT 127°C	HT 127°C	HT 147°C	HT 147°C
BT 48°C_0.1 rad/s	0.01	0.01	0.01	0.01
BT 73°C_0.1 rad/s	0.01	0.01	0.01	0.01
BT 48°C_10 rad/s	1.03	0.95	1.06	1.05
BT 73°C_10 rad/s	1.01	1.03	1.07	1.05
BT 48°C_100 rad/s	3.82	3.54	3.92	3.80
BT 73°C_100 rad/s	3.76	3.77	3.96	3.83
	YT –	NT +	YT –	NT +
	Trimming state		Trimming state	

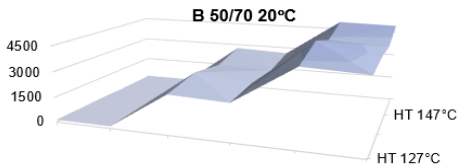

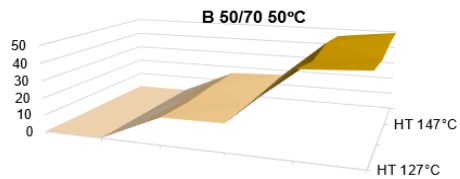

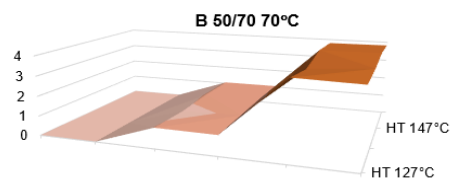

|G*|160/220 at 10°C	HT 121°C	HT 121°C	HT 141°C	HT 141°C
BT 41°C_0.1 rad/s	289.0	401.5	199.1	224.5
BT 61°C_0.1 rad/s	477.3	483.4	289.0	416.3
BT 41°C_10 rad/s	3069.5	4178.7	2670.0	2939.1
BT 61°C_10 rad/s	3899.6	4259.3	3069.5	3993.1
BT 41°C_100 rad/s	5999.3	8093.0	5139.5	5361.5
BT 61°C_100 rad/s	7985.2	8303.0	5945.8	7737.0
|G*|160/220 at 30°C	HT 121°C	HT 121°C	HT 141°C	HT 141°C
BT 41°C_0.1 rad/s	2.87	3.99	2.12	2.12
BT 61°C_0.1 rad/s	4.76	5.13	2.87	3.24
BT 41°C_10 rad/s	78.07	111.44	66.44	72.13
BT 61°C_10 rad/s	103.15	120.50	78.07	93.91
BT 41°C_100 rad/s	239.37	340.86	203.18	213.58
BT 61°C_100 rad/s	322.45	363.71	238.75	280.39
|G*|160/220 at 50°C	HT 121°C	HT 121°C	HT 141°C	HT 141°C
BT 41°C_0.1 rad/s	0.04	0.06	0.04	0.04
BT 61°C_0.1 rad/s	0.04	0.04	0.04	0.05
BT 41°C_10 rad/s	2.84	3.27	2.83	2.76
BT 61°C_10 rad/s	2.72	2.85	2.84	2.94
BT 41°C_100 rad/s	10.58	12.20	10.49	10.05
BT 61°C_100 rad/s	10.17	10.45	10.54	10.77
	YT –	NT +	YT –	NT +
	Trimming state		Trimming state	

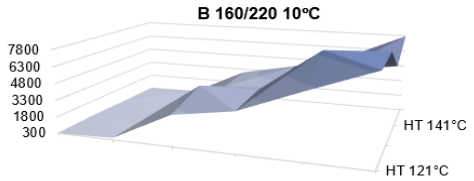

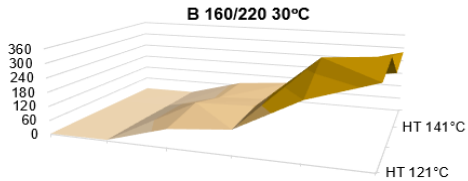

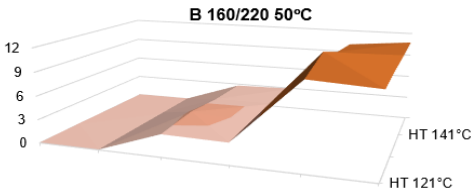

|G*| 70/100 at 20°C	HT 126°C	HT 126°C	HT 146°C	HT 146°C
BT 46°C_0.1 rad/s	82.1	81.0	77.1	114.9
BT 71°C_0.1 rad/s	69.1	98.9	87.1	85.9
BT 46°C_10 rad/s	1578.9	1531.6	1489.1	1981.3
BT 71°C_10 rad/s	1418.9	1825.6	1702.4	1582.7
BT 46°C_100 rad/s	5640.8	5412.4	5334.9	6715.7
BT 71°C_100 rad/s	5177.3	6392.1	6028.0	5554.2
|G*| 70/100 at 45°C	HT 126°C	HT 126°C	HT 146°C	HT 146°C
BT 46°C_0.1 rad/s	0.43	0.42	0.43	0.52
BT 71°C_0.1 rad/s	0.37	0.45	0.43	0.43
BT 46°C_10 rad/s	23.62	22.88	23.81	27.35
BT 71°C_10 rad/s	21.01	23.73	23.60	22.61
BT 46°C_100 rad/s	139.71	135.12	141.14	157.37
BT 71°C_100 rad/s	125.57	137.41	139.24	130.53
|G*| 70/100 at 60°C	HT 126°C	HT 126°C	HT 146°C	HT 146°C
BT 46°C_0.1 rad/s	0.03	0.03	0.04	0.04
BT 71°C_0.1 rad/s	0.03	0.04	0.04	0.03
BT 46°C_10 rad/s	2.75	2.69	2.77	3.27
BT 71°C_10 rad/s	2.58	2.77	2.77	2.68
BT 46°C_100 rad/s	20.17	19.70	20.20	23.41
BT 71°C_100 rad/s	19.02	20.00	20.26	19.29
	YT –	NT +	YT –	NT +
	Trimming state		Trimming state	

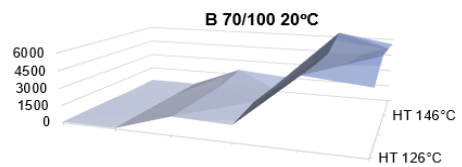

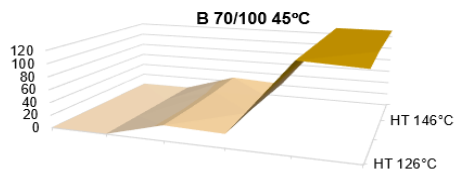

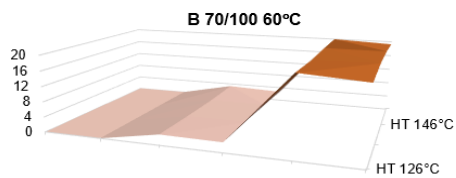

|G*| 70/100+4%SBS at 20°C	HT 147°C	HT 147°C	HT 167°C	HT 167°C
BT 67°C_0.1 rad/s	156.1	146.1	148.9	204.2
BT 92°C_0.1 rad/s	123.1	157.1	146.5	175.9
BT 67°C_10 rad/s	2173.4	1976.2	2108.4	2683.1
BT 92°C_10 rad/s	1805.4	2217.0	2058.5	2333.2
BT 67°C_100 rad/s	6976.6	6228.7	6814.1	8360.7
BT 92°C_100 rad/s	5938.9	7149.2	6572.8	7245.4
|G*| 70/100+4%SBS at 50°C	HT 147°C	HT 147°C	HT 167°C	HT 167°C
BT 67°C_0.1 rad/s	0.77	0.76	0.67	0.68
BT 92°C_0.1 rad/s	0.62	0.69	0.65	0.89
BT 67°C_10 rad/s	27.36	28.44	27.00	26.73
BT 92°C_10 rad/s	25.09	27.56	26.22	29.70
BT 67°C_100 rad/s	122.05	124.50	119.66	118.52
BT 92°C_100 rad/s	113.40	121.75	116.28	128.95
|G*| 70/100+4%SBS at 70°C	HT 147°C	HT 147°C	HT 167°C	HT 167°C
BT 67°C_0.1 rad/s	0.05	0.04	0.04	0.04
BT 92°C_0.1 rad/s	0.03	0.03	0.03	0.05
BT 67°C_10 rad/s	2.75	2.76	2.72	2.68
BT 92°C_10 rad/s	2.43	2.63	2.57	3.25
BT 67°C_100 rad/s	16.45	17.04	16.87	16.63
BT 92°C_100 rad/s	15.55	16.47	16.07	17.69
	YT –	NT +	YT –	NT +
	Trimming state		Trimming state	

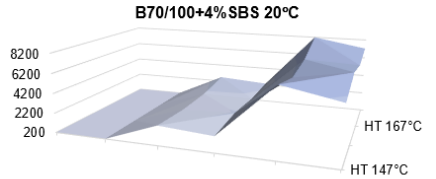

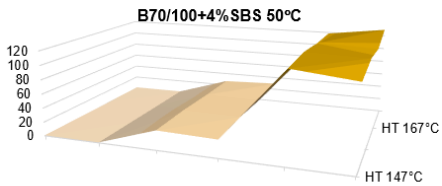

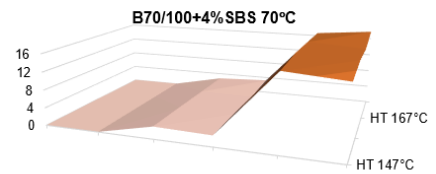

|G*| 70/100+4%wax at 20°C	HT 159°C	HT 159°C	HT 179°C	HT 179°C
BT 79°C_0.1 rad/s	563.0	595.1	631.5	628.7
BT 104°C_0.1 rad/s	594.4	848.8	877.1	1051.9
BT 79°C_10 rad/s	3451.1	3520.0	3987.4	4073.6
BT 104°C_10 rad/s	3478.6	4685.0	4301.4	5648.3
BT 79°C_100 rad/s	8601.5	8537.8	9971.6	10054.0
BT 104°C_100 rad/s	8286.9	10896.5	9645.0	12668.0
|G*| 70/100+4%wax at 65°C	HT 159°C	HT 159°C	HT 179°C	HT 179°C
BT 79°C_0.1 rad/s	8.95	9.15	13.79	10.63
BT 104°C_0.1 rad/s	11.49	19.67	22.88	18.08
BT 79°C_10 rad/s	42.06	38.71	45.57	43.63
BT 104°C_10 rad/s	45.84	73.88	78.59	70.69
BT 79°C_100 rad/s	121.94	114.56	130.50	128.40
BT 104°C_100 rad/s	128.49	196.48	193.79	195.15
|G*| 70/100+4%wax at 80°C	HT 159°C	HT 159°C	HT 179°C	HT 179°C
BT 79°C_0.1 rad/s	0.17	0.23	0.73	0.75
BT 104°C_0.1 rad/s	0.21	0.20	0.23	0.23
BT 79°C_10 rad/s	1.55	1.84	3.14	3.18
BT 104°C_10 rad/s	1.53	1.65	1.70	1.73
BT 79°C_100 rad/s	7.31	8.22	12.25	12.22
BT 104°C_100 rad/s	7.30	7.86	7.84	8.25
	YT –	NT +	YT –	NT +
	Trimming state		Trimming state	

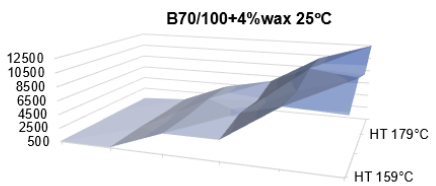

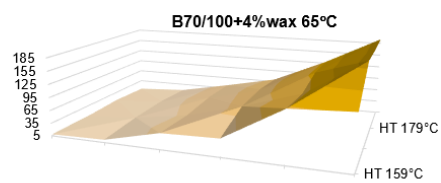

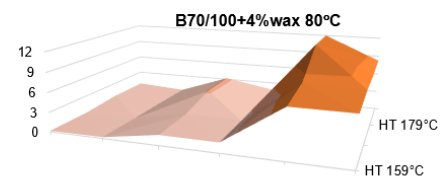

Appendix III:

Papers (I, II, III, IV)

About the author

Maya Sheidaei (second person from right in photo) is a civil engineer with bachelor's degrees in civil engineering and surveying-geomatics from Iran, and a master's degree in infrastructure and environmental engineering from Chalmers University, Sweden. Since 2016, she has worked as a lecturer at Lund University before pursuing her education as a research student at the Division of Transport and Roads (T&R), Lund University Faculty of Engineering (LTH).

In her research, she studied the impact of measurement techniques when using a Dynamic Shear Rheometer (DSR) for rheological investigation of bitumen in road applications (2020-2023). In her last year of research (2024), she concentrated on the influence of filler's geometrical and physical nature on the behaviour of bitumen mixed with filler (mastic), evaluated using conventional penetration and softening point tests as well as with DSR.

Her research findings will be used in road construction courses offered to students to keep them updated as future researchers and industry employees. Additionally, these findings will be shared with the asphalt industry through meetings, seminars, and contact persons involved in standardisation to facilitate communication among parties involved in bitumen testing.

Printed by Media-Tryck, Lund 2025 NORDIC SWAN ECOLABEL 3041 0903

LUND UNIVERSITY

Department of Technology and Society
Faculty of Engineering

ISBN 978-91-8104-365-5
ISSN 1653-1930